ANL-5486

ARGONNE NATIONAL LABORATORY
P. O. Box 299
Lemont, Illinois

QUARTERLY REPORT OF BIOLOGICAL AND MEDICAL RESEARCH DIVISION

A. M. Brues
Director

October, 1955

Preceding reports:

ANL-5456 - July, 1955
ANL-5426 - April, 1955
ANL-5378 - January, 1955

Operated by The University of Chicago
under
Contract W-31-109-eng-38

TABLE OF CONTENTS

TABLE OF CONTENTS

TABLE OF CONTENTS

TABLE OF CONTENTS

GEOGRAPHIC INCIDENCE OF SKIN TUMORS

Harry Auerbach

The literature supporting the relationship between exposure to ultraviolet radiation and skin cancer is very thoroughly reviewed by Blum.[1] Variation in skin tumor incidence rates with differences in latitude in the United States were shown by Dorn.[2] This study used the data collected from ten large metropolitan areas in the years 1937-1938. The relationship is based on total white male and total white female incidence rates and is shown for three non-overlapping latitude areas. The study showed an inverse relationship between the skin cancer incidence rate and the north latitude; in areas closer to the equator the incidence rates were higher.

The National Cancer Institute repeated the survey of these ten large cities (New Orleans, Dallas, Birmingham, Atlanta, San Francisco, Denver, Philadelphia, Pittsburgh, Chicago, and Detroit) in the years 1947-1948; as a result, detailed data are available on the age, sex, and color incidence rates of skin tumors in these cities.

The objective of this study was to use these more detailed data in an attempt to find whether a more precise relationship exists between latitude and skin tumor incidence rates by age and sex. The total white male and total white female incidence rates were first age-adjusted to correct for differences in age distribution of the populations of the ten cities. Table 1 shows the white male and white female incidence rates of skin tumors.

The numbers following the names of the cities indicate the order in which they were surveyed. These numbers are used also to indicate the cities in the graphs. Figures 1 and 2 are semi-logarithmic plots of these data with a least-squares-fitted straight line. The slopes of these lines are not significantly different but at any north latitude, the white male rates are higher than those of the white females.

The age-specific skin tumor incidence rates can be fitted with least-squares straight lines; these are shown in Figures 3 and 4. The broken line in Figure 4 results from an attempt to correct the 55-64-year age line for white females. In the reported data the incidence rate for white females age 55-64 in New Orleans, was less than the incidence rate for white females age 45-54. Since such a decrease occurred in no other age group, male or female, in any other city, the New Orleans figure was not used in fitting the line and the resulting broken line plot was obtained.

Skin tumor incidence rates in the United States in 1947

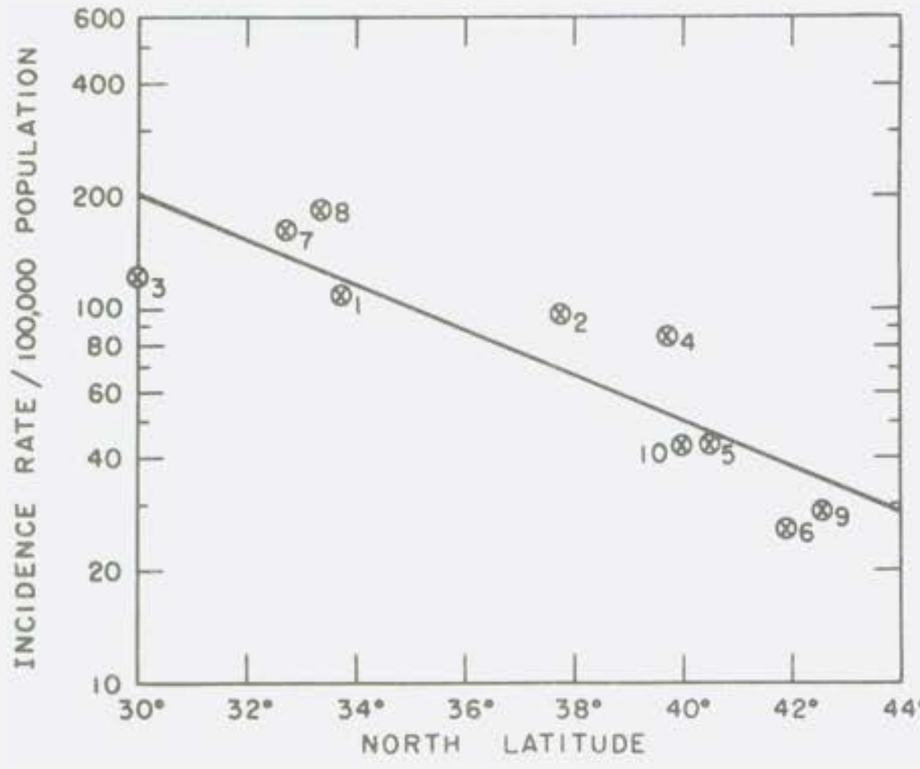

Figure 1 White males
(age-adjusted rates)

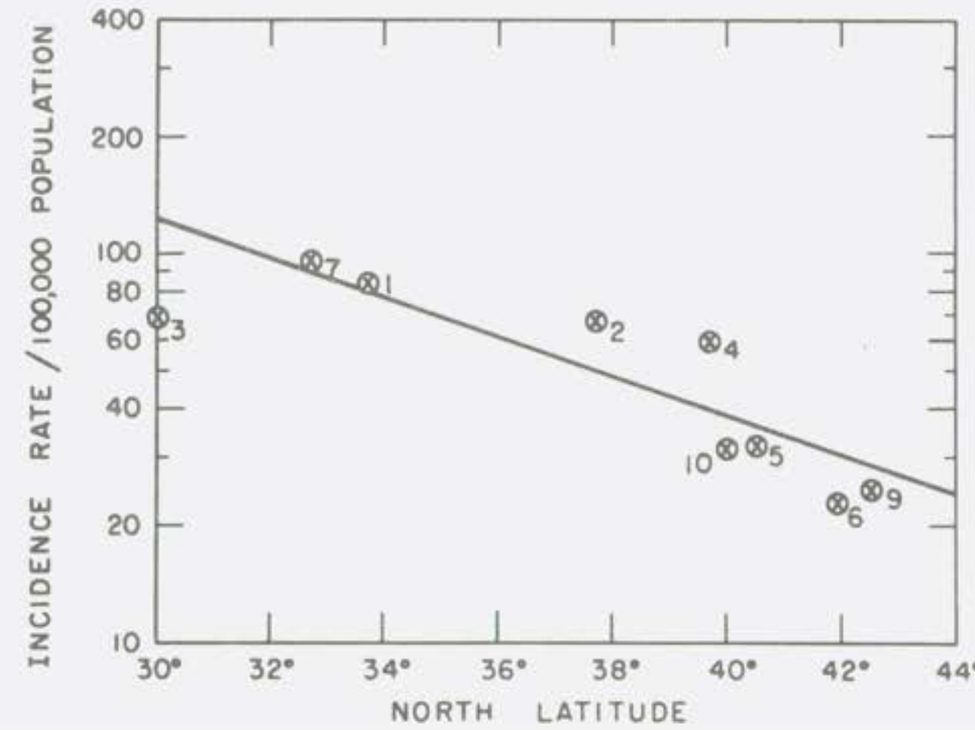

Figure 2 White females
(age-adjusted rates)

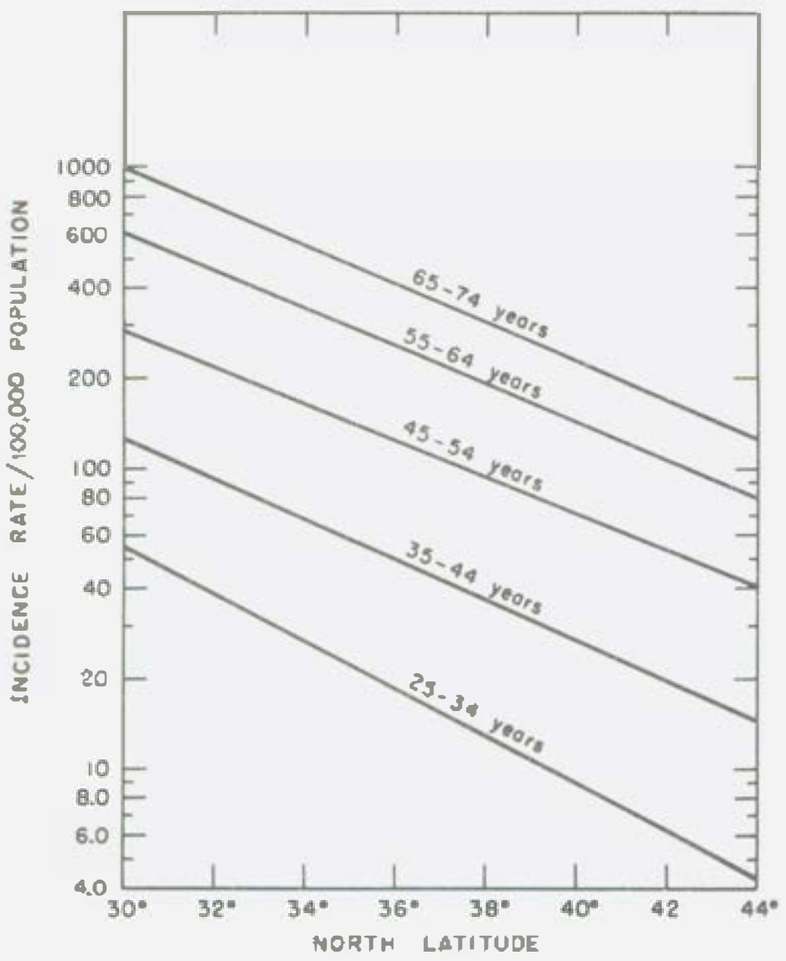

Figure 3 White males
(age-specific rates)

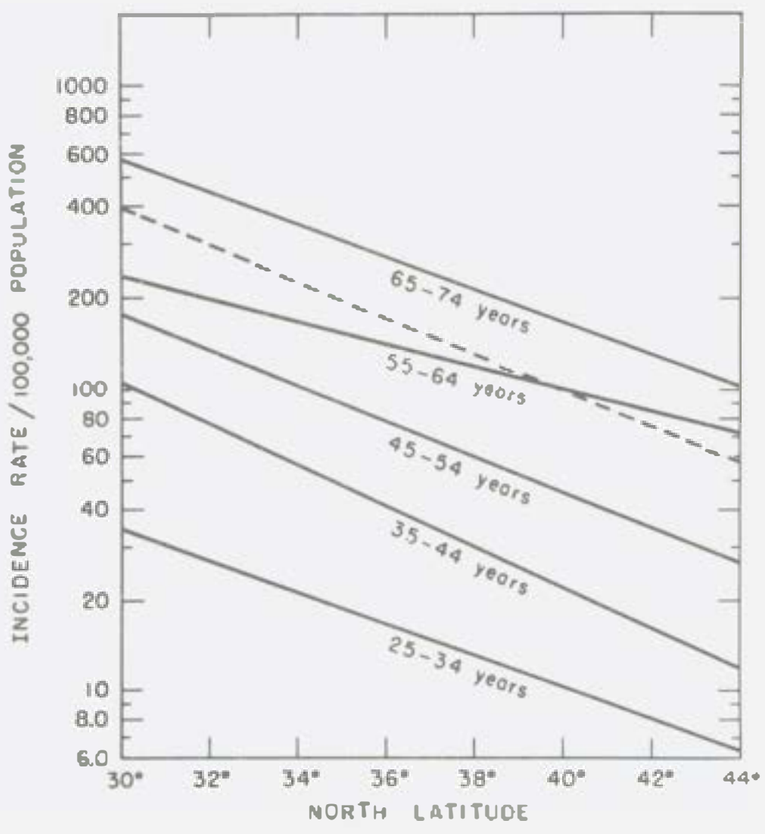

Figure 4 White females
(age-specific rates)

Table 1

Total white male and white female skin tumor incidence rate (per 100,000 population). Ten cities, United States, 1947-1948. Age-adjusted rates.

City	North latitude in degrees	Incidence rate	
		White male	White female
New Orleans (3)	29.95	123.2	68.7
Dallas (7)	32.78	164.4	95.6
Birmingham (8)	33.35	182.2	132.3
Atlanta (1)	33.75	110.0	82.9
San Francisco (2)	37.77	97.1	68.0
Denver (4)	39.73	86.3	60.6
Philadelphia (10)	39.95	41.3	32.8
Pittsburgh (5)	40.43	43.0	32.5
Chicago (6)	41.87	25.3	22.4
Detroit (9)	42.33	33.6	24.2

The parallelism of these lines in a semi-logarithmic plot is due to similar slopes. This would indicate a constant rate of increase in the incidence of skin tumors with decreasing north latitude, i.e., higher skin tumor rates as one examines white populations closer to the equator. This constant rate of increase is independent of age or sex of the population since all the semi-logarithmic slopes are similar. In the absence of exact measurements of the amount of ultraviolet energy arriving at the earth's surface at each of these cities, it can be shown that the total solar radiation energy received at points in the United States decreases with increasing north latitude, i.e., the farther north the area is located, the less the energy received. The displacement of the plotted points from the fitted line may be due to lesser variables such as differences in altitude of the areas, differences in skin susceptibility due to varied ethnic backgrounds of the populations, degree of air pollution, and others.

References

1. Blum, H. F., 1955. Ultraviolet radiation and cancer, in Radiation Biology, Vol. 2, A. Hollaender, ed. New York: McGraw-Hill.

2. Dorn, H. F., 1944. Illness from cancer in the United States. U. S. Public Health Reports, 59, 33-48, 65-77, 97-115.

HEMOLYSIN PRODUCTION IN IRRADIATED RABBITS

Bernard N. Jaroslow and William H. Taliaferro*

In previous reports we have noted that X-irradiated (400 r) rabbits produced antibody in titers approaching those of the unirradiated group if the antigen was mixed 5 or more minutes prior to intravenous injection with minced rabbit spleen, aqueous extract of mouse spleen, minced HeLa cells or aqueous extract of HeLa cells. In irradiated rabbits that received antigen only, the average antibody titers were approximately one-tenth those of the normal rabbits.

Since our last report we have used an autolysate of brewer's yeast which appears to be effective. The autolysate was prepared by suspending dried brewer's yeast in phosphate buffer at pH 7.4 and letting it stand over night at room temperature. The supernatant after centrifugation was mixed with sheep red-cell antigen and injected. The results are shown in Table 2.

Work is being carried on with the aim of characterizing the active principle found in these unrelated substances.

Table 2

Effect of yeast autolysate on hemolysin titer in irradiated rabbits

Group	No. of rabbits	Mean log peak titer	Geometric mean
Unirradiated	33	3.3 ± .2	2000
400 r + autolysate	7	3.1 ± .2	1260
400 r	25	2.4 ± .3	250

*Department of Microbiology, University of Chicago.

PROGRESS REPORT: ACARIASIS OF MICE

Robert J. Flynn

Previous reports[1,2,3,4] have been concerned with the species of mites found on mice, the lesions attributed to the various species, and a search for methods of control. This work is being continued.

In order to determine the incidence of infestation by mites among native laboratory mice and to identify the species of mites involved, 8 strains of mice from 8 commercial sources are being surveyed. The species of mites observed to date include: Myobia musculi Schrank, Myocoptes musculinus Koch, Radfordia affinis Poppe, Psorergates simplex Tyrrell, and Myocoptes sp. This latter myocoptid mite (Figures 5, 6, 7, 8) is similar to Myocoptes tenax Michael, Myocoptes romboutsi Van Eyndhoven, and Myocoptes kalrai Radford, but differs slightly from the published morphological descriptions of each. Samples have been sent for comparison with the type of each of the above and should the unique identity of this mite be confirmed, it will be described as a new species.

Pathology

Myobia musculi The simple denuding of the face and head attributed to this mite in an earlier report[4] has been observed since in mice free of all mites and is apparently due to other causes.

Myocoptes musculinus The report on lesions attributed to this mite[4] has been partially confirmed since these lesions do not occur on mice free of mites; however, similar lesions have been observed in Myocoptes sp. infestations.

Psorergates simplex The microscopic and internal lesions produced by this mite are described elsewhere in this report.[5] No external lesions have been observed or reported.

Radfordia affinis This mite is almost identical with Myobia musculi; it differs principally in the number of claws of the second tarsus. Apparently because of its similarity to the latter, it has not been previously reported on laboratory mice and no lesions have been attributed to it specifically.

Myocoptes sp. This mite at this laboratory has been frequently observed on mice with thin hair and weeping, eczematous lesions of the skin.

Because almost all laboratory mice have mixed mite infestations the true lesions caused by each of these species is in doubt. Mite-free CF#1 mice are now being bred at this laboratory and will be monoinfested to determine the specific lesions.

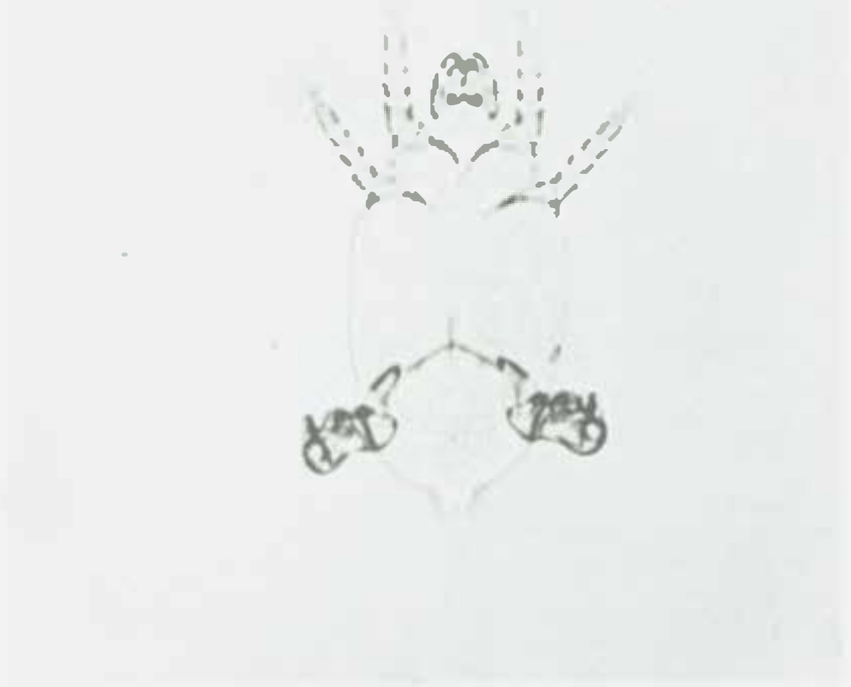

Figure 5 Myocoptes sp. larva

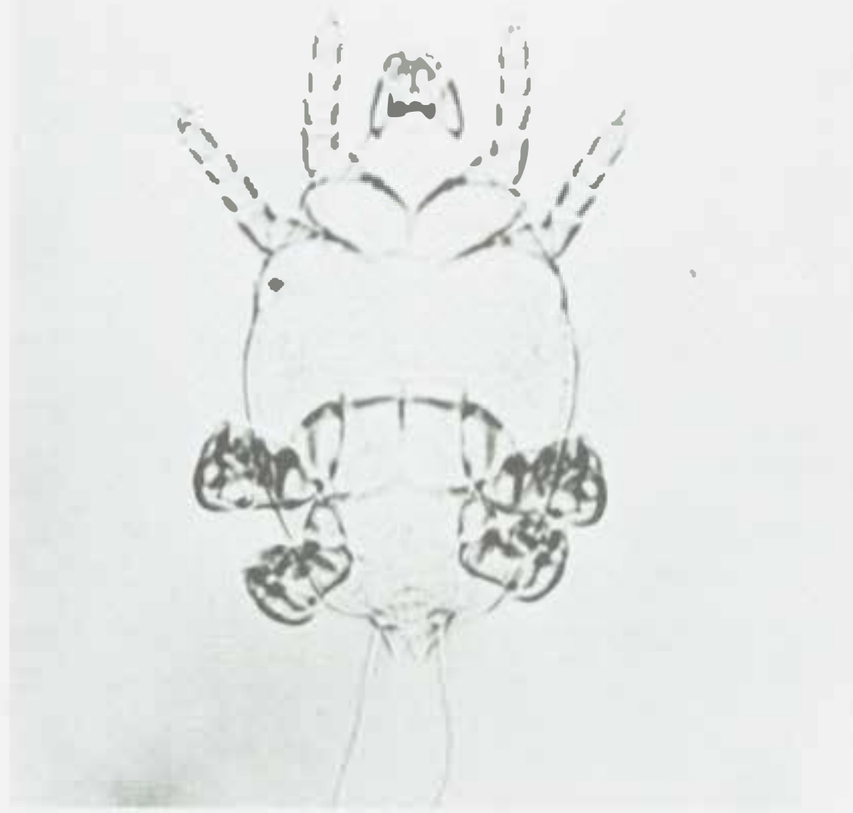

Figure 6 Myocoptes sp. nymph

0.1 mm

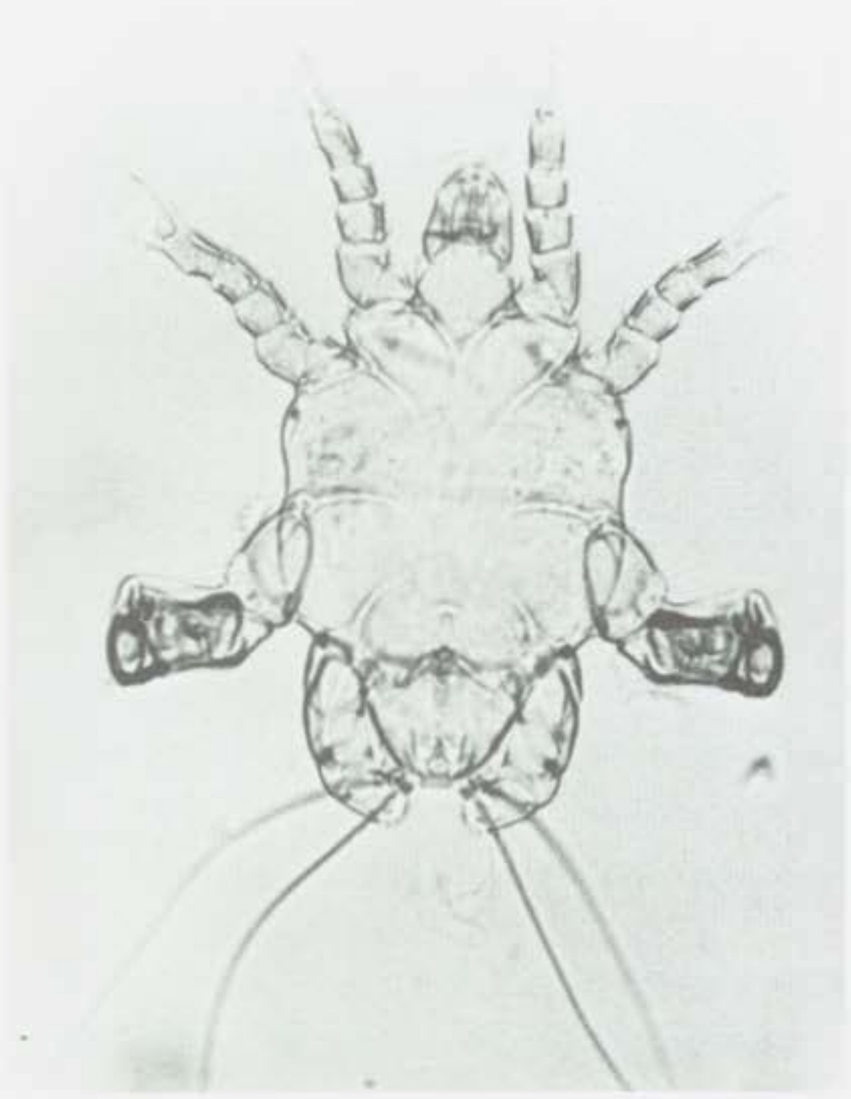

Figure 7 Myocoptes sp. male

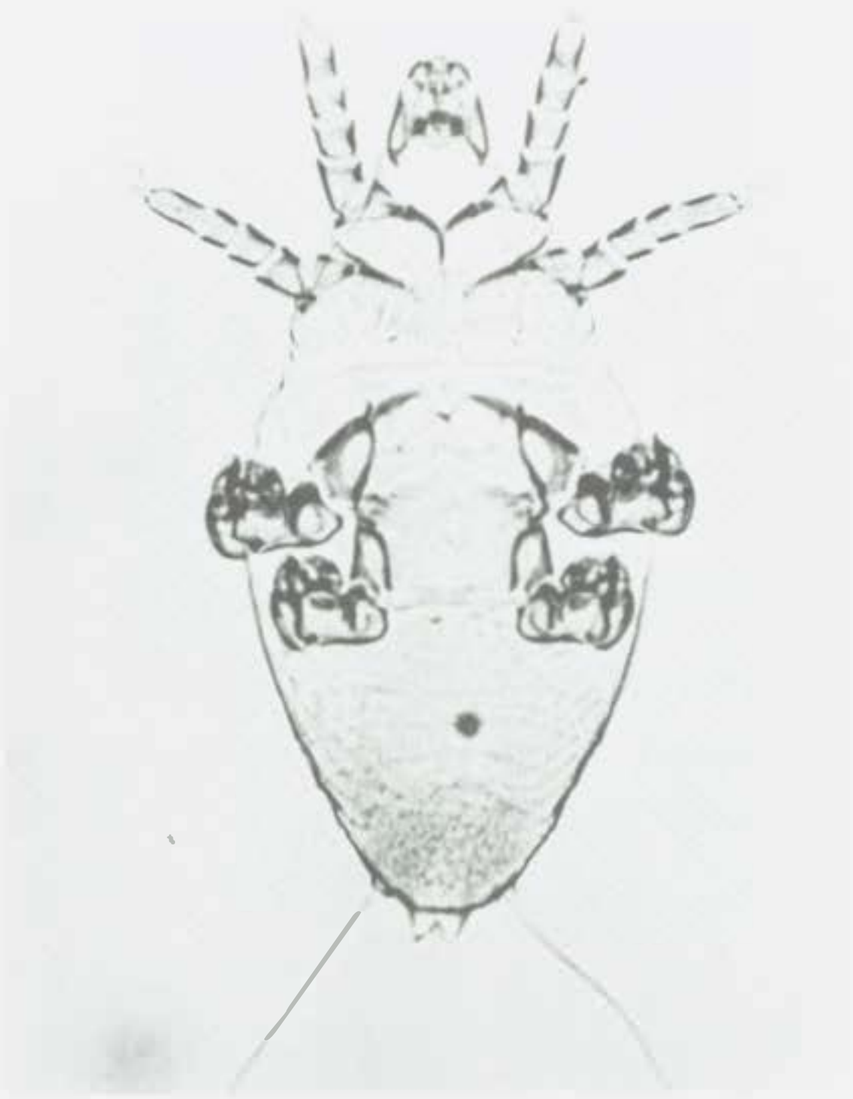

Figure 8 Myocoptes sp. female

Control

Further studies have been made concerning the methods of application, effectiveness, and toxicity of Aramite-15W.*

Methods of application Different methods of dipping have been compared. It appears that any method is effective that includes submerging the animal and completely wetting the hair and skin with acaricidal solution.

Effectiveness Previous reports[2,3] have indicated that one application of 2% Aramite-15W (with Nacconol** 1:1000) was apparently completely effective for the myobiid and myocoptid mites.

CF #1 female mice, over one year of age, dipped once, twice, or three times at weekly intervals or not at all, were examined 90 days after dipping. All non-dipped mice showed thin hair and skin lesions and were found to be heavily infested with myobiid and myocoptid mites. Two-thirds of those dipped once showed no clinical symptoms but were found to harbor small numbers of myocoptid mites. Of the mice dipped two or three times, none showed clinical symptoms or the presence of myobiid or myocoptid mites.

In another group of 100 mice (CAF_1, male and female, 16 months old), 50 were dipped twice and 50 were not dipped. Six months after dipping, sample mice from each group were examined. All the dipped mice were found to be free of pilicolous mites while the controls were heavily infested.

Apparently a few mites may survive one dipping but none survive two dippings.

Clinical Trials The treatment of mice showing lesions attributed to myocoptid mites has been consistently gratifying. In almost every case the hair coat has returned to normal in about 30 to 60 days.

The treatment of mice showing severe facial lesions has not been successful. In most cases, even though mites were no longer present, the lesions failed to heal. Prophylactic treatment at about 60 days of age appears to be more successful. Extensive studies have been initiated in conjunction with the Gamma Ray Toxicity Program. All mice used for these studies are now being predipped twice at about 60 days of age. Post-mortem records of the skin lesions of all those not dipped previously will be kept and compared with similar records of those now being dipped.

---

*Active ingredient 2-(p-tert-butylphenoxy) isopropyl-2-chloroethyl sulfite. Naugatuck Chemical Co.

**Wetting agent manufactured by National Aniline Division, Allied Chemical and Dye Corp.

Toxicity Fifty CAF_1 male and female mice about 16 months of age were dipped twice, and 50 similar mice as controls were not dipped. At six months after dipping, 19 of the dipped animals and 19 of the non-dipped controls had died.

One hundred and five CF #1 female mice 7-8 weeks of age were treated with 1,2,3, and 4% solutions and 30 similar mice were used as controls. At 250 days only 9 animals have died and no conclusions can be made.

Experiments are currently under way to determine the additive toxicity of X-irradiation plus dipping in Aramite-15W.

References

1. Flynn, R. J., and B. N. Jaroslow. 1955. Murine mange control program. Quarterly Report, Biological and Medical Research Division, Argonne National Laboratory. ANL-5378, pp. 182-186.

2. Flynn, R. J. 1955. Mouse mange II. Acaricide screening experiments. Quarterly Report, Biological and Medical Research Division, Argonne National Laboratory. ANL-5426, pp. 167-169.

3. Flynn, R. J. 1955. Mouse mange III. Effectiveness and toxicity of Aramite-15W. Quarterly Report, Biological and Medical Research Division, Argonne National Laboratory. ANL-5426, pp. 170-173.

4. Flynn, R. J. 1954. Mouse mange. Proc. Animal Care Panel, pp. 96-105.

5. Flynn, R. J., and B. N. Jaroslow. 1955. Nidification of a mite (Psorergates simplex Tyrrell, 1883: Myobiidae) in the skin of mice Quarterly Report, Biological and Medical Research Division, Argonne National Laboratory ANL-5486, p. 13.

NIDIFICATION OF A MITE (PSORERGATES SIMPLEX TYRRELL, 1883: MYOBIIDAE) IN THE SKIN OF MICE

Robert J. Flynn and Bernard N. Jaroslow

When skin flaps were reflected during surgical procedures in mice, small whitish areas on the inner aspect of the skin were observed[1] (Figure 9). Microscopic section showed these areas as pouches in the skin. Dissection of a pouch from unfixed skin revealed the presence of mites that were subsequently identified by Dr. E. Baker of the U. S. Department of Agriculture, as Psorergates simplex Tyrrell, 1883. Other investigators[2,3] have reported the occurrence of these nodules. In this investigation we studied different stages in the process of nidification.

Pouches were found in the skin on all parts of the body - over the legs, back, thorax, abdomen, shoulders, and particularly the head. The largest pouches, up to 2 mm in diameter, were found on the back of the neck where the skin is loose, and where growth of the pouch is not restricted by pressure. Conversely, on the legs and face where the skin is tight, most of the pouches observed were small. When a nest was incised and the contents expressed, mites (Psorergates simplex) in all stages of development were observed (Figure 10).

In section, the nest is seen as an invagination of the skin with normal epidermis continuous with the outside. It develops from a punctate invagination of the epidermis containing one or few mites (Figure 11), to a large flask-shaped pouch full of mites and debris (perhaps sloughed, cornified epidermis) as depicted in Figures 12 and 13. In the large nest shown in Figure 13, comparable in size to those in Figure 9, the epidermis was continuous and normal in appearance along the lateral borders, but compressed along the fundus of the pouch which was deep in the sub-cutis. At this stage, the opening was quite large and the mites could freely migrate or be accidently expressed out of the nest.

An encysted nest is shown in Figure 14. The lumen was lined with a layer of connective tissue and no trace of epidermis remained. The cyst had no orifice and a marked invasion by inflammatory cells was in progress. Figures 15 and 16 are enlargements of a portion of the normal pouch in Figure 13 and the cyst in Figure 14, respectively. In the former, the epidermal lining was intact and normal and no inflammation was seen. In the latter, the epidermis had been replaced by connective tissue and inflammatory cells had penetrated well into the cyst.

The life cycle of the mite apparently is completed in the nest as indicated by the presence of all stages of the cycle in any fair-sized pouch. They may feed on the detritus in the nest which appears to be cornified epidermis which has sloughed off the walls of the pouch. The relatively large size of

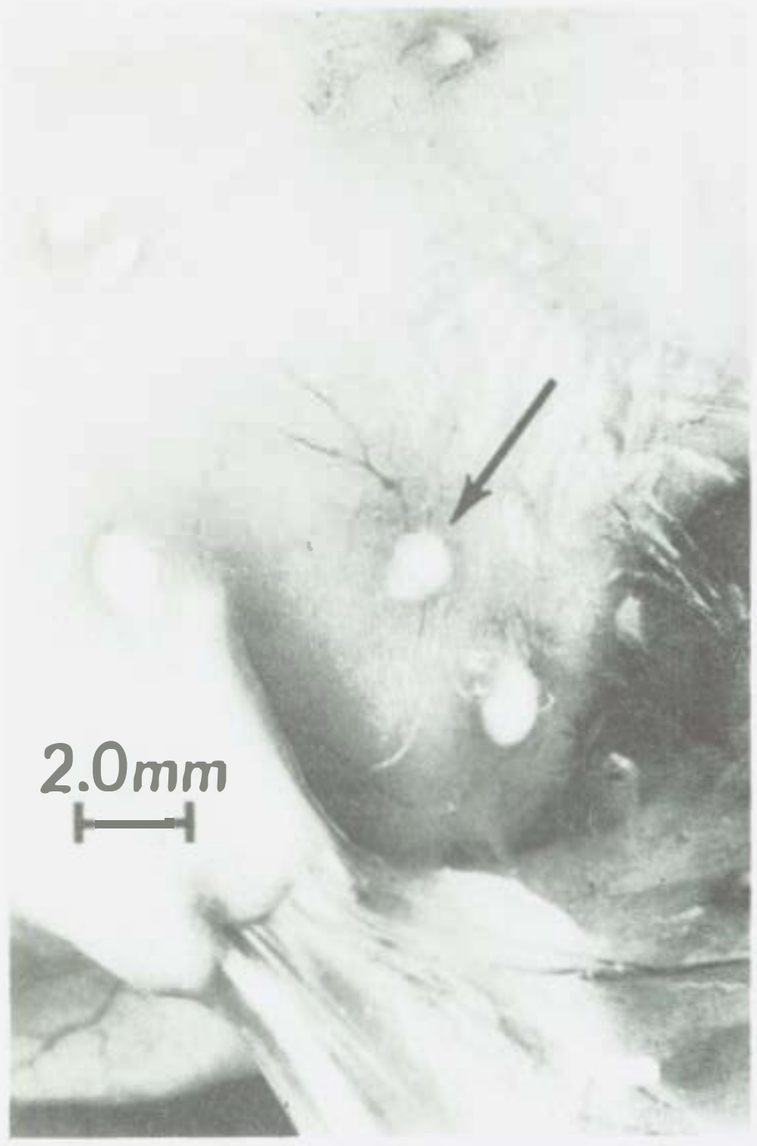

Figure 9 Inner aspect of mouse skin showing macroscopic pouches (arrow).

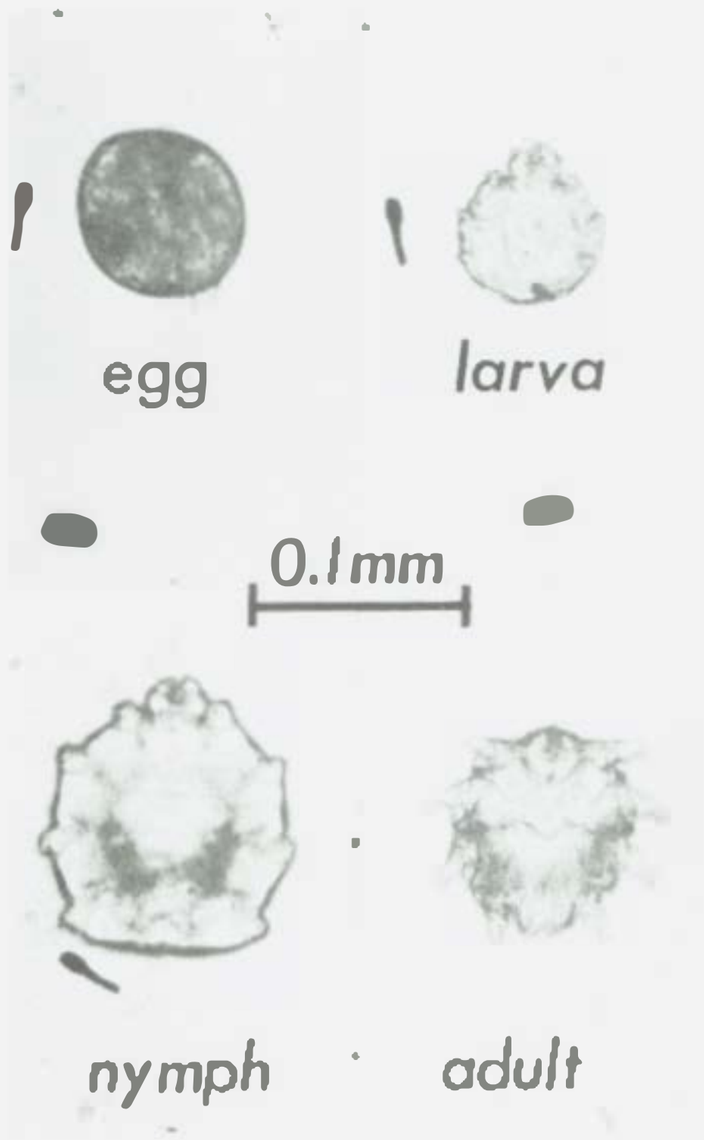

Figure 10 Various stages obtained from one pouch.

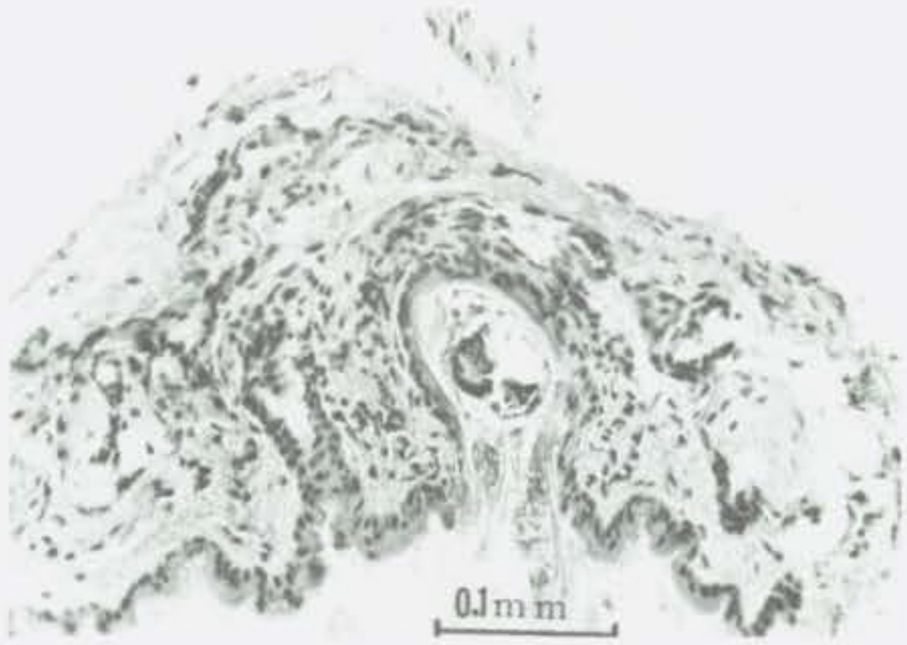

Figure 11 Early pouch. Note the normal appearance of the epidermis around the lumen and its continuation with the external epidermis.

Figure 12 Pouch filled with mites and debris. Considerably larger than early pouch. Epidermal lining still intact and normal.

Figure 13 Pouch like that in Figure 12 but considerably larger.

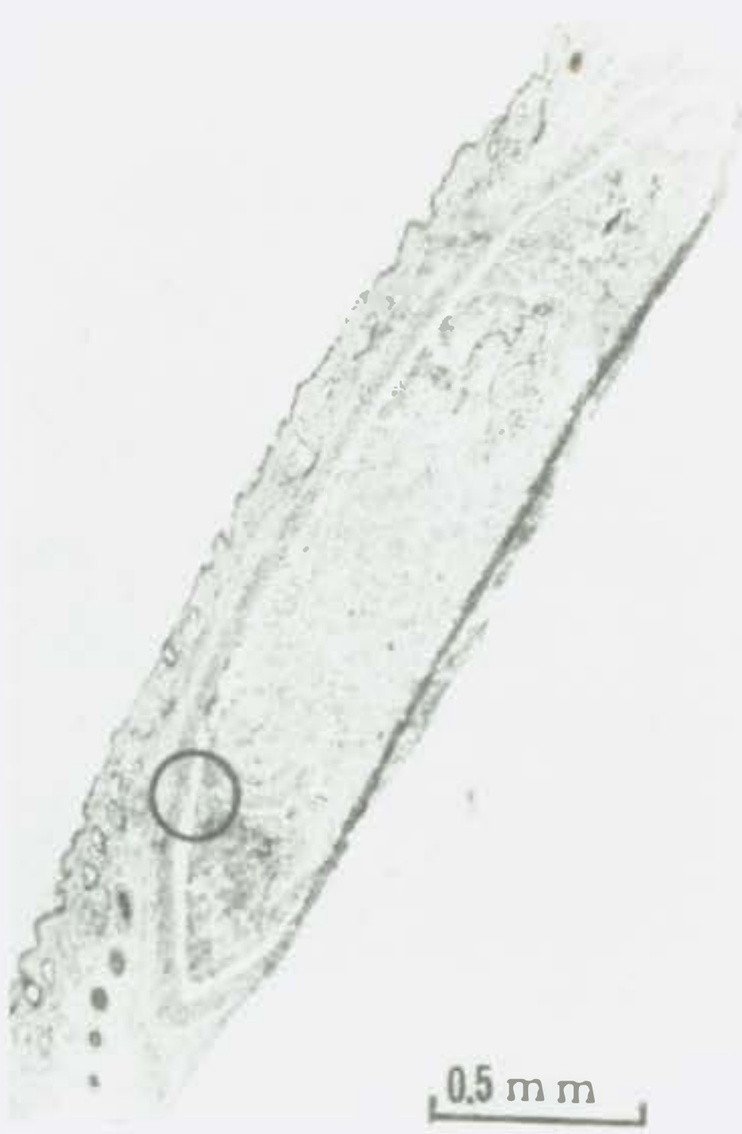

Figure 14 Encysted pouch. No orifice.

Figure 15 Magnification of circled area of Figure 13. Note normal epidermal lining and complete absence of inflammatory exudate.

Figure 16 Magnification of circled area of Figure 14. Note connective tissue lining around nest. Depth of penetration of inflammatory cells around periphery very clearly delineated.

the opening in the typical nest (Figure 13) permits ready escape either by chance movements or accidental expulsion. Colonization may occur as the result of the entry of a wandering gravid female into another hair follicle. It is likely that exchange of hosts takes place through contact.

References

1. Wassermann, F. 1951. Personal communication.

2. Piana, G. P. 1886. Cisti cutaneo contenenti acari nei topi. Ann. Scuola Med. Vet., 1, 122. (Cited by Neumann (1893).)

3. Neumann, M. G. 1893. Sur un acarien (Psorergates simplex Tyrrell) de la souris. Bull. Soc. Hist. Nat. Toulouse, 27, 13-21.

PROGRESS REPORT: BIOLOGICAL EFFECTS OF COSMIC RADIATION

Howard Walton, Jr.

By the use of high-altitude balloons, samples may be exposed directly to primary cosmic radiation. Since the properties of this radiation are not precisely known and cannot be duplicated under laboratory conditions, information on responses of biological samples so exposed is desirable.

Through the courtesy of Col. John M. Talbot and with the collaboration of Lt. C. H. Steinmetz, U.S.A.F., several exposures have been completed on a variety of plant and animal materials of diverse radiosensitivities and the materials are now being studied. The initial survey involves about 25,000 organisms; results will be reported as they become available.

PREVIOUS HYPOTHESES OF CELL DIVISION IN MICROORGANISMS

Herbert E. Kubitschek

In an earlier report[1] we indicated that the interdivision times of mother and daughter cells of E. coli were uncorrelated. However, this is not the case for sister cells, for which the correlation coefficient is significant at less than the 0.1% level. These observations are in agreement with the work of Powell[2] on six other species of bacteria (B. aerogenes, B. coli anerogenes, S. faecalis, P. vulgaris, B. mycoides and B. subtilis) and with the work of Burns[3] on yeast (saccharomyces cerevisiae). They indicate conclusively that the previous hypotheses of Rahn[4] and Kendall[5] are untenable for all of these microorganisms since they assume all divisions to be independent of one another.

Burns' work provides further proof of the invalidity of their hypotheses for yeast, since he has measured the mean division time and the standard deviation for a diploid strain of yeast at three temperatures, 20°C, 30°C, and 38°C. The coefficients of variation CV and their standard deviations σ_{CV} at these temperatures are shown in Table 3.

Both hypotheses predict a frequency distribution dependent upon two parameters, only one of which can be temperature-dependent. Furthermore, the temperature-dependent parameter is always coupled to the independent variable. Thus, according to these hypotheses, a change in temperature should give a linear transformation of the frequency distribution. But it can be shown that the coefficient of variation should remain constant. Table 3 shows that this is not the case. On this basis the chance that either Rahn's or Kendall's hypotheses could be correct is less than 1%.

Table 3

Statistical parameters for diploid yeast

Temperature, °C	CV	σ_{CV}
20	.93	.096
30	.90	.075
38	1.67	.234

References

1. Kubitschek, H. E., and H. E. Bendigkeit. 1955. Some studies on the growth and size of bacteria. Quarterly Report, Biological and Medical Research Division, Argonne National Laboratory. ANL-5462, pp. 99-109.

2. Powell, E. O. 1955. Some features of the generation times of individual bacteria. Biometrika 42, 16-44.

3. Burns, Victor W. 1954. Physical studies of cell division. University of California Radiation Laboratory. UCRL-2812, pp. 1-95.

4. Rahn, O. 1932. A chemical explanation of the variation of growth rate. J. Gen. Physiol. 15, 257-277.

5. Kendall, D. G. 1948. On the role of variable generation time in the development of the stochastic birth process. Biometrika 35, 316-330.

A SIMPLE MICROPIPETTE PULLING DEVICE

Edward W. Daniels

Micropipettes with microtip measurements in the range of 1 to 3 μ I.D. and 2 to 5 μ O.D. have been made conveniently with the device shown in Figure 17. This micropipette puller was made from a glass tube, a lead pencil, 3 rubber bands and a metal pin 3 cm long.* A hole was made through one end of the glass tube at right angles to the lumen. Both ends of the pencil were cut off and 2 holes (1.2 mm) were drilled through it, the first 1 cm and the second 2.5 cm from the exposed end. The metal pin was placed through the latter hole. A notch was sawed halfway through the side of the pencil at approximately 1 cm from the opposite end. A rubber band was hooked into this notch, and the notch end of the pencil was inserted into the glass tube until it was stopped by the metal pin. The free end of the rubber band was then drawn out through the hole in the glass tube and secured under slight tension by wrapping around the tube. A second rubber band was wound around the pencil at the point of insertion of the metal pin to prevent chipping of the glass. A third rubber band was placed around the exposed end of the pencil to hold the capillary.

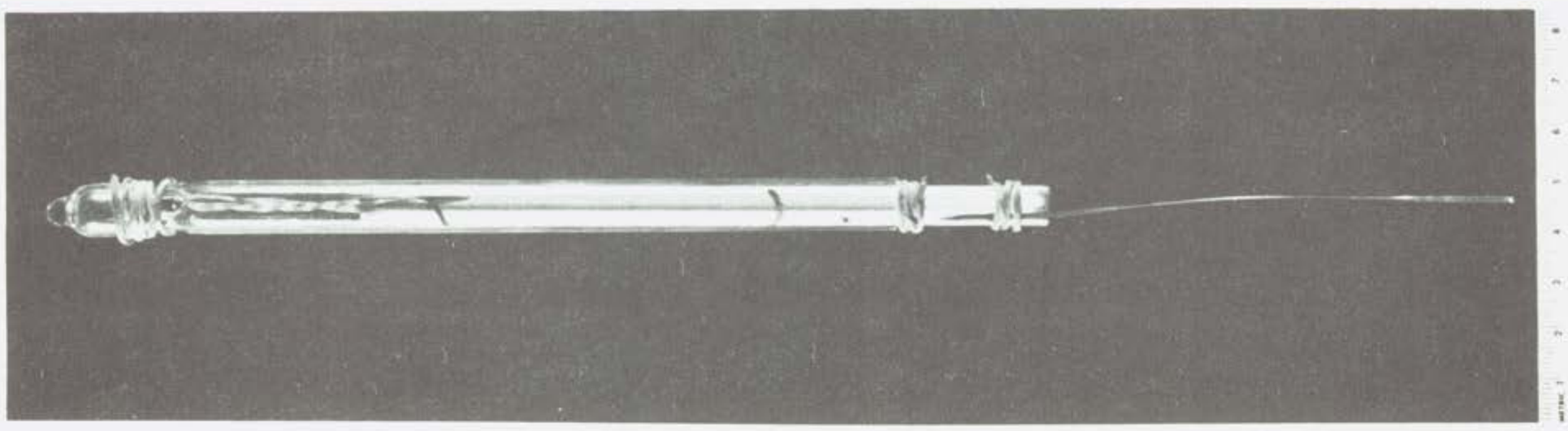

Figure 17 Micropipette pulling device

To operate the device, a thin-walled glass capillary tube (0.7 to 1 mm O.D.) is broken off into lengths of some 15 to 20 cm. One end of a length of tubing is held over a microflame until an L is formed. The short arm of the L is then put into the hole at the free end of the pencil and the long arm is fitted into a groove sawed along the side to accommodate it; the third rubber band is then slipped over the glass capillary to keep it in the groove. The free end of the capillary is held by the thumb and finger of one hand and the pipette puller is held in the other hand,

---

*For dimensions, note scale at left border of Figure 17.

while tension is placed on the capillary as it is passed through a gas Bunsen flame. As the capillary is pulled out, the first step is completed (Figure 17). The capillary is then passed through a gas microflame while the lumen and outside dimension are further reduced. A second or third pass through the microflame will complete the pulling of the pipette.

The micropipette is then observed under the dissecting microscope and discarded if the lumen is closed. If it appears open, the end opposite the microtip is placed on a small amount of modeling clay mounted on a slide. The microtip is then examined further and measured with a compound microscope. after which it may be cut off with sterile scissors at a point where the diameter is appropriate for the intended use. A hot filament may be used to firepolish the tip or to bend it if desired.[1] Hot filaments are used in the de Fonbrune and Reyniers[2] instruments for the entire process of micropipette manufacture.

The writer wishes to thank Mr. Atlee S. Tracy for making the photograph.

References

1. Fonbrune, Pierre de. 1949. Technique de Micromanipulation. Monographies De L'Institut Pasteur; Masson.

2. Reyniers, J. A. 1933. Studies in micrurgical technique. J. Bacteriol. 26, 251-287.

A LIQUID MICRURGY CHAMBER

Edward W. Daniels

An experimental liquid chamber for the manipulation of microtools under high magnification has been designed which eliminates some of the problems inherent in the conventional hanging drop preparation. This chamber does not have optical distortions due to the curvature of the hanging drop surface; it is particularly satisfactory for use with phase microscopy. Motile cells are restricted in vertical movements and can be limited in movements along the horizontal plane by the insertion of stationary glass needles of the desired size and shape, exclusive of the movable microtools.

Fluid loss through evaporation is not rapid, but in some chamber types the fluid lost is constantly replaced by a reserve supply from a well which is adjacent to and connected with the area of micrurgical operation. Chambers with adjacent wells have remained exposed to the atmosphere (70° F and 40% relative humidity) from 3 to 12 hours without drying out. All parts of the chamber can be sterilized.

In its simplest form the fluid chamber is composed of a microscope slide and a No. 1 cover glass of small dimensions, i.e., a 12 mm circle or an 8 x 20 mm rectangle (Figure 18). The cover glass can be cut with a diamond pencil into the shape best suited for the experiment. Aluminum foil paper, 15 μ in thickness, was used to make 2 mm squares used as cover glass supports. If, for example, a 30 μ space was required between cover glass and slide, two thicknesses were used. The space required between the slide and cover glass is determined by the size of the cells used. The microtools can be made to satisfy the requirements of the experiment. Sterile petrolatum is used to make a firmer fit of portions of the cover glass to the slide and to reduce the area of the film edge which is exposed to the atmosphere. Following micrurgical operation, the cell can be cultured in this type of fluid chamber provided that a moist chamber cap is placed over it and sealed (Figure 18).

Figure 19 shows a similar chamber which is merely raised above the slide a few millimeters by a collar. The advantage of this is to permit more freedom for movement of the bulky part of microtools. However, in phase microscopy the greater distance between condenser and objective is a disadvantage. A solution for this is to cut a large hole in the center of a wide slide and to support the fluid chamber on an inverted cone with the apex cut off. The difficulty can also be obviated by using a U-shaped slide with a bridge across, the bridge being made from another slide or coverglass and supported at each end by a column several millimeters in height. The fluid chamber is mounted on the bridge. The condenser is adjusted so that it can be placed above the microscope stage between the arms of the U-slide.

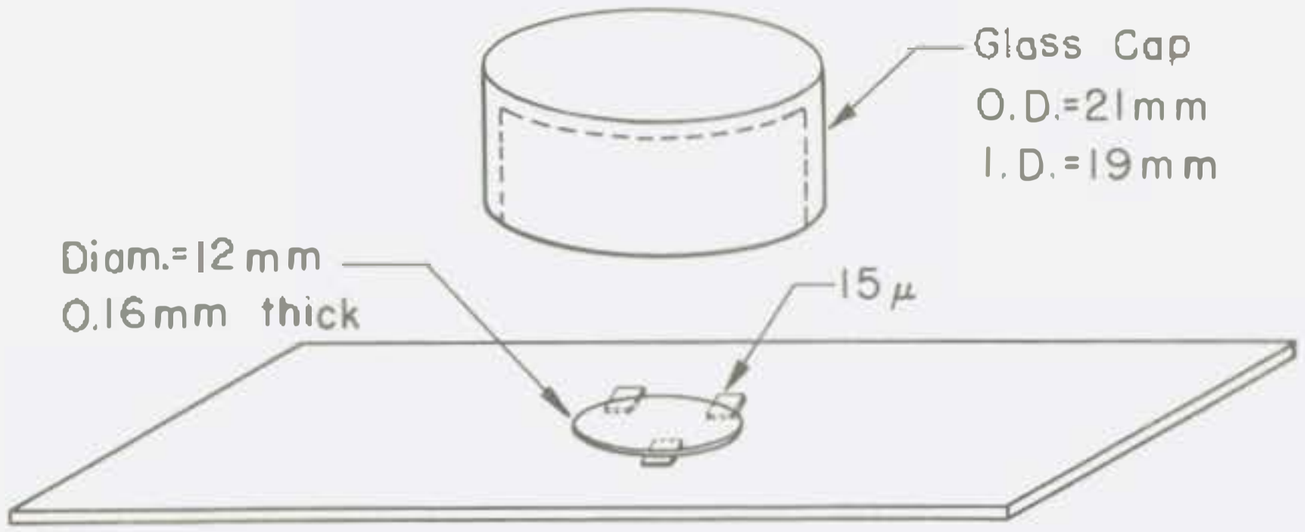

Figure 18

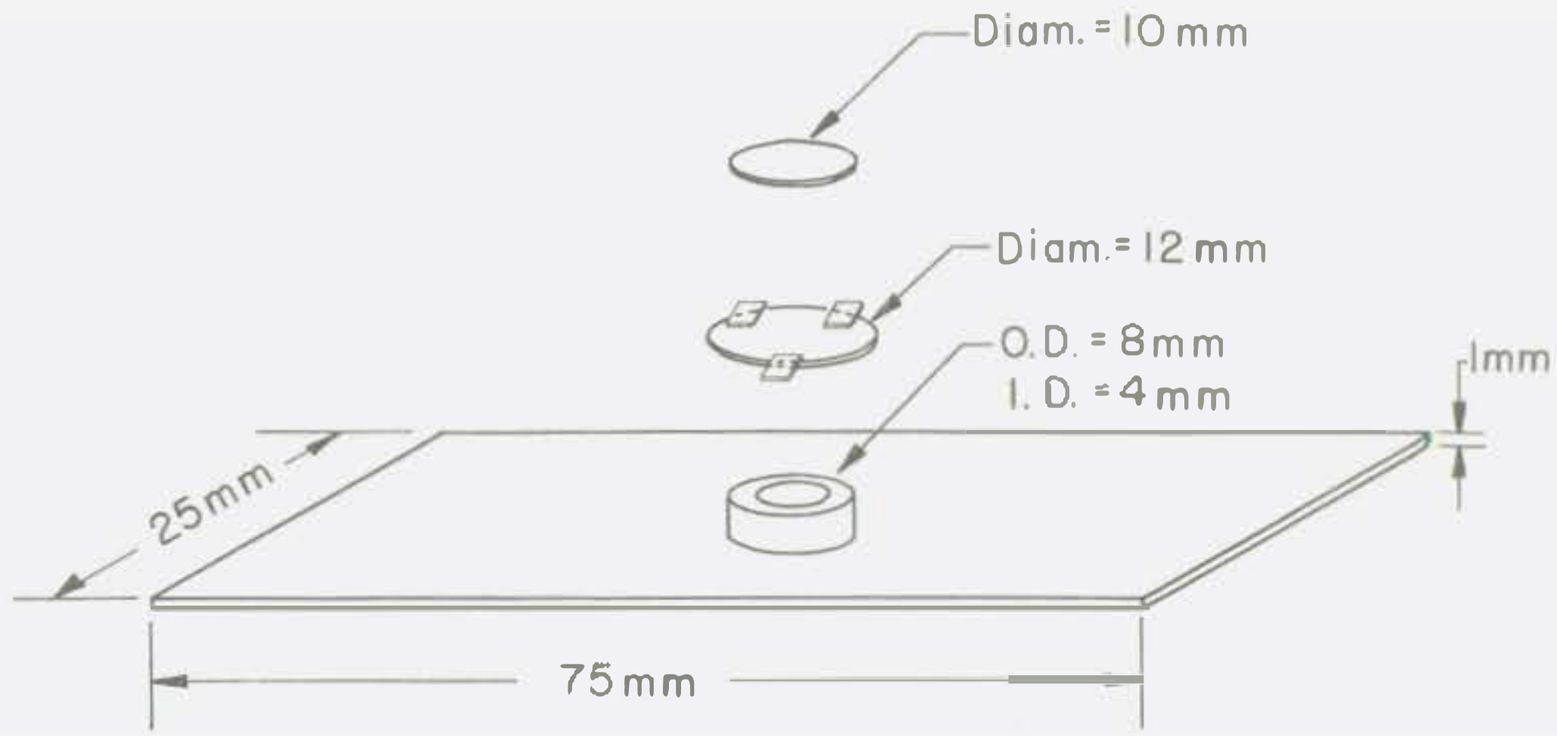

Figure 19

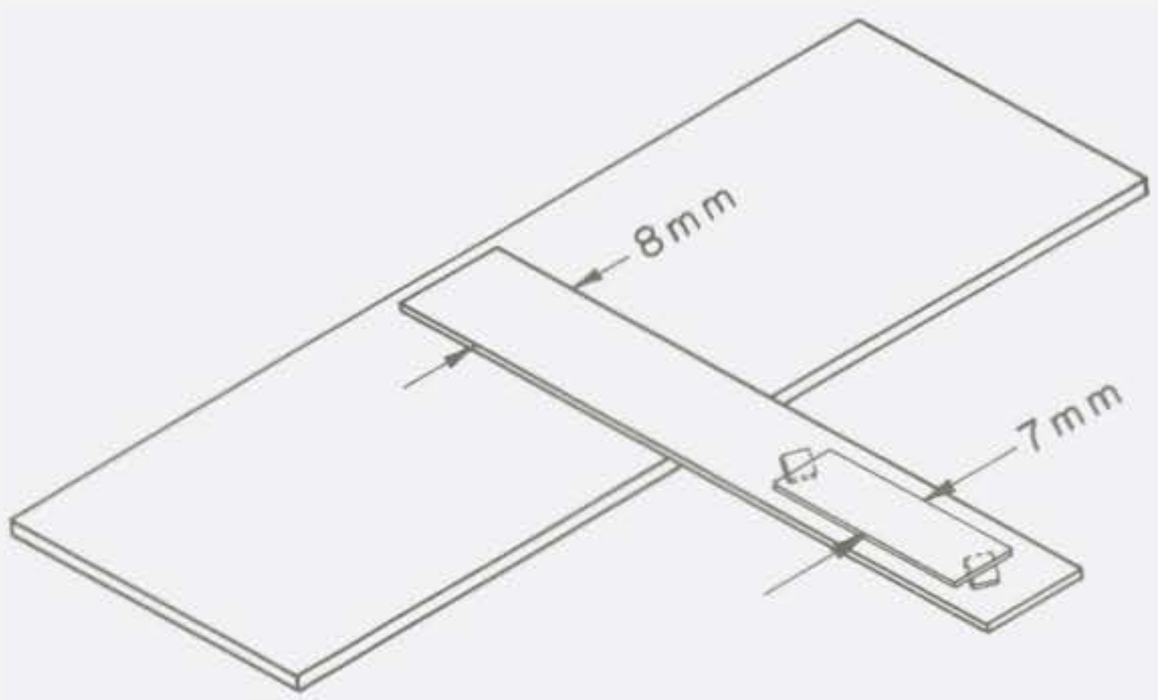

Figure 20

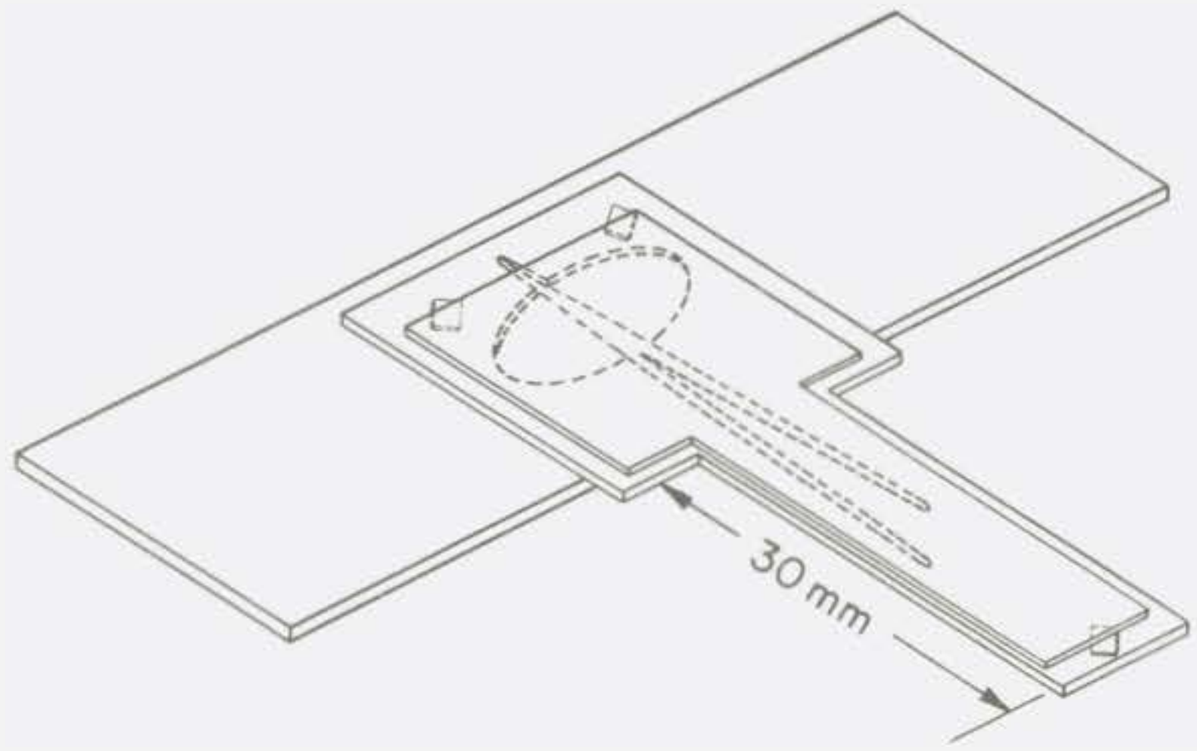

Figure 21

Figures 20 and 21 represent types of fluid chambers which permit sufficient space for microtool shank movement without sacrifice of the advantages of phase microscopy. These chambers are modifications of the more bulky U-shaped chamber type just described. To construct the type shown in Figure 20, a No. 1, 24 x 50 mm cover glass cut lengthwise into halves or thirds is used as a support. Petrolatum is put on one end and pressed between the cover glass and a slide. A rectangular cover glass is then cut so that it is about 1/3 the length of the cover glass support and about 1 mm less in width. This type of chamber (Figure 20) will suffice for certain purposes, such as the isolation of microorganisms. Its advantages are its thinness and the fact that it can be broken off near the slide. The fluid chamber can then be dropped into sterile media. This is analogous to the practice of breaking off the microtip of a micropipette following removal of one microorganism.[1] The experimental cell can then be observed and cultured in the fluid chamber provided that the entire unit is kept humidified in a Petri dish.

Figure 21 shows a fluid chamber which has a standard microscope slide as a base. A second slide is cut lengthwise with a glass saw into the form of a T. A depression well is made in the wide portion of the T and a kerf is cut which joins the depression well with the chamber. The kerf extends posterior to the well and serves as an inlet for air. Petrolatum fills the space at the edge of the cover glass, between slide and cover glass, except at the inlet and at the chamber where the microtools enter. A cover glass support of desired thickness is placed at the free base of the T, and also, if necessary, at the ends of the bar.

Reference

1. Wright, W. H., and E. F. McCoy. 1927. An accessory to the Chambers apparatus for the isolation of single bacterial cells. J. Lab. Clin. Med. 12, 795-800.

RADIOSTRONTIUM AND FELIS DOMESTICUS

Miriam P. Finkel, Juanita Lestina, and Dorice Czajka

Nine cats have been added to the family of animals comprising the radiostrontium studies. They belong to two litters that were seven or eight weeks old in May, 1953, when they were given to the laboratory, and two years old when they became a formal part of the experiment. It was decided that the best use could be made of these animals by maintaining one male and one female as untreated controls and giving the others a similar single, intravenous dose of strontium^{90} in the subacute, carcinogenic range. It was presumed that the initial response of the cat to radiostrontium would be more like that of the dog ($LD_{50/30}$ approximately 0.15 mc/kg) than the mouse ($LD_{50/30}$ 6mc/kg). For this reason the first animal was given 0.15 mc/kg of strontium^{90} in equilibrium with yttrium^{90} and observed closely for six weeks. The expected decrease in circulating leucocytes, particularly heterophils, was noted at one week after injection, but at no time did the animal appear to be seriously ill. Consequently, the remaining cats were given the same specific dose.* The variation in total dose and the distribution of litters and sexes can be seen in Table 4.

Table 4

Strontium^{90} cats

Animal number	Litter number	Sex	mc/kg	Total μc
202	2	Male	0.15	546
251	2	Female	0.15	368
254	1	Female	-	-
255	1	Female	0.15	357
256	1	Female	0.15	378
257	1	Male	0.15	588
258	2	Male	-	-
259	2	Male	0.15	504
280	1	Male	0.15	557

* We are indebted to Robert Flynn for injecting the radiostrontium and also for facilitating the handling of these animals by surgically removing their claws.

Peripheral blood samples taken from a marginal ear vein prior to isotope administration gave average values for the nine animals as follows: hemoglobin--13.7 grams % (range 11.6 - 17.4), leucocytes--9811/mm^3 (6300 - 13,400), heterophils--5142/mm^3 (2931 - 7446), lymphocytes--3884/mm^3 (2738 - 5720), eosinophils--756/mm^3 (126 - 1206), and monocytes--29/mm^3 (0 - 106). The response to radiostrontium can be seen in Figure 22, where the averages for the treated animals have been plotted. Although there was some variation among individuals and minimum values are masked by averaging, these curves adequately represent the course of events. The average values obtained 91-98 days after injection were only slightly greater than those observed at 70 days.

Figure 22 Average peripheral blood counts of strontium^{90} treated cats

Cat #251 refused food on the 21st day after injection, failed to respond to friendly overtures, and sat quietly in a corner of the cage. A peripheral blood sample showed 8.7 grams % hemoglobin and 1700 leucocytes/mm^3, of which only 255 were heterophils. Daily doses of 300,000 units of penicillin were given for the next two weeks with the hope of keeping the animal free of infection during this extreme depression of

Table 5

Radiostrontium content of cat #251
(0.15 mc/kg (368 μc)) at 40 days

Organ	μc/gm	Estimated Total μc
Spleen	.001	.004
Liver	.001	.10
Kidneys	.001	.02
Gastrocnemius muscle	.001	.01
Heart	.001	.01
Lung	.003	.04
Larynx	.004	.006
Trachea	.007	.01
Caudal vertebrae	.30	5.37
Feet	.33	11.89
Lumbar vertebrae	.45	21.31
Thoracic vertebrae	.52	16.51
Cervical vertebrae	.57	12.44
Pelvis and sacrum	.59	22.04
Radii and ulnae	.65	8.49
Tibiae	.70	12.22
Mandible	.75	5.07
Femora	.79	15.60
Humeri	.83	13.95
Cartilaginous ribs	.87	9.06
Scapulae	.97	10.69
Bony ribs	1.19	18.49
Sternum	1.24	3.17
Parietal bone	3.25	-
Skull (minus the mandible)	(.75)	65.70
Total		252.20

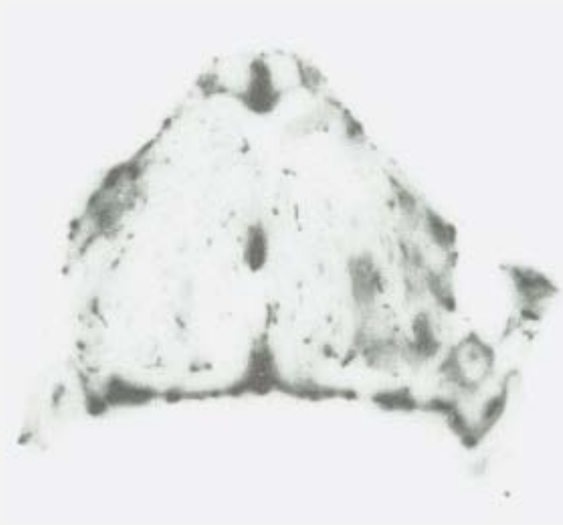

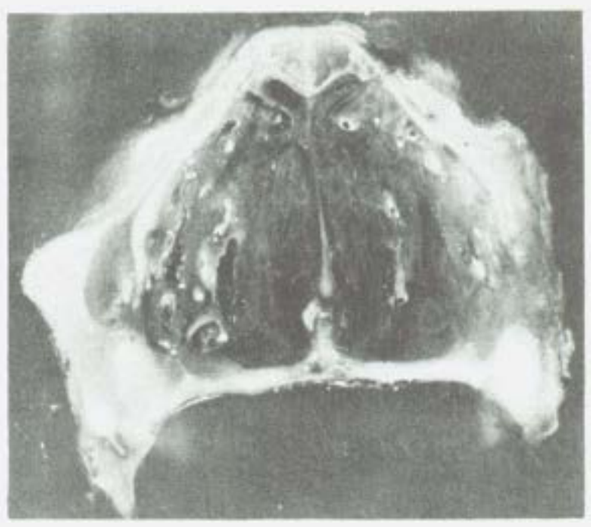

Transverse section through face x-1.25

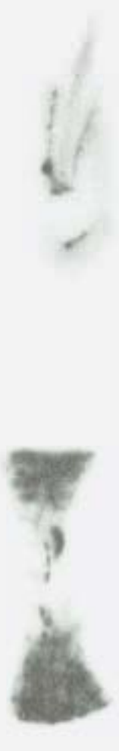

Tooth x-1.66

Sternum x-2.0

Femur x-1.56

Cartil. rib
x-1.18

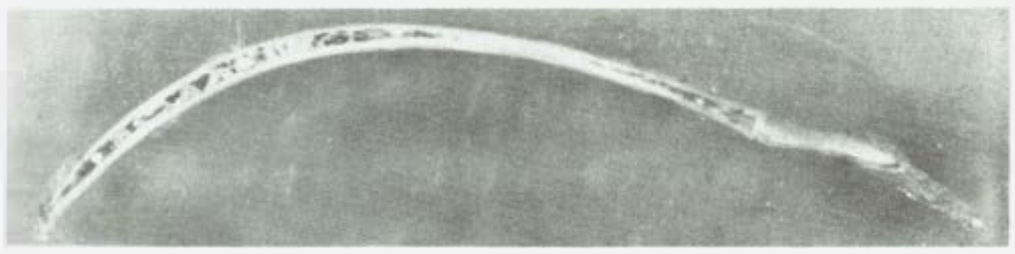

Bony rib
x-1.21

Figure 23 Specimens and autoradiograms of skeletal parts of cat #251

hematopoietic activity. Although the white count increased to 3185 cells/mm^3. of which 1019 were heterophils, hemoglobin values continued to fall, and 4.4 grams % were recorded on the 35th day after injection. Forced feeding and the subcutaneous injection of 120 cc of saline and 10 cc of serum on the 39th and 40th days proved of little value, and the animal died. Autopsy revealed multiple subcutaneous hemorrhages extending from the face to the tip of the tail and ranging in size from pin-point to 1 cm. The site of saline injection was surrounded by a hemorrhagic area 6 cm in diameter. The immediate cause of death appeared to be hemorrhages of the cardiac wall which produced a hemopericardium and tamponade. Except for a few inconspicuous petechiae in the small intestine, the other viscera were free of hemorrhages.

Representative samples of most of the viscera and approximately half of the skeleton of cat #251 were analyzed for strontium^{90}; the results are given in Table 5. It is interesting that the cartilage of the respiratory system and that of the skeleton displayed such diverse affinity for radiostrontium; although the concentration in the larynx and trachea was only 4 and 7 times, respectively, the concentration in the soft tissues, it was as great in the cartilaginous portion of the ribs as in the skeleton as a whole. The greatest specific activity was found in a small sample of the parietal bone. In estimating the total body content of radiostrontium, this value could not be taken as representative of all the skull bones; instead it was assumed that the specific activity of the entire skull was equal to that of the mandible. No addition was made for the radiostrontium content of the skin or skeletal muscle since the amount in these organs was insignificant. The estimated body burden of 252 μc (68.5% of the injected dose) was considerably greater than anticipated.

Autoradiograms of selected bones were prepared by exposing photographic film to the specimens embedded in Scotchcast. These have been reproduced in Figure 23, where it can be seen that greater darkening occurred over trabecular bone and bone marrow than over dense, cortical bone. Note the relatively homogeneous distribution in the cartilaginous rib in contrast to the irregular distribution in the bony rib.

COUNTING STABILITY IN LIQUID SCINTILLATION SYSTEMS

Walter E. Kisieleski and Frank Smetana

The photomultipliers used in liquid scintillation systems give large and variable numbers of small thermionic noise pulses which contribute significantly to the background count. Since the thermionic pulses are of essentially the same amplitude as the beta pulses, they cannot be eliminated by pulse height selection as they can in gamma counting. To eliminate these thermionic pulses it is necessary to cool the photomultipliers; this is accomplished by containing the counting chamber in a freezer chest at -10° C.

Under these conditions it became necessary to evaluate the effect of cooling time (as influenced by the type of container) on the stability of the observed counting rate.

Tritium as water was used for the study. The samples were prepared by adding 1 ml. of tritiated water to 15 ml. of absolute alcohol. This mixture was added to 35 ml. of the scintillation solution (2 mg. of 2,5-diphenyloxazole per ml. of toluene). The samples, which had been prepared in the light and at room temperature, were then placed in the counting chamber and a continuous recording was made of the counting rate over an extended period of time.

The types of containers which were evaluated were: (1) Pyrex vials with cork stoppers. (2) Pyrex bottles with plastic screw caps and (3) sealed Pyrex vials. The results are shown in Figure 24.

In general the counting rate increases for a short time until a limited plateau period is reached. This is then followed by a slight continual decrease in the counting rate.

The Pyrex vial with the cork stopper exhibits the shortest rise time as well as the shortest stable counting period. The sealed Pyrex vial, on the other hand, has the longest rise time and the longest and most stable counting period. Corked vials are quite satisfactory for the rapid counting of the samples under the conditions of this system, provided that the sample is cooled for 20 minutes and that it is counted within one hour. For the preparation of standards or for more precise measurements sealed vials are more desirable. The screw cap bottle has characteristics somewhat between the above extremes; however, it is more convenient for routine handling.

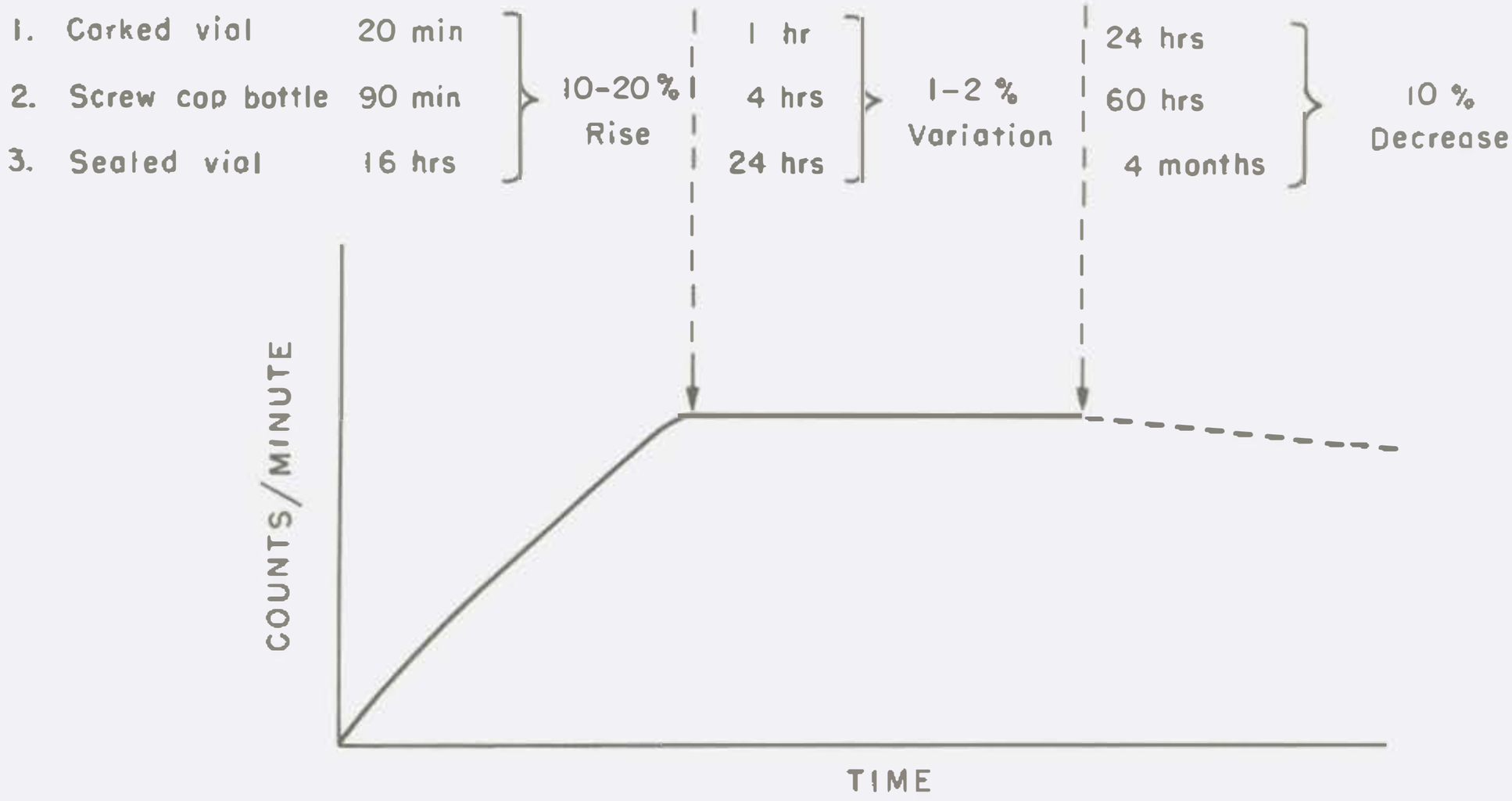

Figure 24 Effect of container and cooling time on the counting rate. Tritium as water in a toluene-alcohol mixture. Photomultipliers 1200 volts; discriminator 10 - 50 volts.

PRESUMED TOXIN IN URINE OF IRRADIATED ANIMALS

Robert N. Feinstein

In a recent series of papers [1 - 3], Burger and his colleagues claimed the demonstration of the following two phenomena. (a) Polyvinylpyrrolidone (PVP) is of therapeutic value to animals receiving a lethal dose of whole body X-radiation, and (b) the urine of irradiated, PVP-treated rats is more toxic when injected into normal rats than is the urine of irradiated, uninjected rats. The latter observation, they feel, accounts for the former; the PVP treatment causes a more rapid excretion of radiation toxin(s).

In preliminary experiments here, the effect described appeared to be erratic. Lethality of urine appeared to be much more dependent upon the concentration of the urine (i.e., the inverse of the volume of urine) than upon any treatment received. Some of the urine samples were analyzed for total nitrogen. The assumption was then made that all nitrogen represented urea, and on this basis urea solutions in water were prepared and injected in amounts comparable to the urine injections.* Such solutions proved to be as toxic as the urines. It is therefore concluded that no evidence has been produced for the existence of a radiation toxin in the urine of irradiated animals, and that the effect, if any, of PVP injection on the toxicity of urine is probably due to the water-retaining, anti-diuretic properties of the agent.

After completion of this work, a note was received from Dr. Burger, in answer to a request for reprints, saying that for reasons unknown to him, he has been unable to reproduce his results.

References

1. Burger, H., H. Grabinger, and J. Lehmann. 1954. Uber die Schutzwirkung von Periston N bei Anwendung energiereicher Strahlen. Strahlentherapie 95, 399-406.

2. Burger, H., and J. Lehmann. 1954. Strahlenschutz durch Periston N. Naturwissenschaften 41, 190.

3. Peters, K., and H. Burger. 1954. Intrazellularer Strahlenschutz durch Entgiftung mit Kollidon (Polyvinylpyrrolidon). Naturwissenschaften 41, 261-262.

---

*For this suggestion we are indebted to Dr. F. Schlenk.

PROLONGED CLOTTING TIME OF PERITONEAL FLUID AFTER X-IRRADIATION

Douglas E. Smith and Yevette S. Lewis

Shortly after the withdrawal of 2 - 3 ml of Tyrode's solution which has been injected 10 minutes previously into the peritoneal cavity of the rat or the hamster, a fibrin clot forms within the fluid. After exposure of the animal to total-body X irradiation clot formation in this fluid is greatly retarded (Table 6). The addition of protamine sulfate to such fluids is immediately followed by clot formation.

The findings indicate that X irradiation induces the liberation in the peritoneal cavity of an anticoagulant with heparin-like properties. It is possible that the anticoagulant may come from the tissue mast cells in the serous membranes of the peritoneal cavity, since these cells probably contain heparin[1] and undergo widespread disruption at the time when the clotting defect is present.[2]

Table 6

Influence of total-body X-irradiation upon clotting time of peritoneal fluid

Hamster		Rat	
Treatment	Clotting time (minutes)*	Treatment	Clotting time (minutes)*
Control	2	Control	<1
	1		1.5
	0.5		2.5
	1	3 days post 1200 r	>13
	1		>10
	2		
	0.5	4 days post 600 r	>15
3 days post 1200 r	>120		> 8
4 days post 1200 r	> 10		4
5 days post 1200 r	4		4
	> 10		
	> 12		

*These values are from individual animals.

References

1. Jorpes, J. E. 1946. Heparin, 2nd ed., Oxford University Press.

2. Smith, D. E., and Y. S. Lewis. 1953. Effects of total-body X-irradiation on the tissue mast cell. Proc. Soc. Exptl. Biol. Med. 82, 208-212.

THE BIOSYNTHESIS OF METHIONINE IN NORMAL BACTERIA AND IN ULTRAVIOLET-INDUCED METHIONINE MUTANTS

Stanley K. Shapiro

The utilization of homocysteine and methylmethionine sulfonium salt (MMS) for the biosynthesis of methionine in growing cells and in cell-free extracts of Aerobacter aerogenes has been reported previously.[1] In order to determine the distribution of this reaction in other micro-organisms, similar studies have been undertaken with several additional groups of bacteria which require methionine for growth. The organisms tested so far include Streptococcus faecalis, Lactobacillus arabinosus, Lactobacillus casei, Leuconostoc mesenteroides, Escherichia coli W (2 methionine-requiring mutants), Escherichia coli B (2 methionine-requiring mutants), Escherichia coli K_{12} (2 methionine-requiring mutants), and Aerobacter aerogenes 199 (4 methionine-requiring mutants).

None of these bacteria will grow when homocysteine or MMS alone is substituted for methionine. With the exception of L. arabinosus these cultures will not utilize homocysteine and MMS to replace methionine when both compounds are added simultaneously; L. arabinosus will grow on this mixture as well as on methionine. Cell-free extracts have been obtained from wild type A. aerogenes 199 which can produce methionine from homocysteine and MMS as effectively as extracts of methionine auxotroph 68 of A. aerogenes. E. coli K_{12} yielded active extracts, but E. coli B and E. coli W have thus far failed to produce active extracts. L. arabinosus has yielded an extract of low activity.

The extracts of A. aerogenes can product methionine from cystathionine and MMS as well as from homocysteine and MMS. Typical results are summarized in Table 7.

Table 7

The biosynthesis of methionine in cell-free extracts of Aerobacter aerogenes*

Substrate	Methionine formed (μM/ml)
None	<0.1
2 μM D,L-homocysteine	<0.1
2 μM L-MMS	<0.1
2 μM D,L-cystathionine	<0.1
2 μM D,L-homocysteine + 2 μM L-MMS	2.1
4 μM D,L-homocysteine + 2 μM L-MMS	3.2
2 μM D,L-cystathionine + 2 μM L-MMS	1.5

*Reaction mixtures adjusted to pH 7.0 and incubated at 35°C for 2 hours; extract was added to give a concentration of 3 mg protein per ml mixture

In the presence of 4 μM D, L-homocysteine and 2 μM L-MMS, more than 3 μM of methionine was recovered; this is higher than the theoretical yield from a simple demethylation of MMS, and clearly supports the hypothesis that a transmethylation of homocysteine is involved. Tracer studies are planned to substantiate this more directly.

The production of methionine from cystathionine and MMS seems to support the hypothesis that cystathionine is split to yield serine and homocysteine; the latter in the presence of MMS could then be methylated to methionine:

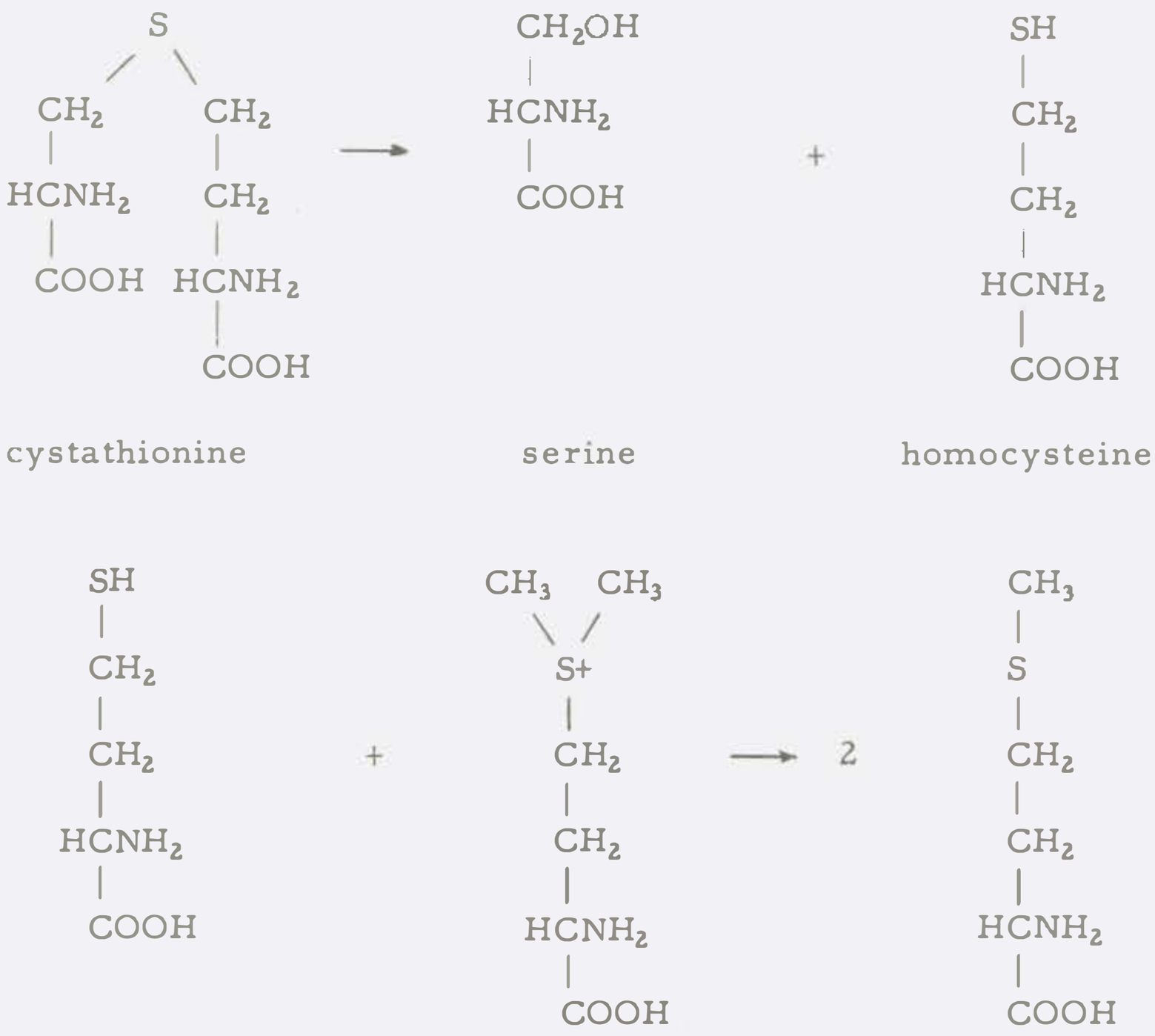

Purification of the enzymes involved should facilitate the study of the mechanism of biosynthesis of methionine in these postulated reactions. It may also be possible to gain some information on a biochemical level concerning the type of change produced by ultraviolet irradiation in the mutant cultures being studied.

Reference

1. Shapiro, S. K. 1955. The biosynthesis of methionine from homocysteine and methylmethionine sulfonium salt. Biochim. et Biophys. Acta, in press.

PRELIMINARY REPORT: ELECTRON MICROSCOPE STUDIES OF THE MORPHOLOGY OF THE GREGARINE

Harold W. Beams, Rosemarie L. Devine, and
Theodore N. Tahmisian

Up to the present time, there has been no definite description of the sporozoan symbionts found in Orthoptera. The electron microscope was employed to study the sporadin stage of Gregarina melanopli from the intestine of the grasshopper, Melanoplus differentialis, and particularly to analyze the puzzling type of biological motion of the protozoan on a morphological basis. The cell membrane forms longitudinal outpockets over the entire surface of the animal. Within the ectoplasm, a loose fibrillar network is in association with poorly-defined bands of fibers (possibly primitive or very simple myonemes), which are arranged either transversely or spirally. These apparently aid in locomotion, suggesting contractility at certain regions.

In addition, studies are being made of the nature of the endoplasm, the mode of connection of the deutomerite to the protomerite, and the mode of endwise attachment (syzygy) of the sporadins.

PRELIMINARY REPORT: THE GOLGI BODY OF THE CRICKET TESTIS

Harold W. Beams, Theodore N. Tahmisian, and Rosemarie L. Devine

The Golgi apparatus has been reported and described for many species during the last fifty years. In some cases the nomenclature has varied, but the structures described were basically comparable. In others, cytoplasmic inclusions of a variety of forms and natures - caps, spheroids. granules, networks, etc. - have all been termed the Golgi apparatus. A more recent question, aside from the controversies concerning its identification, is that of the similarity of this inclusion in the vertebrate and invertebrate cell. Gatenby[1] has discussed the problem and has proposed the homology of the Golgi apparatus of the higher vertebrates and the dictysomes of invertebrates. In an attempt to test his hypothesis, electron microscope studies of the testis of the cricket are being made in this laboratory. The earlier stages of spermatogenesis reveal that two or more dictysomes and their accompanying archoplasm are often found within one cell. Although we are lacking electron photomicrographs as yet, it is assumed that these bodies coalesce to form the single Golgi apparatus of the spermatid. This body is composed of small vacuoles and membranes arranged in dense concentric circles or portions thereof, and is thus similar to the Golgi substance of the mouse, as described by Dalton and Felix.[2] Electron photomicrographs of older spermatids demonstrate the development and deposition of the acrosomal body on the nuclear wall by the Golgi body. Since this very nearly corresponds to the origin of the acrosomal granule in the cat, as described by Burgos and Fawcett,[3] it too suggests that a similarity exists between the vertebrate and invertebrate Golgi apparatus.

References

1. Gatenby. J. B. 1955. The Golgi apparatus. J. Roy. Microscop. Soc. 74, 134-161.

2. Dalton, A. J. and M. D. Felix. 1954. Cytologic and cytochemical characteristics of the Golgi substance of epithelial cells of the epididymis - in situ, in homogenates and after isolation. Am. J. Anat. 94, 171-207.

3. Burgos, M. H. and D. W. Fawcett. 1955. Studies on the fine structure of the mammalian testis. J. Biophys. Biochem. Cytol. 1, 287-300.

DIFFERENTIATION OF CORTEX OF FROG OOCYTES

Norman E. Kemp*

A report has appeared previously on the origin and development of the formed inclusions in frog oocytes, as investigated by electron microscopy.[1] Further study of growing oocytes of Rana pipiens has revealed new details of differentiation of the cortical cytoplasm and its relationship to cells of the inner follicular epithelium. Prior to the appearance of lipochondria in the cytoplasm the plasma membranes of both oocyte and follicle cells are in close contact so that the boundary is perfectly smooth. As lipochondria develop, cortical granules appear in a peripheral layer just beneath the cortex, and the cortical cytoplasm begins to push outward in the form of microvilli. These projections protrude into the spaces formed when localized regions of the follicle cells pull away from the oocyte.

After the advent of yolk synthesis, the surface of the oocyte, in addition to forming microvilli, undergoes folding so that it appears to possess alternating ridges and valleys. The microvilli now project from the peaks of the ridges, and processes of cytoplasm from the follicle cells project into the valleys. The transfer of formed particles between follicle cells and oocyte has not been detected, but droplets appearing in the cytoplasm of the cortical ridges are interpreted as visible evidence of the transfer of nutrients from the follicle.

According to this new information the cortex has two distinct zones, (1) the basal zone which contains droplets and includes the cortical ridges, and (2) the zone of microvilli; the layer containing cortical granules is interpreted as the most peripheral part of the endoplasm. The region between the microvillous layer and the follicle cells. formerly interpreted as vitelline membrane derived from the oocyte, is in reality composed of processes of the follicular cells plus intercellular spaces. Stages of development of the vitelline membrane in older oocytes have not yet been investigated.

Reference

1. Kemp, N. E. 1954. Electron microscopy of frog oocytes. Quarterly Report. Biological and Medical Research Division, Argonne National Laboratory. ANL-5332, p. 78.

---

*Resident Research Associate from the University of Michigan.

THE USE OF GRADIENT CENTRIFUGATION FOR THE SUBFRACTIONATION OF PREPARATIONS OF CYTOPLASMIC PARTICULATES

John F. Thomson

In previous studies on intracellular enzyme distribution as determined by gradient centrifugation techniques, it was observed that the distribution of most of the enzymes studied followed a bimodal pattern; e.g., although the major portion of cytochrome oxidase and succinic dehydrogenase was associated with a peak at about 0.4μ on our semi-arbitrary scale (representing mitochondria), a significant fraction was associated with another maximum at about one-third the diameter.[1]

It was thus of interest to prepare cytoplasmic particulate fractions using a standard procedure of differential centrifugation,[2] and then to subject these preparations to further fractionation using gradient centrifugation. In this manner we hoped to establish whether or not the occurrence of so-called mitochondria-linked enzymes in the smaller particulates might be an artifact produced in the gradient centrifugation technique.

Data obtained in such experiments for succinic dehydrogenase, uricase, and cytochrome oxidase are presented in Figures 25 - 27. Three experiments have been carried out with each enzyme; although the examples chosen for the figures were the most satisfactory from a standpoint of precision and quantitative recovery, the results of the others were in essential agreement with those presented here. These data show that the subfractionation of bulk preparations yielded only a single peak; i.e., in the case of succinic dehydrogenase and cytochrome oxidase, gradient-centrifuged mitochondria showed no activity maximum associated with particles of microsome size, while both the poorly-sedimentable and the microsome fractions possessed negligible activity at 0. 4μ. It is apparent that the succinic dehydrogenase and cytochrome oxidase activities were associated with smaller particles whether gradient or bulk centrifugation was employed, and that if the microsomal activities are artifactitious, the artifacts did not arise during gradient centrifugation. The recovery of activity (curve 5 in Figures 25 - 27) is reasonably good, considering that the nuclei fraction contained appreciable amounts of the three enzymes.

Kuff and Schneider[3] had previously employed centrifugation with a discontinuous sucrose gradient to show the lack of homogeneity of their mitochondrial fraction. We have substantiated their findings by showing that on a nitrogen basis, the most active zones of subfractionated mitochondria are about 25 per cent more active than the bulk preparation in respect to succinic dehydrogenase and cytochrome oxidase, and nearly 5 times as active in respect to uricase.

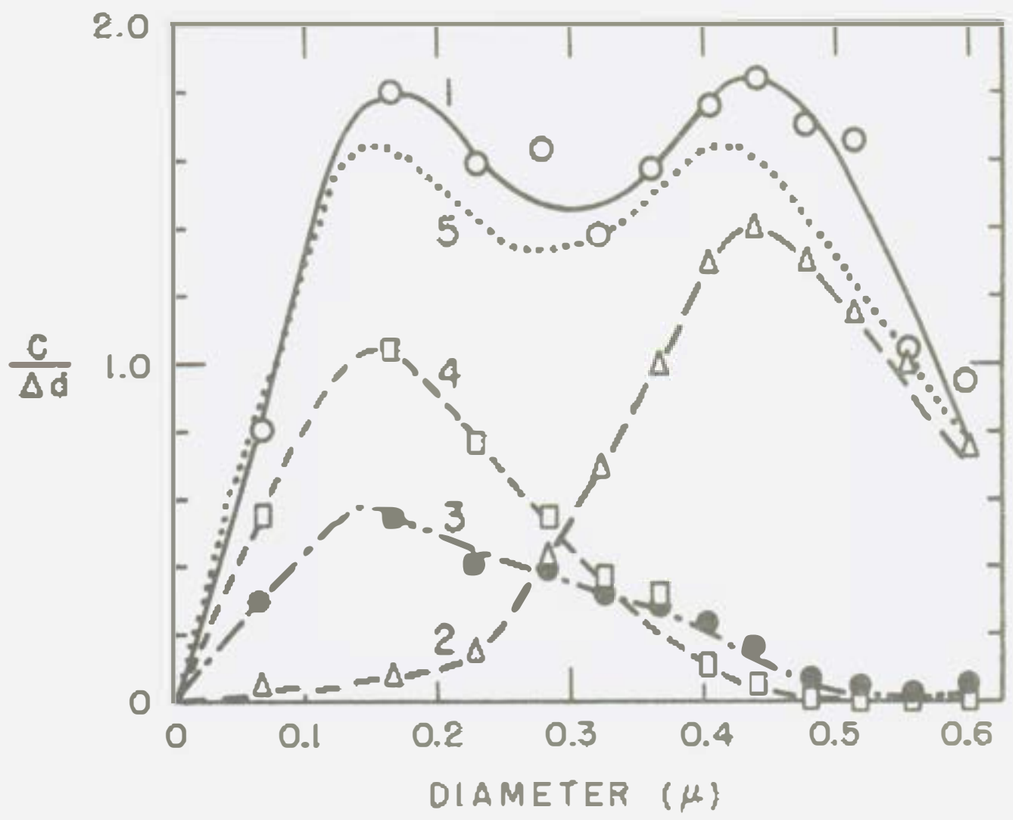

Figure 25 Distribution of succinic dehydrogenase activity of rat liver and of cytoplasmic fractions obtained therefrom. Curve 1, liver homogenate; 2, mitochondria; 3, poorly-sedimentable layer; 4, microsomes; 5, sum of curves 2, 3, and 4.

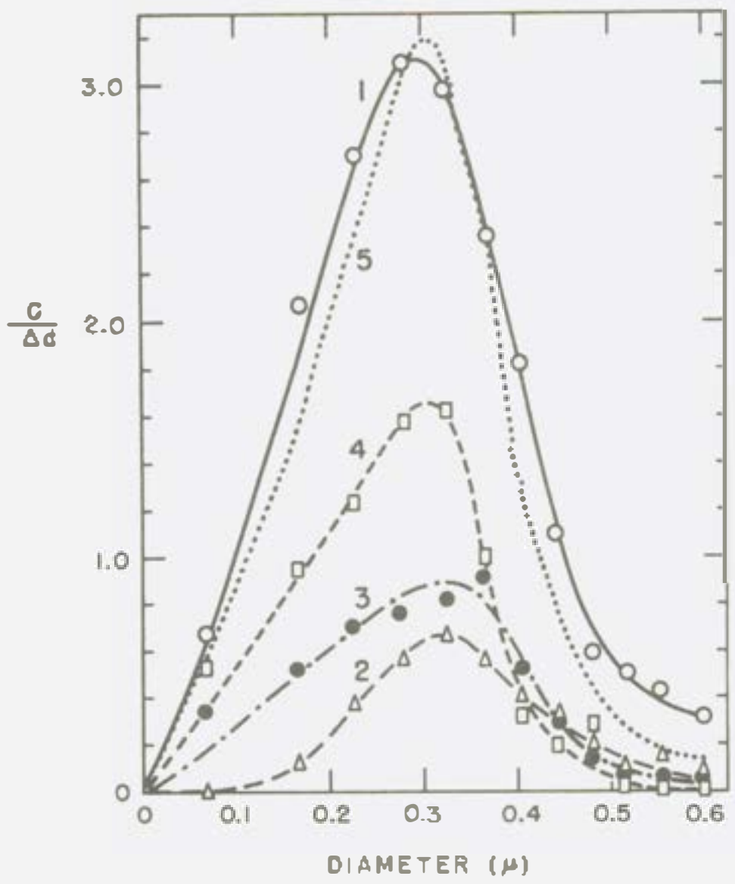

Figure 26 Distribution of uricase. Curve numbers same as in Figure 25.

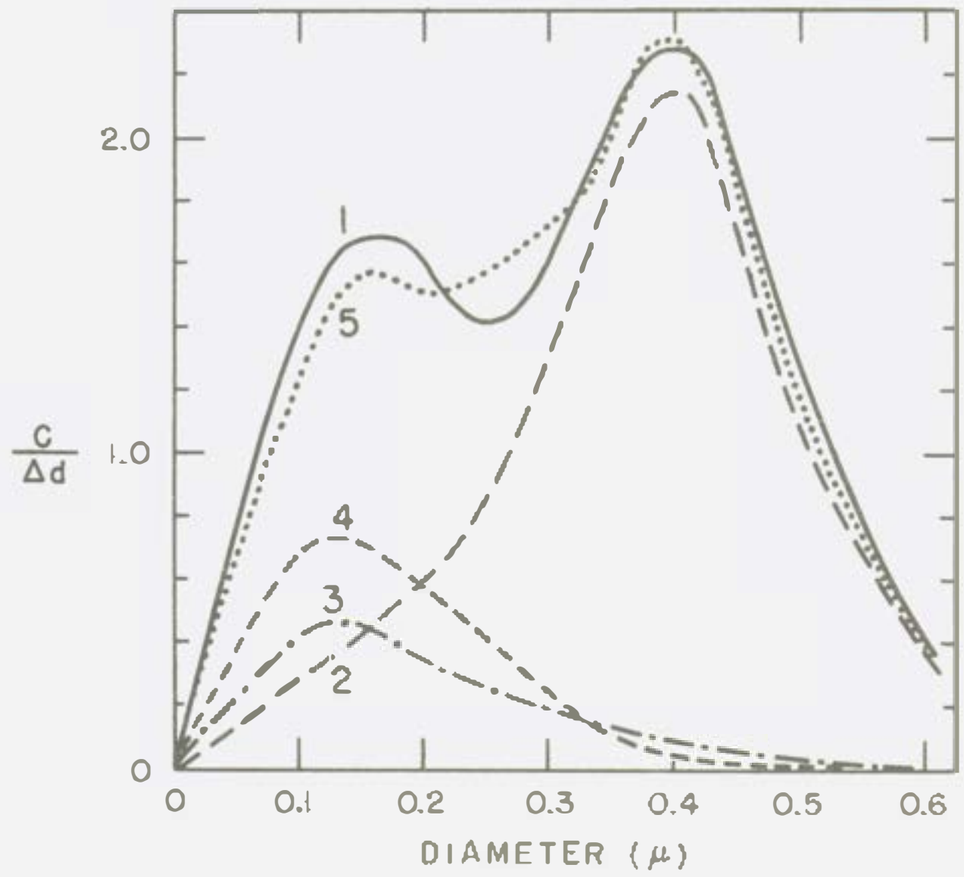

Figure 27 Distribution of cytochrome oxidase. Curve numbers same as in Figure 25; for the sake of clarity, the individual points are not shown.

References

1. Thomson, J. F., and E. T. Mikuta. 1954. Enzymatic activity of cytoplasmic particulates of rat liver isolated by gradient centrifugation. Arch. Biochem. Biophys. 51, 487-498.

2. Klein, P. D., and R. M. Johnson. 1954. Changes in age in the unsaturated fatty acids content of subcellular particles of rat livers. Arch. Biochem. Biophys. 48, 172-177.

3. Kuff, E. L., and W. C. Schneider. 1954. Intracellular distribution of enzymes. XII. Biochemical heterogeneity of mitochondria. J. Biol. Chem. 206, 677-685.

PROGRESS REPORT: GAMMA RAY TOXICITY PROGRAM

I. SURVIVAL OF LAF_1 MICE IRRADIATED DAILY FOR THE DURATION OF LIFE

Katherine F. Hamilton, Jean Drallmeier, Douglas Grahn, and George A. Sacher

Recruitment of mice into the various phases of the program is proceeding on schedule. In the duration-of-life program, two or more replications of thirty mice each have been completed at seven daily dose levels from 43 to 220 r/day of Co^{60} gamma rays. Results are summarized in Table 8 in terms of the mean survival times (sexes combined). In addition to the daily exposure levels reported here, exposures are under way at 32, 24, 12, and 6 r daily, but data are still too incomplete for reporting at present.

The mortality statistics are being assembled, not only for analysis in their own right, but also for comparison with histologic and hematologic changes. The comparison will be made by correlating the physiologic changes with the age- and disease-specific mortality rates. Although the data are not yet complete enough for such detailed analysis, the mean survival times reported here can be compared with the preliminary hematologic findings reported in Part II.

Table 8

Survival of LAF_1 mice exposed to Co^{60} gamma rays daily for the duration of life

Daily dose (r)	220	170	125	97	74	56	43
Mean after-survival	15.8	20.3	31.2	40.9	57.4	91.1	147.5
No. of mice	90	90	90	120	60	60	60

Mortality data are also being accumulated on four inbred mouse strains, namely the BALB/c, C57 Bl, A/Jax, and C3H/f, exposed at the seven levels from 43 to 220 r daily. Approximately 300 mice have yielded data at this time. The over-all strain differences in radiosensitivity are similar to those determined by the single dose procedure, but the curves for survival time vs. dose rate differ in detail between strains. This suggests that the hypothesis of multiple-factor strain differences in radiosensitivity will be vindicated. The schedule of histologic and hematologic studies on the inbred lines will be determined by the pattern of strain differences established by the mortality studies presently under way.

The survival of mice exposed to a very high daily γ-ray doses (220 to 2500 r) is currently being investigated. Exposures are given over a 12-hour period each day; LAF_1 mice and 5 inbred strains are used. Mean survival times are summarized in Table 9 except for the 220 r level, which is not yet complete. The predicted pattern of behavior is observed, namely,

(1) the existence of a sharp break in the survival time vs. dose rate relationship at about 5 days, consistent with the finding with single dosages, and
(2) the disappearance of the rank order of strain differences that is characteristic at longer survival times.

In the coming quarter a test will be done at ultra-high levels ranging from 1650 to 27000 r daily. Exposure in this case will be 24 hours per day, with short interruptions for death checks at 4-hour intervals. At a later time the investigations of the ultra-high range will be completed by tests in the range 10^4-10^6 r/day.

Table 9

Survival of mice of four inbred and one hybrid genotype given very high daily dosages of Co^{60} gamma rays for the duration of life

	330 r/day		500 r/day		750 r/day		1100 r/day		1650 r/day		2500 r/day	
	MAS*	N**	MAS	N	MAS	N	MAS	N	MAS	N	MAS	N
LAF_1	13.1	30	10.8	30	7.98	24	5.67	24	5.23	24	5.17	18
BALB/c	12.0	6	8.8	6	7.67	6	6.25	2	6.08	6	6.00	2
A/He	13.0	6	8.7	6	7.25	6	6.33	6	5.50	3	5.00	3
A/Jax	13.0	6	-	-	7.33	6	-	-	5.00	3	-	-
C3H/f	12.8	6	11.0	3	6.75	6	5.50	3	4.92	6	-	-
C57 Bl/6	12.8	6	9.8	6	7.17	6	5.33	3	5.17	3	5.00	3

*MAS = Mean after-survival in days

**N = Number of mice

PROGRESS REPORT: GAMMA RAY TOXICITY PROGRAM

II. HEMATOLOGIC RESPONSES OF LAF_1 MICE GIVEN DAILY DOSAGES OF GAMMA RAYS

Marietta Miller and George A. Sacher

Sampling of the hematologic and histologic responses of the LAF_1 mice in the duration of life exposure program continues. The accompanying figures illustrate some effects on the blood in the exposure levels for which survival times are reported in Part I. Each point is based on 2 to 6 counts. Sexes are combined. Some counting times within this series have not yet been sampled. This program has reached about one-third completion at these exposure levels.

The reticulocyte and erythrocyte pictures are especially interesting; it is believed that the complete data will give a good basis for the analysis of the response of the erythropoietic system to ionizing radiation. Bone marrow, spleen and lymph nodes from the same animals will also be counted.

The very low neutrophil levels in the mouse make counting difficult, especially the determination of immature forms. Procedures are therefore being developed for concentrating white cells.

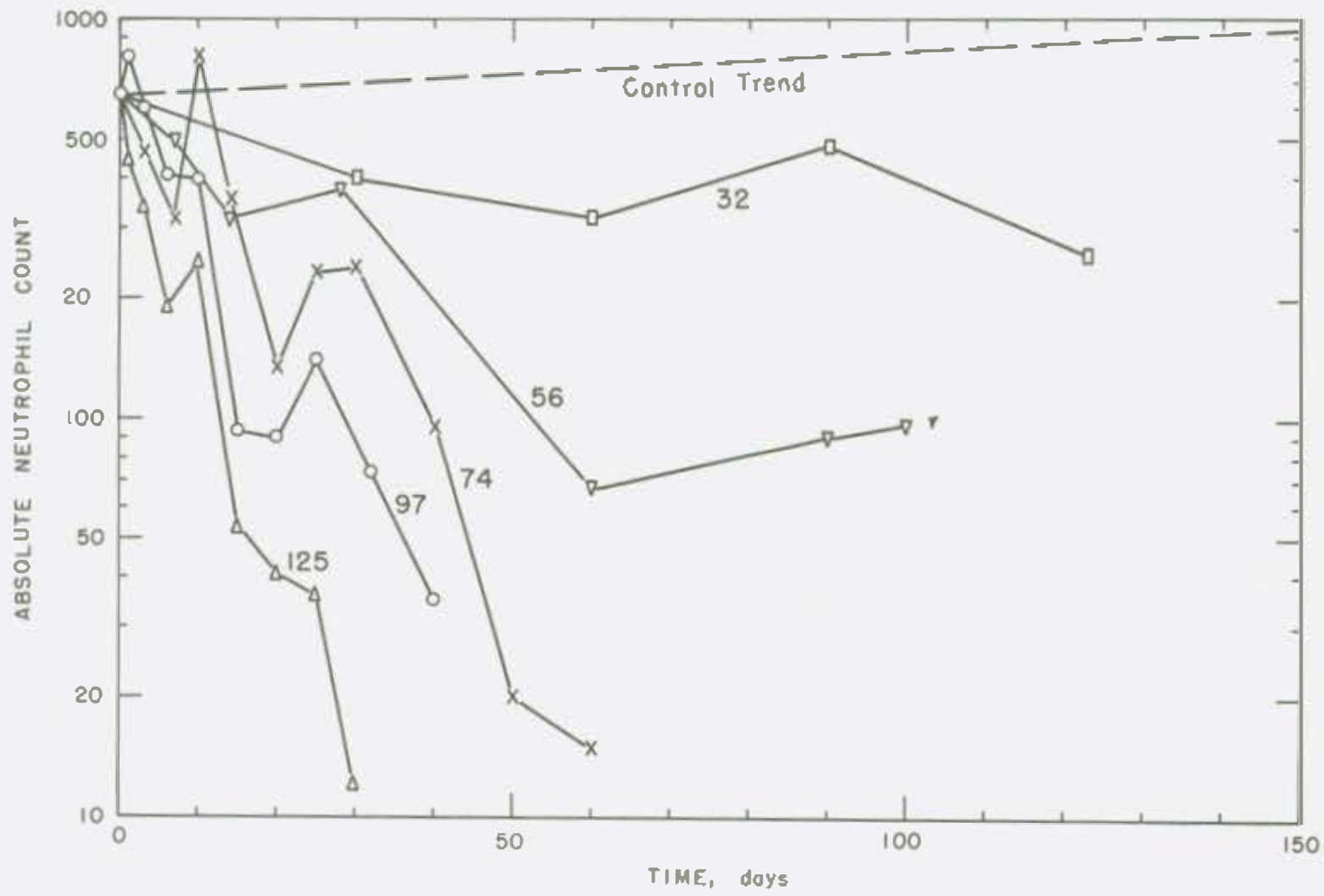

Figure 28 Neutrophil response of LAF mice given daily doses of X rays. The daily dose is indicated alongside the curve.

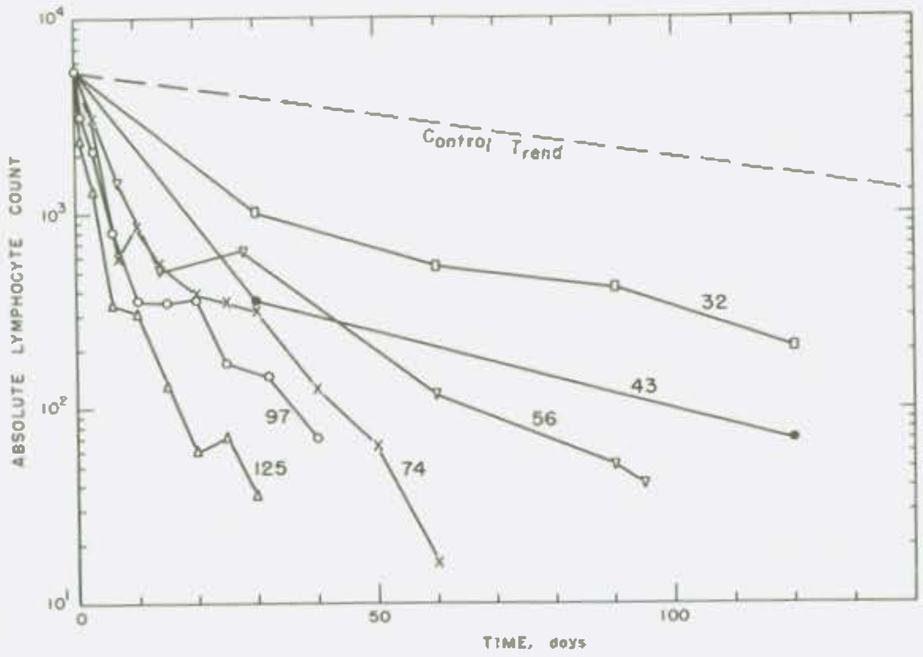

Figure 29 Lymphocyte response

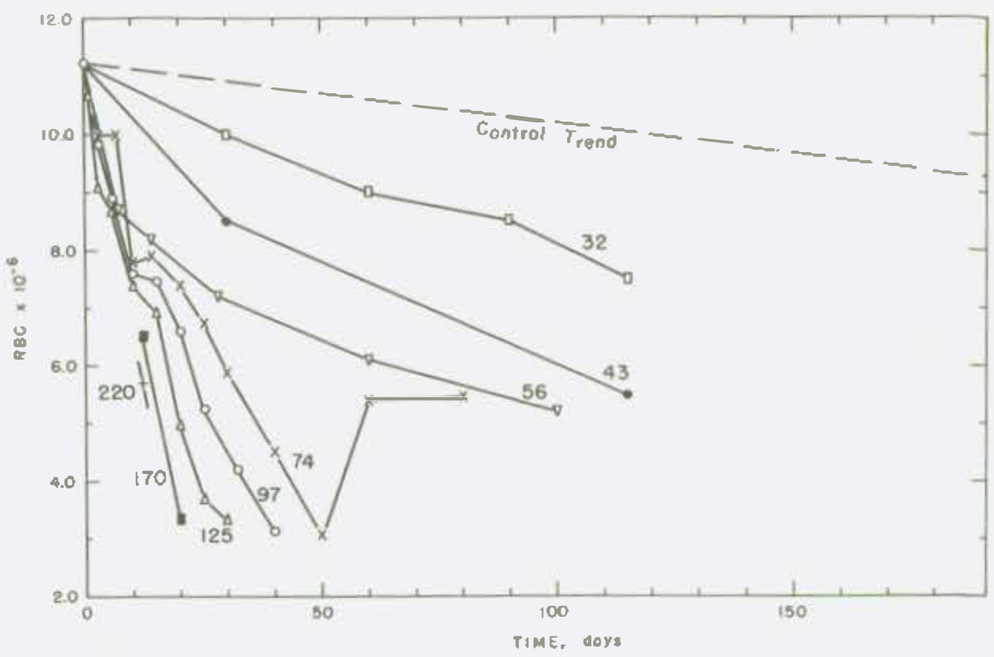

Figure 30 Erythrocyte response

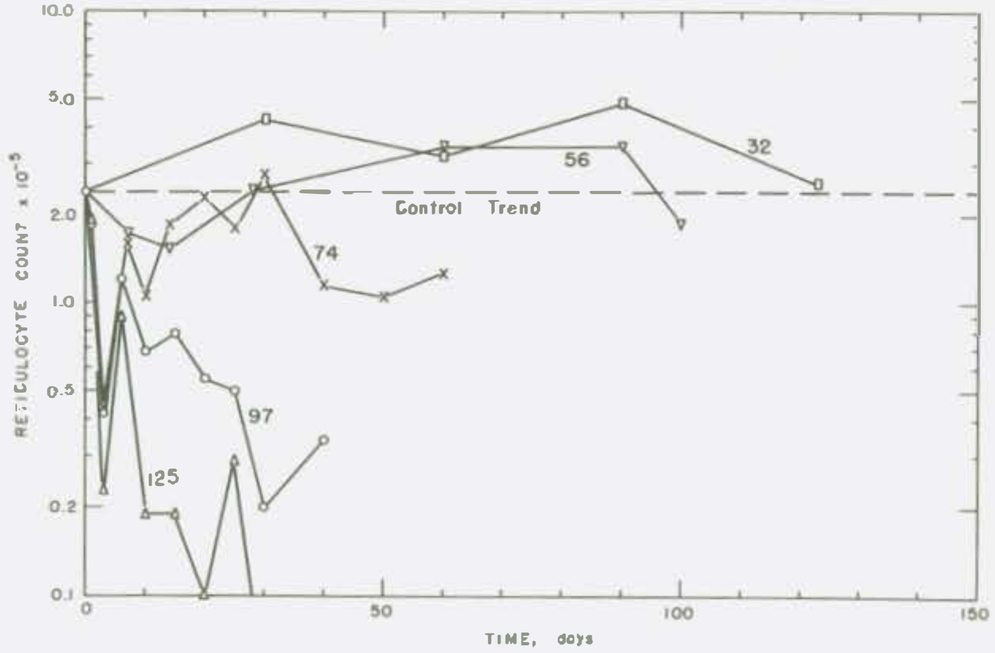

Figure 31 Reticulocyte response

Hematologic responses of LAF mice given daily doses of X rays. The daily dose is indicated alongside each curve.

PROGRESS REPORT: GAMMA RAY TOXICITY PROGRAM

III. MATHEMATICAL ANALYSIS OF THE BEHAVIOR OF CELLULAR SYSTEMS

George A. Sacher

Introduction

The purpose of this investigation is to give a quantitative account of growth, injury, and recovery processes in tissues in terms of concepts of cell physiology and population dynamics, such as birth, migration, maturation, and death. It may further be specified that the rates of birth, maturation, and migration, and perhaps the death rates as well, are governed by feedback loops. Little is known about the quantitative nature of the above processes and relations considered individually, and even less about the interactions that determine the characteristics of even a simple functioning tissue.

The program consists of describing each process in a mathematically simple yet realistic manner, and then combining them in successively more elaborate networks. The goal is to synthesize a network that reproduces the salient characteristics of a tissue. For our purposes a circulating formed blood element plus the productive center for that element are together considered to be a tissue.

The general principles of network synthesis and the mathematical procedures required are now new; they are presented with admirable lucidity by Bode[1] in his treatise on the design of feedback amplifiers. One respect in which the biological problem is more difficult is that one is required to deal with non-linear response characteristics. This is due not to any difference in kind between biological and electronic systems, but rather to the adventitious fact that biological and medical interest and experimentation is centered on the breakdown of normal function. Breakdown occurs beyond the range of normal (linear) response, and therefore the response characteristic must be specified in a reasonably adequate non-linear fashion.

In the very first stages of such a program one is confronted with systems of equations that are quite intractable insofar as desk computations are concerned. A considerable part of the work reported here was done on electronic computing machines.

Concepts and Definitions

A tissue is considered to consist of a very large number of distinct elements called cells. A cell within a simple tissue is characterized by its age and by an index of geographical location. For reasons of computational convenience and necessity, the aging process is considered to occur in a small number of discrete stages (maturation stages) and geographical localization is reduced to the case of homogeneous distribution within a small number of compartments. This approximation is fortunately in good accord with the actual situation. Maturation is therefore treated as an irreversible transition from one maturation stage to the next. Present formulations allow the possibility that maturation rates are functions of other parameters of the system. Where this assumption is made, maturation age is not equivalent to age in the actuarial sense, i.e., that at a given age there is a determinate after-expectation of life. New cells are produced by binary fission. Fission of a cell at a given age produces two daughters of equal age.

The First Model Studied

Even the above incomplete description cannot be handled in an initial treatment. Let us consider first a system of two compartments. The proliferative compartment contains a homogeneous population of cells that reproduce themselves and can also mature into "adult" cells that are incapable of reproduction. The behavior of this system is determined by a pair of simultaneous non-linear differential equations that can be written explicitly when the expressions for the birth and migration terms are fixed. The first system to be investigated is

$$\frac{dx}{dt} = h_1 x(1-x) - h_2 x(y^* - y) - h_3 x \tag{1}$$

$$\frac{dy}{dt} = h_2 x(y^* - y) - h_4 + y$$

Here x and y are the total numbers of proliferative and adult cells respectively. The birth, migration, and death terms are chosen to be

$$b = h_1 x(1-x) \tag{2a}$$

$$m = -h_2 x(y^* - y) \text{ for emigration from x to y} \tag{2b}$$

$$d = h_3 x,\ h_4 y \text{ for x and y respectively} \tag{2c}$$

The birth term is the product of terms for growth proportional to x and a growth limitation term that is a linear decreasing function of x. This birth term is the simplest form that satisfies the requirements that (a) new

cells cannot be formed except from cells already present, and (b) there is a maximum population size set by space and substrate limitations, etc. The migration term is similarly the simplest form embodying the properties that (a) the rate of migration is dependent on the number of cells present that are potentially able to migrate, and (b) the rate of migration is regulated by the level of y in a way that tends to reduce the effect of external or internal fluctuations on the value of y. The death terms are linear.

In the region of interest ($0 \leqslant x \leqslant 1$) there can be three equilibrium points. The largest is always stable, and is denoted x_s, y_s. These are the steady state values of the system. The point x=0, y=0 is also stable and the third point is unstable if it lies between 0, 0 and x_s, y_s. The approach to the steady state is non-periodic.

The dependence of the steady state values of the system on the values of the parameters is illustrated in Figures 32 and 33, where x_s and y_s are plotted against h_3 for fixed values of h_1, h_2, y* and h_4. Since h_3 is the death rate of proliferative cells, an increase in h_3 corresponds to one aspect of the effects of continuous exposure to ionizing radiations, hence h_3 can be considered to be proportional to the dose rate of a continuous exposure.

Increase in the value of the ratio h_2/h_4, or increase in h_2y^*, other things being equal, stabilizes the level of adult cells. This stabilization is seen in the decreased slope of y_s at small h_3 and in an increase of the value of h_3 at which instability occurs. As in all feedback networks, this stabilization is achieved at the expense of a loss of efficiency, as seen in the decreased level of y_s that accompanies increased stability. The stabilization of y_s in the present model is achieved at the expense of x_s, for there is no provision in this network to adjust the production of new x to the demand from y. In real tissues such an adjustment occurs, by processes of hypertrophy which consist of either (a) increased productivity within a fixed volume (hyperplasia) or (b) increase in the productive volume (e.g., extramedullary hemopoiesis). Introduction of a birth term of the form

$$b = h_1 x(1-x)(a-y) \qquad (3)$$

tends to stabilize x. The stabilization is achieved at the expense of the remainder of the organism and this imposes limitations on the completeness of compensation. The parameter "a" describes the degree of compensation that can occur. Compensation is complete if a = 1, and incomplete if $a > 1$. The best approximation of the model to the real system will presumably be attained with $a > 1$.

Steady state values, x_s and y_s, as a function of h_3, for values of the other parameters indicated. The encircled points indicate approximately the minimum values of x_s and y_s for which the particular system is stable.

	h_1	h_2y^*	h_2/h_4
A	5	3.5	10
B	5	3.5	2.5
C	5	2.0	10
D	5	2.0	2.5

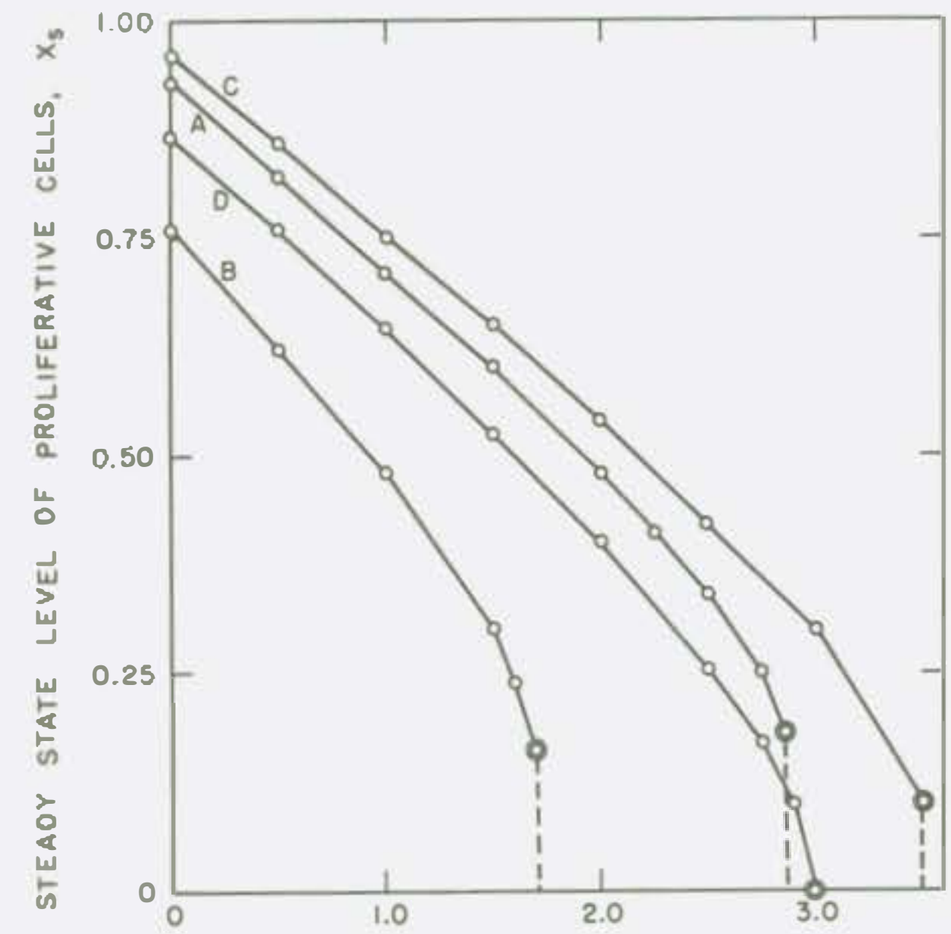

Figure 32

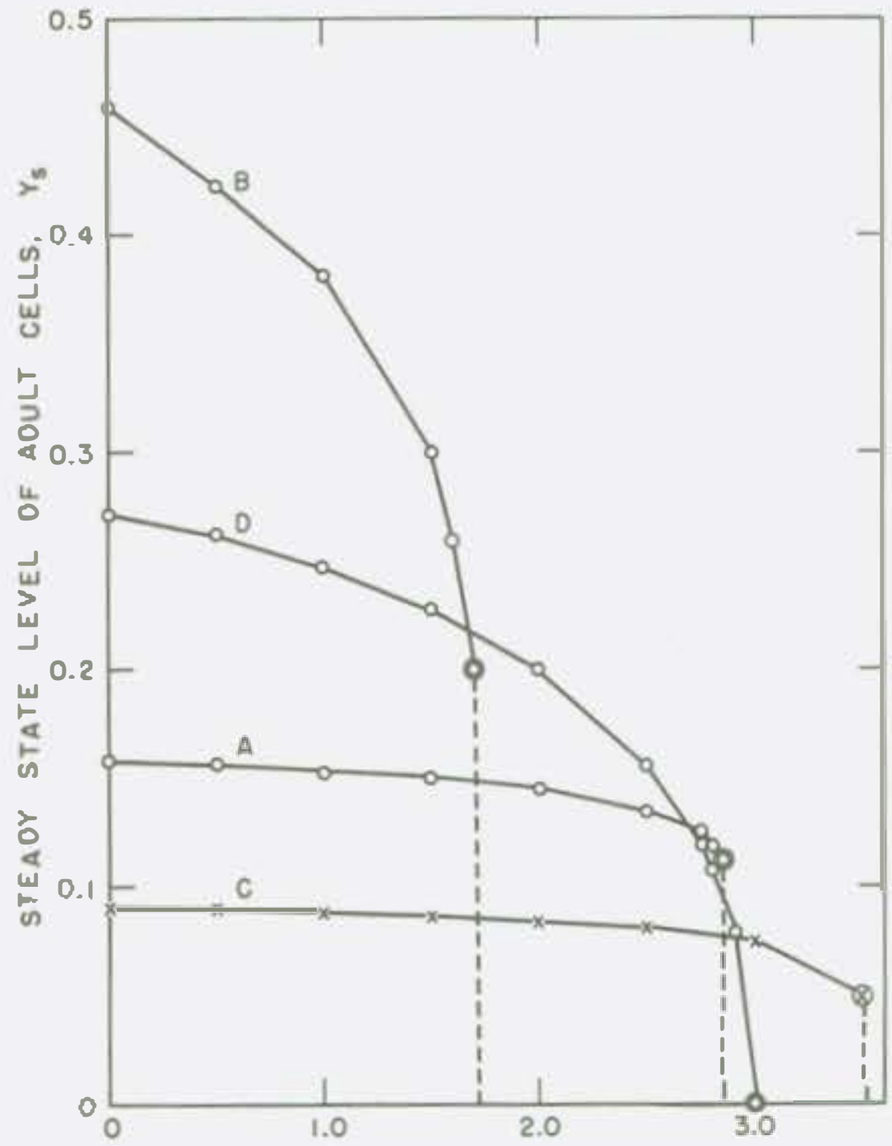

Figure 33

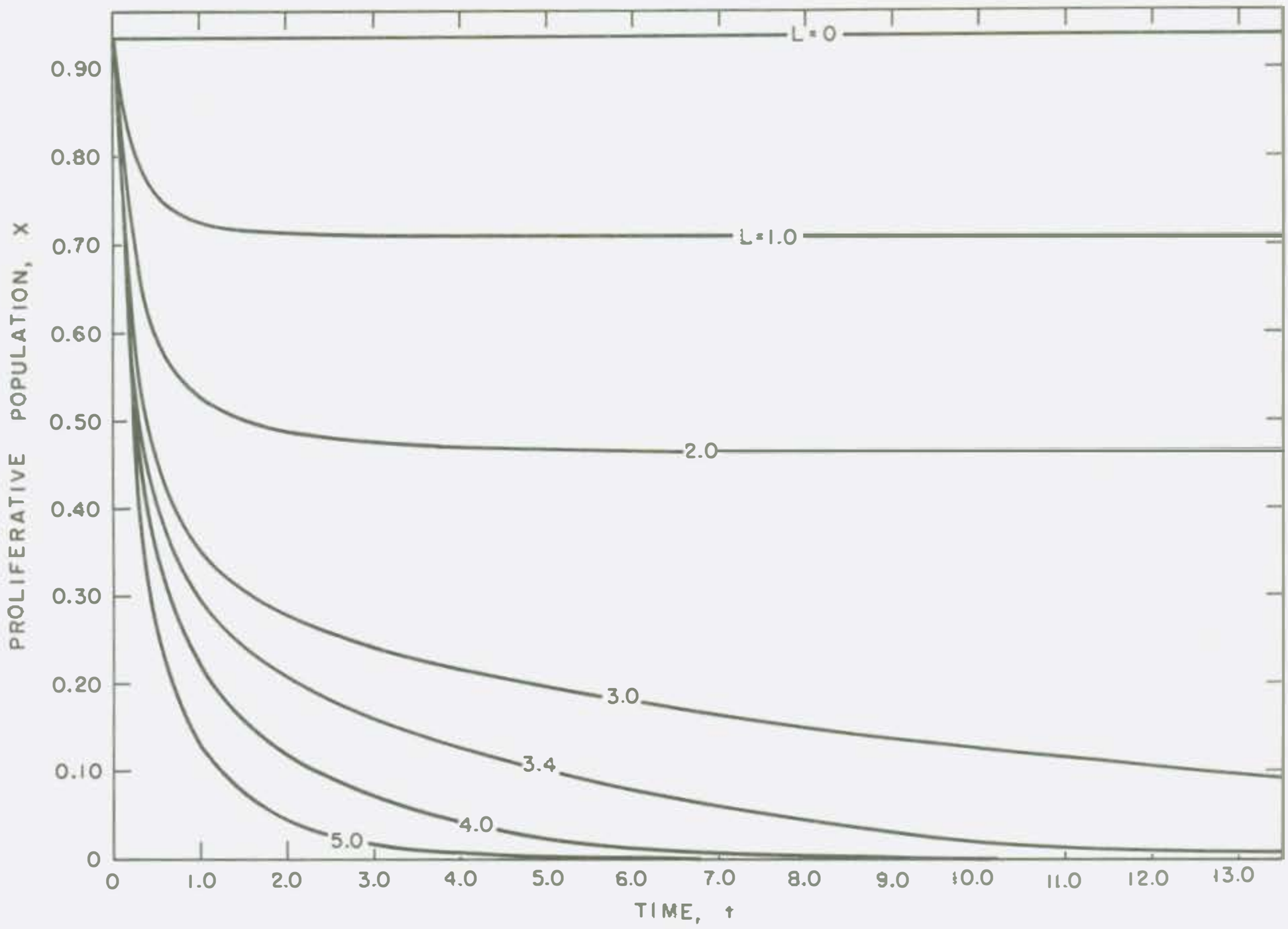

Figure 34

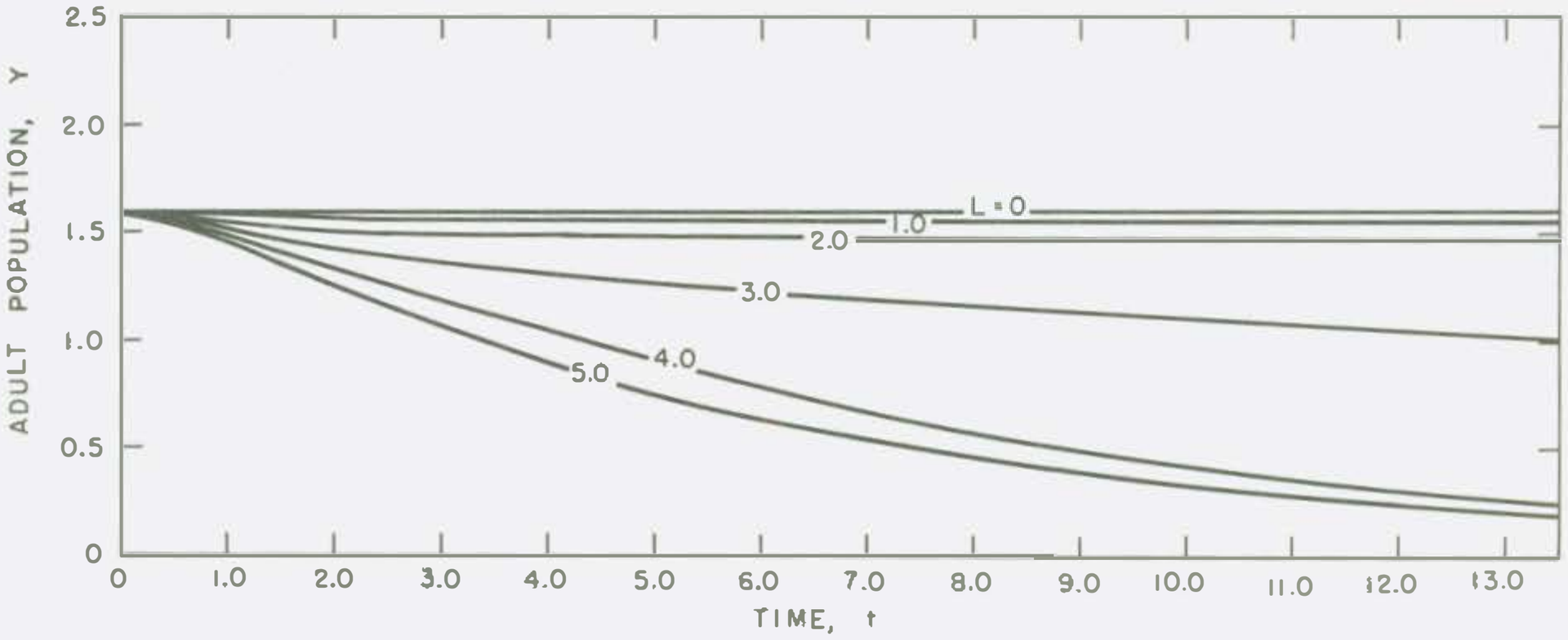

Figure 35

Transient responses of x and y following a stepwise change of h_3 from zero to the value indicated on the curve. Values of other parameters are: $h_1 = 5$, $h_2 = 20$, $y^* = 0.175$, $h_4 = 2$. In this case, the adult form is comparatively short-lived and there is considerable feedback (Figure 32).

The transient reponses of the model are illustrated by one example. Figures 34 and 35 show the responses of x and y to change in value of h_3. As noted above, this is partially equivalent to the imposition of a continuous exposure at a rate proportional to h_3. If non-zero steady state values of x and y exist for a given h_3, the system approaches these values. As h_3 increases, however, the steady state is reached more slowly, and if h_3 increases beyond the point of instability then x and y decline steadily to zero. A comparison of Figures 32 and 33 with the blood counts of mice given daily exposures (Figures 28-31) shows some interesting similarities. It is encouraging to observe that, although we are far from attaining an adequate model of a tissue-like system, nevertheless the present model agrees better with actuality then do the customary linear models.

Transient responses of the model described by Equation 1 have been computed and plotted by the REAC (Reeves Electronic Analog Computer) for several sets of values of the parameters and for various initial conditions. The next features to be investigated are (a) modification of the birth term and (b) introduction of intermediate maturation stages. Continued development of this program should lead to the synthesis of models that can account reasonably well for the behavior of the hemopoietic system in response to a variety of disturbances. The particular problem of the response to ionizing radiations is, however, the most difficult of all, because it introduces the complications of delayed injury and injury whose expression is a function of past states of the system. It remains to be seen whether the description of such behavior is feasible in terms of kinematic equations. If not, it will be necessary to proceed to stochastic models.

The electronic computations were carried out on the facilities of the Computing Section, Physics Division. The writer is indebted to Drs. Donald Flanders, Joseph Cook and Nye F. Morehouse for their cooperation and advice.

Reference

1. Bode, H. W. 1945. Network Analysis and Feedback Amplifier Design. New York: D. Van Nostrand.

THE EFFECT OF X RAY ON FERTILITY IN THE FEMALE MOUSE

Margaret H. Sanderson and S. Phyllis Stearner

Investigations were continued on fertility, mean litter size, and sex ratio of offspring in female LAF_1 mice following total body X-ray exposure. Dosages of 10, 25, 50, 75 or 100 r were administered to 70-day-old animals. Matings were begun one month after exposure and were continued monthly for periods of seven or of nine months.

Data on litters produced from these mating trials are presented in Table 10. Although the results of the first few matings were reported previously,[1] they are included here for the sake of comparison and completeness. There was some reduction in the number of litters born to the 10 r and 25 r groups, but the average litter size did not decrease perceptibly from that of the control until the ninth mating. In the group exposed to 10 r the first four matings produced litters slightly larger than the control group. In the 10 r as well as in the 25 r group, there was a slight preponderance of female offspring. Spontaneous abortions were observed after the third, fourth and sixth matings in the 10 r group and after the third mating in the 25 r group. In the 50 r group, the first four matings produced smaller than normal litters, with altered sex ratios after the first and fourth matings. After the fourth mating no litters were born and no abortions were observed. In the 75 r group the mean litter size was reduced and sex ratio was altered after the first mating; subsequent matings produced no offspring. Mice exposed to 100 r did not produce any litters. The incidence of nulliparous females in each exposure group is noted.

In the control group the number of pregnancies decreased somewhat after the fourth mating, but the average litter size and sex ratio remained fairly consistent throughout the experimental period.

It has been known for many years that the exposure of female mice to relatively low doses of radiation results in reduction in mean litter size and, eventually, permanent sterilization. Russell et al.[2] and Russell and Spear[3] have reported an increased mortality in embryos in the pre-implantation stage when female mice are mated within five days after exposure to X-radiation, although ovulations during this period are normal or increased in number. After the third post-irradiation week, decreased numbers of ova are available for fertilization; this, together with the high mortality of pre-implantation embryos, explains the reduced litter size.

Table 10

Percent parous, litter size, and sex ratio of offspring of mice exposed to total-body X ray before mating

	Controls	10 r	25 r	50 r	75 r	100 r
Mating 1						
No. animals	71	48	32	32	32	32
% parous	68	58	53	25	16	0
% observed abortions	0	0	0	0	0	0
Average litter size	7.7	7.5	7.2	4.1	4.0	0
% males	44.4	49.5	45.0	37.5	40.0	0
% females	55.5	50.5	55.0	62.5	60.0	0
Mating 2						
No. animals	71	48	32	32	32	32
% parous	58	62.5	69	22	0	0
% observed abortions	0	0	0	0	0	0
Average litter size	8.4	8.7	8.1	2.3		
% males	45.9	46.2	49.7	53.3		
% females	54.1	53.8	50.3	46.7		
Mating 3						
No. of animals	70	48	31	32	31	32
% parous	63	54	55	25	0	0
% observed abortions	0	4	3	0	0	0
Average litter size	7.7	8.8	9.4	2.0		
% males	47.5	44.3	47.5	50.0		
% females	52.5	55.7	52.5	50.0		
Mating 4						
No. animals	65	46	25	29	31	32
% parous	46	41	40	6.9	0	0
% observed abortions	0	10.9	0	3.4	0	0
Average litter size	7.1	9.2	7.9	1.5		
% males	45.3	45.4	40.5	33.3		
% females	54.7	54.6	59.5	66.7		
Mating 5						
No. animals	63	45	25	29	31	32
% parous	59	53	40	0	0	0
% observed abortions	0	0	0	0	0	0
Average litter size	9.0	8.9	8.6			
% males	48.2	41.1	45.3			
% females	51.8	58.9	54.7			
Mating 6						
No. animals	63	44	25	29	30	32
% parous	50	39	36	0	0	0
% observed abortions	0	2.6	0	0	0	0
Average litter size	9.3	7.9	8.8			
% males	50.7	43.7	41.8			
% females	49.3	56.3	58.2			
Mating 7						
No. animals	63	44	25	29	30	32
% parous	48	48	32	0	0	0
% observed abortions	0	0	0	0	0	0
Average litter size	8.2	7.5	8.3			
% males	46.2	43.9	47.0			
% females	53.8	56.1	53.0			
Mating 8						
No. animals	44	44	25	29	-	32
% parous	50	36	24	0	-	0
% observed abortions	0	0	0	0	-	0
Average litter size	9.1	7.5	8.0			
% males	45.8	46.7	43.8			
% females	54.2	53.3	56.2			
Mating 9						
No. animals	42	42	25	29	-	32
% parous	48	50	36	0	-	0
% observed abortions	0	0	0	0	-	0
Average litter size	8.1	6.4	5.2			
% males	48.8	40.7	36.2			
% females	51.2	59.3	63.8			
% nulliparous throughout 9 mating trials	0.0	0.0	8.0	48.3	83.3*	100

*7 trials

References

1. Sanderson, M. H., and S. P. Stearner. 1955. The effect of X-ray on fertility in the mouse. Quarterly Report, Biological and Medical Research Division, Argonne National Laboratory. ANL-5426, pp. 119-120.

2. Russell, L. B., W. L. Russell and R. J. Spear. 1954. Dominant lethals induced in female mammalian germ cells by X rays. Oak Ridge National Laboratory. ORNL-1766, pp. 52-54.

3. Russell, L. B., and R. J. Spear. 1955. Changes in the sensitivity of oocytes to the induction of dominant lethals. Oak Ridge National Laboratory. ORNL-1863, pp. 61-63.

ACUTE LETHAL RESPONSE OF FIVE INBRED MOUSE STRAINS TO SINGLE DOSE TOTAL-BODY X-IRRADIATION

Douglas Grahn and Katherine F. Hamilton

The irradiation of five inbred mouse strains with single doses of 200 kvp X rays has been completed and the results are presently being analyzed. The data represent 15 to 20 independent test groups for each strain. Generally, from 2 to 4 different doses were employed in each test, with 12 to 16 mice per dose. The age at exposure ranged from about 60 to 110 days; the mean age per strain ranged from 84 to 87 days. In any test, the delivered doses were distributed across litter-mates and sexes. Essentially equal numbers of the two sexes were used; however, this feature was controlled by the normal sex ratio which differed somewhat from strain to strain.

The $LD_{50/30}$ doses and dosage mortality slopes for individual strains were first estimated by pooling all data at each dose, using an arc-sine transform of the mortality percentages against dosage in roentgens. The results of this analysis are given in Table 11.

Table 11

Estimated $LD_{50/30}$ doses for indicated mouse strains. Estimates derived from pooled data where n is total number of animals tested.

Strain	n	$LD_{50/30}$ (r)	S.E. (r)	Slope	S.E.
BALB/c	672	504.4	± 3.3	.330	± .019
A/Jax	522	547.7	± 4.6	.357	± .030
A/He	486	554.6	± 6.2	.393	± .044
$C3H_f$/He	845	592.2	± 6.1	.403	± .060
C57 BL/6	687	629.1	± 3.0	.473	± .040

The maximum difference between the strain LD_{50} values is 125 r, or a factor of 25% increase over the low strain. The dosage-mortality slopes are positively correlated with the LD_{50} doses. Thus increasing resistance is associated with a greater change in mortality per unit dose, so that strain differences are minimal at the high lethality level and maximal at

low lethality. Factors for resistance are indicated by an apparently greater uniformity and narrower dose range of response, where short term recovery factors are presumably more rapid in their rate of action. The apparent differences in uniformity, as demonstrated by the differences in slope, can not be considered due to differences in the residual genetic variation of the several strains (with increasing resistance related to increasing genetic homogeneity), since all of the tested inbreds are of long standing and can be assumed to be at an equal and high level of genetic homogeneity. High dosage mortality slopes are normally expected to yield less variable estimates of response, since the variance of such estimates is inversely proportional to the slope. Pooled-data estimates of the variance of the LD_{50} values are not considered by some to be the most realistic estimates.(1) These data concur, as is demonstrated by a re-estimation of the variance that accounts for the differences between independent test groups.

By fitting the pooled-data mortality slopes through each individual test group and estimating the LD_{50}, an approximate distribution of LD_{50} values was obtained for each strain. Although a tendency to negative skewness exists in these distributions, they were shown to be homogeneous with regard to the deviations of individual test values from the mean value. The means themselves (Table 12) are nearly identical to those obtained from the pooled data, while the standard errors (and variances) now show the expected negative correlation with the LD_{50} values. These variance estimates, which assume the distributions to be normal, clearly indicate that strains with higher LD_{50} values are less variable in their response and vice versa.

Table 12

Mean LD_{50} values for indicated mouse strains.
Data based on individual test groups; n:
number of independent tests.

Strain	n	$LD_{50/30}$ (r) S.E. (r)	Variance S.D. (r)	Limits: x ± 2S.D. (r)
BALB/c	17	504.5 ± 9.2	1446 ± 38.0	428.5 - 580.5
A/Jax	15	545.7 ± 7.5	845 ± 29.1	487.5 - 603.9
A/He	15	551.5 ± 6.2	578 ± 24.0	503.5 - 599.5
$C3H_f$/He	19	593.4 ± 6.3	747 ± 27.3	538.8 - 648.0
C57 BL/6	16	629.9 ± 5.3	446 ± 21.1	587.7 - 672.1

As seen in the last column of Table 12, the limiting values that would include approximately 95% of a distribution cover a broad range of doses. The range for the lowest-LD_{50} strain is about 150 r, while it is only a little

over 80 r for the highest-LD_{50} strain. Any paired comparison of the two outside strains, when carried out under the conditions of this experiment, could show a difference of as much as 250 r or as little as 7 r, a 35-fold range, even though the LD_{50} for each individual strain remains within the customarily accepted range of expectation.

The variance estimates given in Table 12 include all underlying variation that can be attributed to age or to any contribution of the litter history (such as litter size), as well as random environmental or otherwise unaccountable variation. As such, the data are similar to those which would be obtained from commercially available stocks.

Preliminary analysis has shown that age makes a significant contribution to the variance, resistance increasing with age. Parity and litter size are minor variables. A multivariate analysis is being applied to the data in order to remove the effects of these factors and to provide estimates of the LD_{50} and variance that are independent of age, parity and litter size. Similarly, other factors, such as sex differences, survival time, body weight and the like, are being investigated and should be presented in detail in the near future.

Reference

1. Dews, P. B., and J. Berkson. 1954. On the error of bioassay with quantal response, in Statistics and Mathematics in Biology, O. Kempthorne et al., ed., Ames, Iowa: Iowa State College Press.

INDOLEACETIC ACID OXIDASE AND PHOTOPERIOD

Robert E. Stutz

In an attempt to determine the role of indoleacetic acid (IAA) oxidase in growth, the study of the distribution of this enzyme in the stems and buds of Lupinus alba L. grown on 8-, 12-, and 16-hour photoperiods was undertaken. The greenhouse-grown plants were on an 8-hour day of sunlight supplemented with incandescent light to give the total photoperiod.

After 8 weeks the plants had the same number of leaves (internodes), showed typical photoperiod response as to height, and gave an apparent photoperiod response for the level of free enzyme, or inhibitor concentration, in the stem (Table 13). The oxidase was found at about equal levels of activity in the buds from each photoperiod. The crude enzyme preparation from the stems showed an increasing time lag for activation with increasing photoperiod, indicating a higher level of natural inhibitor. Although this effect is accompanied by an apparently lowered level of enzyme, dialysis and addition of 2,4-dichlorophenol as activator results in maximum oxygen uptake; addition of 2,4-dichlorophenol to the crude enzyme preparation does not grossly alter the response.

Table 13

Effect of photoperiod on Lupinus alba L.

Photoperiod (hours)	Av. leaf number	Av. height (inches)	IAA oxidase from stems	
			Lag in O_2 uptake (min)	O_2 uptake at lag + 60 min (microliters)
8	12	5.5	20	350
12	12	9	50	310
16	12.5	13	120	270
			10*	417
			0**	400

*Buds

**Dialyzed stems + 2,4-dichlorophenol

Since the stem length varies with photoperiod, cell number and cell size were examined cytologically.. No appreciable differences as to cell size were found, but there was an increase in cell number.

The photoperiod response of lupine seems to be related superficially to the level of naturally occurring inhibitor for IAA oxidase. However, on the basis of the cell numbers found in the stems, it appears that the growth response is not regulated by IAA or IAA oxidase but shows a kinetin-like[1] response.

Reference

1. Miller, C., and F. Skoog. 1955. Regulation of growth in tobacco tissue cultures. Plant Phys. Supplement xxxv.

THE EFFECT OF DOSE RATE OF Co^{60} GAMMA RADIATION ON 30-DAY MOUSE MORTALITY, AND ITS RELATIONSHIP TO THE "ADDITIVITY" OF FAST NEUTRONS AND GAMMA RAYS

Howard H. Vogel, Jr., John W. Clark, and Donn L. Jordan

It has been reported[1] that when CF#1 female mice were exposed to Co^{60} γ-radiation (single 90-minute whole-body exposures), the 30-day lethal range was found to lie between ca. 750 and 1100 r; these exposures had been carried out in the gamma-neutron radiation chamber[2] at the CP-3' reactor at dose rates between 8 and 12 r/min. We have also reported[3] that there was a significant departure from additivity when mice were exposed to mixtures of fission neutrons and Co^{60} γ-rays. The maximum departure from additivity was found in mixtures of 2/3 neutrons and 1/3 γ-rays. The mice were exposed to both radiations concurrently during a 90-minute period, since it was considered desirable to keep the overall radiation time constant during both the pure and the mixed exposures. This, however, necessitated a variation in dose rate, so that animals received 250-300 r of γ-rays during the 1.5 hours at a dose rate of approximately 3 r/min in these high-neutron, low-γ-ray mixtures.

Thomson and Tourtellotte[4] have shown that the 30-day LD_{50} for mice exposed to γ-radiation was relatively independent of dose rate between 4 and 40 r/min, but that at lower rates the LD_{50} was appreciably higher. We have reported[3] that when the γ-irradiation time of CF#1 female mice was increased from 1.5 to 24 hours, the LD_{50} increased from 930 to 1325 r. In contrast, no such dose-rate dependence was evident following similar exposures of mice to fission neutrons.

The following experiment was undertaken to determine whether the departure from additivity reported following such mixtures of the two ionizing radiations might be explained, wholly or partially, as a dose-rate effect of the gamma component.

Methods and Materials

Approximately 400 female CF#1 mice were randomly selected from two shipments. The mice were approximately 5 weeks old when recieved in the laboratory and were 8-10 weeks old when irradiated. A total dose of 990 r was delivered to 191 mice in the low-level gamma room (Bldg. 202) at a rate of 11 r/min. The following day 187 mice were irradiated with the same total dose at a rate of 3 r/min. At the time of exposure the weights of the mice of both groups varied between 18 and 25 g. The average weight of the mice in the first experiment was 20.6 g; in the second group, 21.5 g.

The mice exposed at the higher dose rate were irradiated at 11 r/min for a 90-minute period. Their 50 exposure cages were distributed concentrically in the gamma room on shelf #4, 59 inches from the 1200 curie Co^{60} source. The mid-animal floor distance was 56-1/2 inches. The exposure cages were the standard plastic cages used routinely by the Gamma Toxicity Group.[5] Each cage held 3 or 4 mice. After the irradiation period of 90 minutes the mice were retained in the exposure cages with the source shielded for an additional 4 hours, without food or water, to conform to the 5.5-hour radiation period in the lower dose-rate exposure. For the latter, 187 mice were exposed in 50 cages at the same height and in the same room; however, the centers of the cages were 117 inches from the source so that the dose rate was 3 r/min and the total exposure time for 990 r was 5.5 hours.

Results

The comparative mortality in the two experiments for the 30-day period after irradiation is illustrated in Figure 36. Of the 191 mice exposed to 990 r at 11 r/min, 167 died within 30 days (87.4%). On the other hand, only 113 mice of the 187 exposed at 3 r/min (60.4%) died during this same interval. It is therefore clear that the dose rates of Co^{60} γ-rays do influence mortality in this mouse.

The mortality picture in these γ-irradiated mice was similar to that observed in mice exposed in the gamma-neutron radiation chamber, with deaths starting at the end of the first week and reaching a peak by the end of the second week after irradiation. In the mice exposed in the gamma room, however, the highest mortality peak in both experiments was found on day 12, whereas this peak did not occur until day 14 in animals previously exposed to similar doses in the radiation chamber. Whether this temporal variation was due to the differences in exposure techniques or to changes in the CF#1 mice over a 2-3 year period is difficult to determine.

The 30-day LD_{50} values calculated for these data for 990 r delivered at 11 r/min and at 3 r/min were 847.9 r and 957.2 r, respectively. The ratio of these values (0.886) could be used to indicate the effect of dose rate on survival. In mice exposed to mixtures of 2/3 neutrons and 1/3 γ-rays the 30-day LD_{50} was found to be 1021 $\pm$ 7 roentgen equivalents.[6] These mixture doses had been calculated by adding the gamma dose in roentgens to the product of the neutron dose in rep and the relative biological effectiveness (RBE) of 4.43. When we introduce the dose-rate factor and calculate the mixture doses by the formula (neutron dose in rep x 4.43) + (gamma dose in roentgens x 0.886), we find the LD_{50} reduced from 1021 to 987 roentgen equivalents. Thus, we can estimate that exposure of mice to 300 r of Co^{60} γ-rays at 3 r/min rather than at 11 r/min increases their radioresistance by approximately 34 roentgen equivalents. Thus, as is shown in Figure 37, one third of the departure from additivity seen in the 2/3 neutron

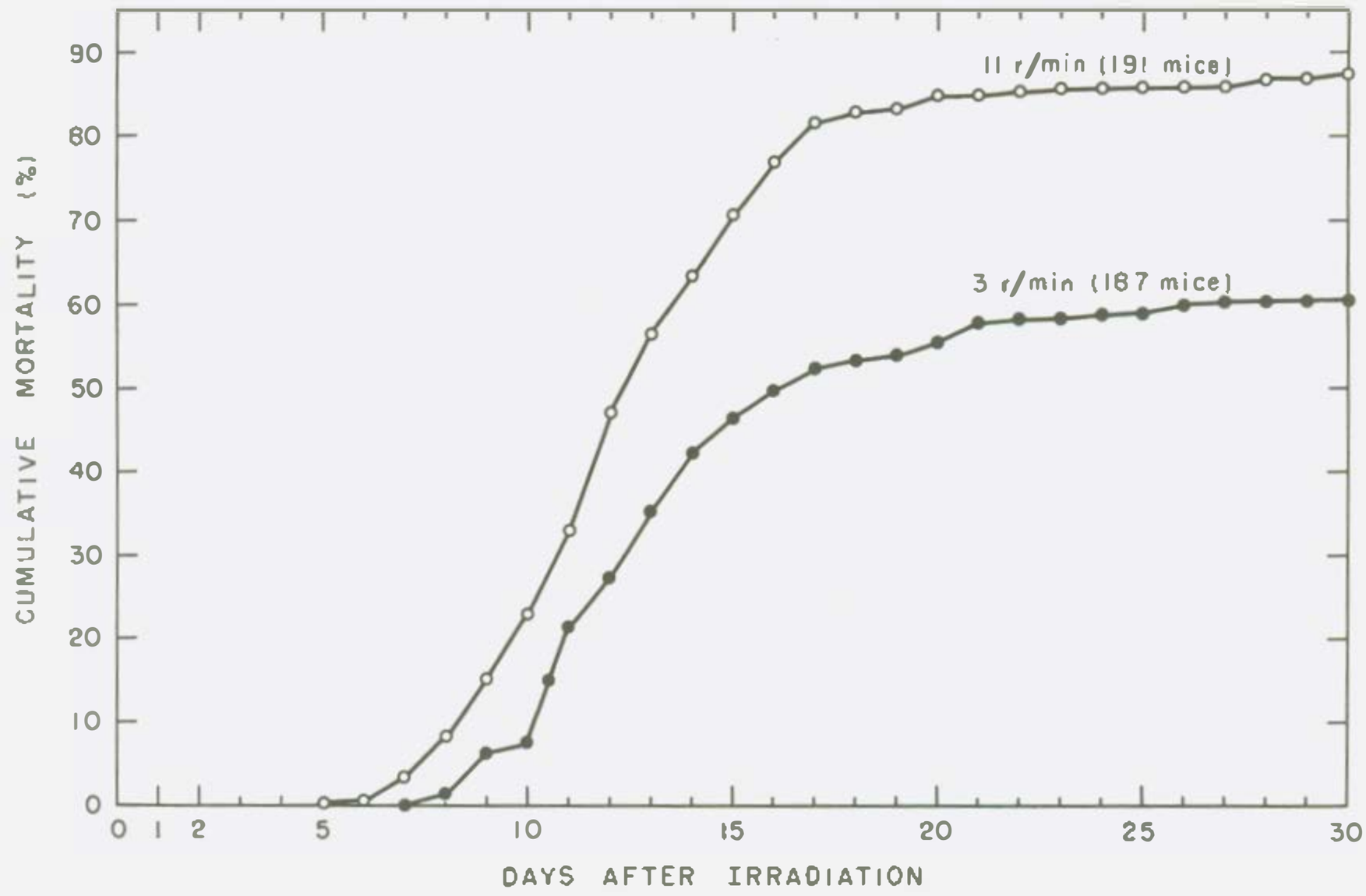

Figure 36 Comparative mortality of CF#1 female mice exposed to 990 r Co^{60} γ-radiation at dose rates of 11 r/min and 3 r/min.

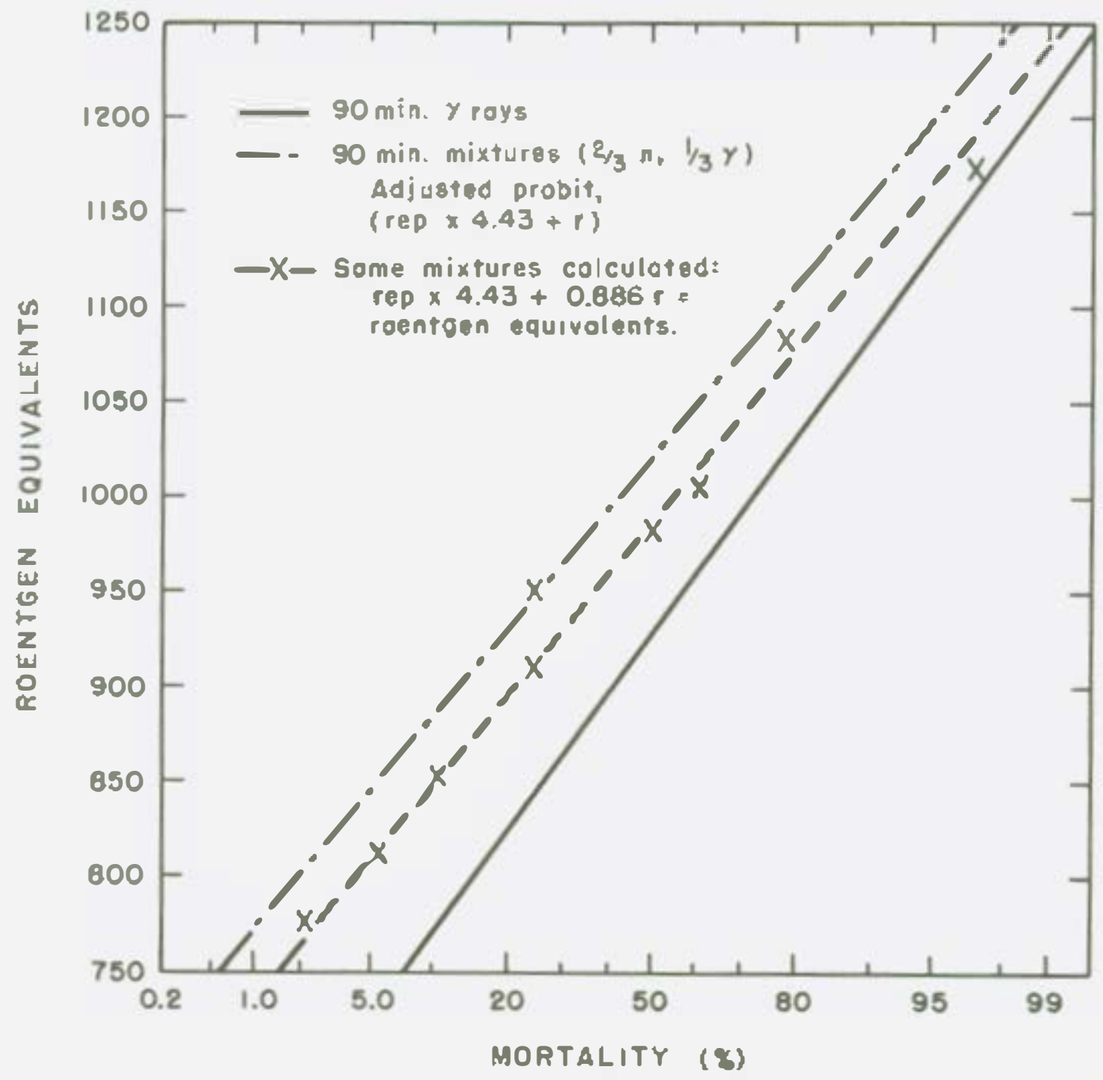

Figure 37 Effect of γ-ray dose rate on departure from additivity in 2/3 neutron and 1/3 γ-ray mixture.

and 1/3 gamma mixtures can probably be explained by the lower dose rates of the gamma radiation in the mixture experiments. However, it is clear from this figure that variation in dose rate does not completely explain this departure from additivity.

References

1. Clark, J. W., D. L. Jordan, and H. H. Vogel, Jr. 1954. Survival of CF#1 female mice after single acute exposures to Co^{60} gamma rays, to fast neutrons, and to mixtures of these ionizing radiations. Radiation Res. 1, 128. Abstract.

2. Vogel, H. H., Jr., R. A. Blomgren, and N. J. G. Bohlin. 1953. Gamma-neutron radiation chamber for radiobiological studies. Nucleonics, 11, No. 3, 28-31.

3. Vogel, H. H., Jr., J. W. Clark, D. L. Jordan, N. Bink, and V. M. Story. 1954. Status of neutron toxicity studies in mice. Quarterly Report, Biological and Medical Research Division, Argonne National Laboratory. ANL-5247, pp. 30-42.

4. Thomson, J. F., and W. W. Tourtellotte. 1953. The effect of dose rate on the LD_{50} of mice exposed to gamma radiation from Co^{60} sources. Am. J. Roentgenol. Radium Therapy Nuclear Med. 69, 826-829.

5. Sacher, G. A., D. Grahn, S. Lesher, and K. Hamilton. 1955. The gamma ray toxicity program: calibration and equipment. Quarterly Report, Biological and Medical Research Division, Argonne National Laboratory. ANL-5378, pp. 91-94.

6. Clark, J. W., D. L. Jordan, and H. H. Vogel, Jr. 1955. Biological effects of fast neutrons and gamma rays. Proceedings of International Conference on Peaceful Uses of Atomic Energy, Geneva, Switzerland, Paper No. 81, in press.

THE DESIGN AND USE OF A HIGH-ALTITUDE CHAMBER

Peter D. Klein and Robert W. Swick

This report deals with the construction and application of a chamber for the simulation of high altitudes. The first section describes the mechanical features of the chamber while the second lists some of the biochemical and physiological problems whose study is facilitated by this device.

Construction

Since the effect of high altitudes (greater than 15,000 feet) on mammals is a function of the oxygen concentration, the simulation of these altitudes may be brought about in two ways. First, a mixture of oxygen and nitrogen may be flushed through an enclosed area and, by varying the concentration of oxygen in the mixture, any altitude may be imitated while maintaining sea level atmospheric pressure. This method has the advantage that structural requirements of strength, volume and airtightness are easily fulfilled, since an overpressure of 1-2 pounds is sufficient to insure the proper atmosphere. On the other hand, such an apparatus requires a supply of pre-mixed gases which cannot be varied in composition once the flow is begun and, therefore, long periods of altitude acclimatization are not practical. In the second method, the pressure within the chamber may be reduced by pumping out air until the proper level is attained; thereafter the air inflow is balanced against the capacity of the pump. While this procedure calls for a much more sturdy type of construction as well as for adequate regulation of the pressure, the period for which animals may be maintained in the chamber is prolonged indefinitely.

The second system was adopted in the construction of the high-altitude chamber now in use (Figure 38). The chamber consists of a glass tube 6 inches in diameter having a wall thickness of 0.5 inches and an over-all length of 48 inches (A). This will accommodate approximately 6 guinea pigs, 10 rats, or 40 mice. Each end section (B) is equipped with metal flanges and an outlet tube for disassembly and loading of the chamber. A metal tray, curved about the longitudinal axis, serves to hold the bedding, food and water (Figure 39). Pressure reduction is carried out by a vacuum pump attached directly to the chamber (C) (Figure 38); pressure regulation may be effected by one of two systems. The regulator in current use (D) is adapted to negative pressures by applying a vacuum to the atmospheric side of the regulating diaphragm. Alternatively, a contact switch operated by the mercury manometer (E) has been used to activate a bleeder valve. The latter system has the advantage of continuous and ready variability, but operates only on the negative side of the pressure desired. A second circuit might be provided for a periodic momentary shutoff on the intake tube to bring the pressure below the desired level; this would increase the stability and eliminate a positive pressure

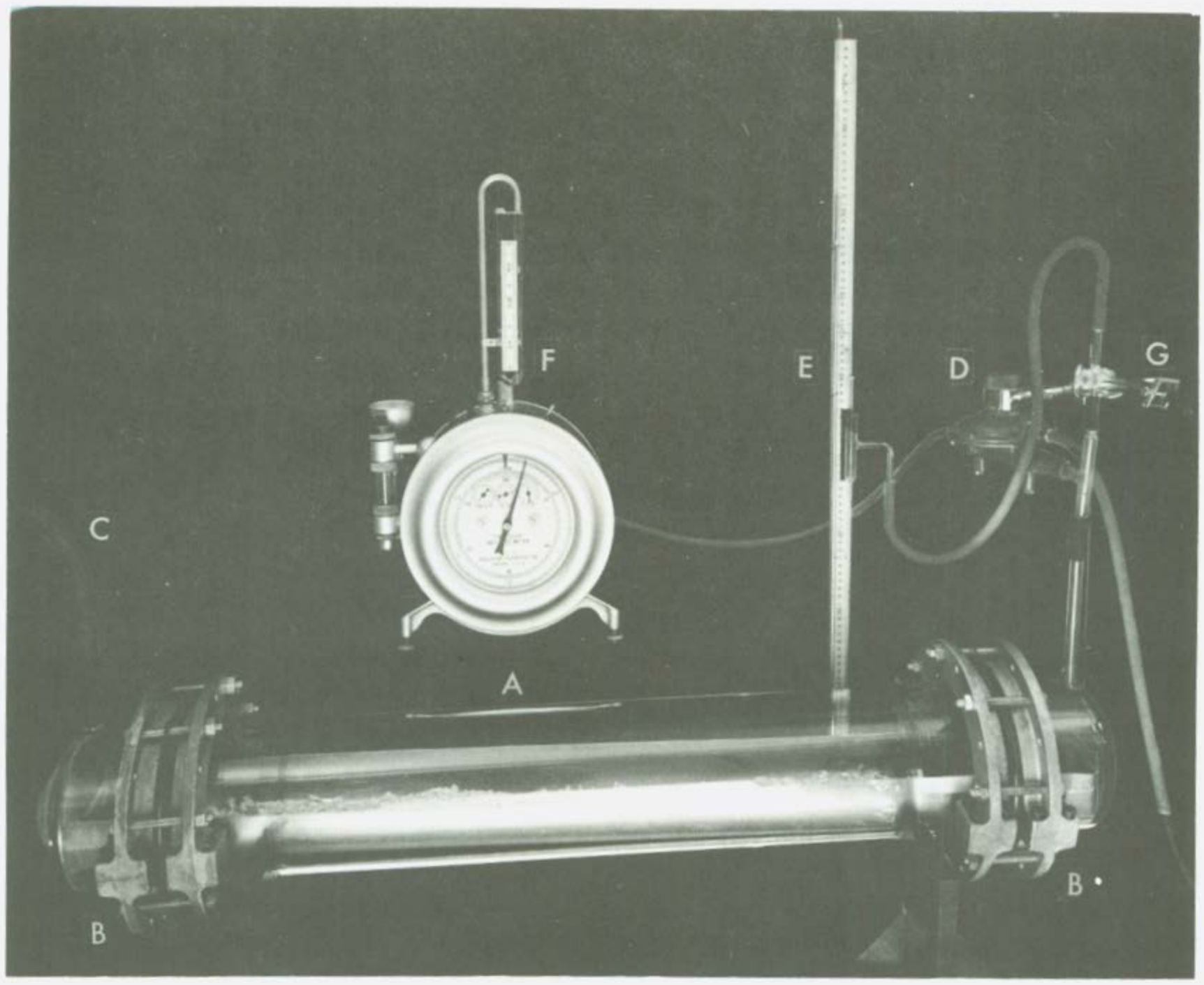

Figure 38 High altitude chamber and associated apparatus.

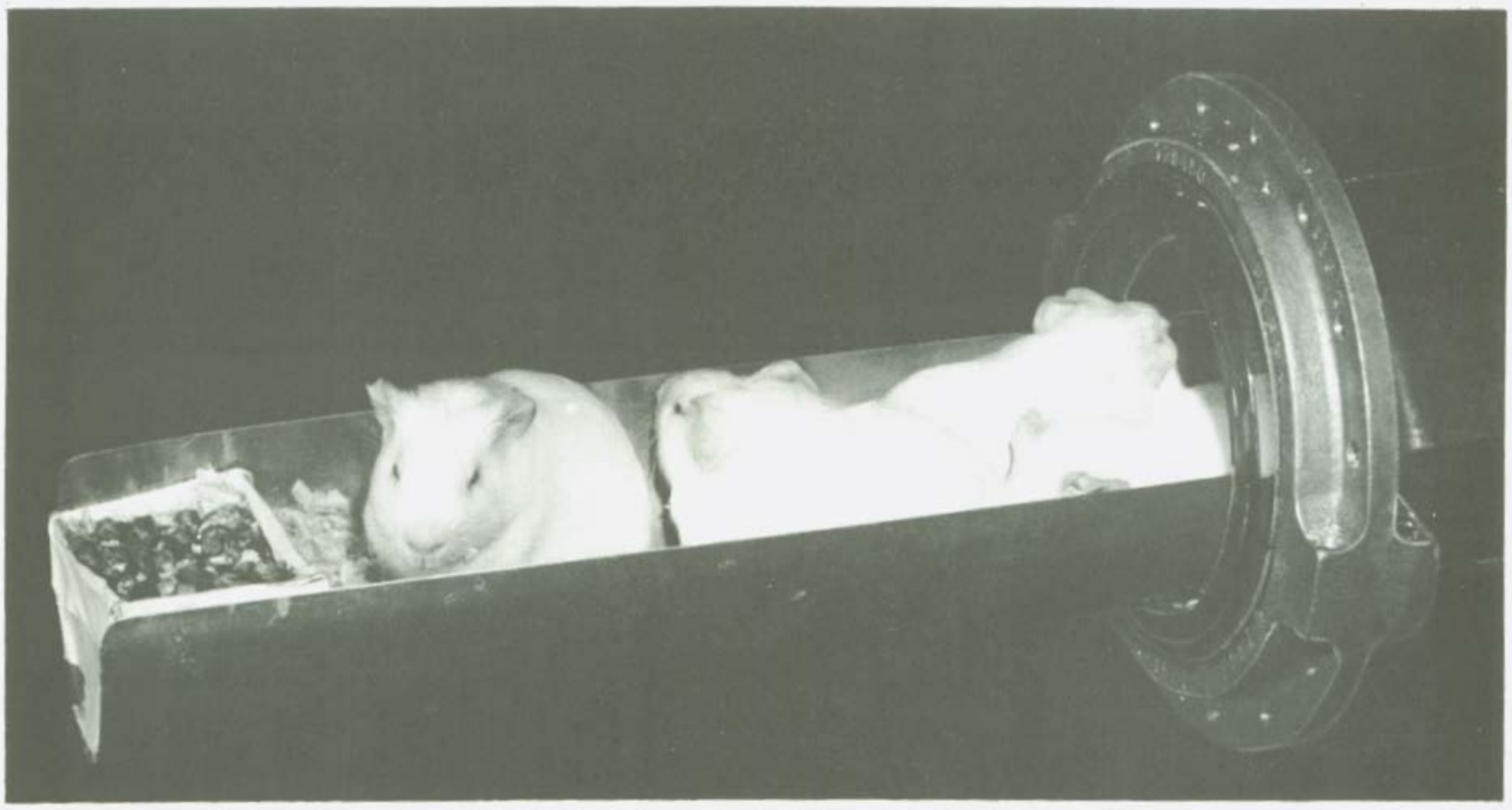

Figure 39 Loading of animals preparatory to initiation of hypoxia.

"escape" of the system. The airflow through the chamber is measured by a flow meter (F) attached to the intake tube; the capacity of the pump is sufficient to provide a flow of 12 liters per minute. Decompression of the animals is carried out slowly, by means of a screw clamp on a section of hose connected to a three-way valve (G). During the period of decompression, all air entering the chamber passes through the hose; when the desired pressure is reached, the three-way valve is reversed in position, allowing the regulated air passage to operate. The return to sea-level is carried out in a similar fashion, reversing the procedure.

The animals are usually loaded in the chamber in the late afternoon and maintained in the hypoxic condition overnight. This permits operation for a period of 16 hours out of every 24. They are removed in the morning to provide a normal atmospheric pressure during part of the day and to encourage their feeding. (Food and water which are provided in the chamber do not appear to be consumed in the usual quantities.)

Uses of the Chamber

The effect of high altitude on the mammalian organism has long been known to be predominantly on the hematopoietic system. Hypoxia therefore can be used to stimulate erythropoiesis, and thus to emphasize the associated metabolic pathways under nutritional or other conditions in which limitations prevail.

The proliferation of the spleen also presents an opportunity to investigate rapidly dividing tissue under physiological conditions, i.e., conditions in which all growth is new growth rather than regeneration such as that following sub-total hepatectomy. We have found that an adult guinea pig spleen will increase in weight from 400 mg. to 2000 mg. during 4 days of anoxia. At the same time, the uptake of P^{32} by deoxyribonucleic acid (DNA) increases by a corresponding factor; hence this technic lends itself to the study of DNA formation. There appears to be considerable species variation in the response of the spleen to hypoxia. While the guinea pig spleen enlarges some 5-fold, that of the mouse or rat will, during the same time interval, enlarge only by about 50% if at all. Here, then, is a possible means of ascertaining the nature of the triggering mechanism for the spleen response.

Another problem already under investigation, concerns the protection of animals against lethal doses of X-irradiation by the administration of perfusates of hypoxic spleens. A further description of this will be found in another report.(1)

We are grateful to Dr. Arthur Koch and to Messrs. Thomas Doody and William Eisler for their contributions to the construction of the pressure regulation systems. We wish also to thank Mr. Atlee S. Tracy for his excellent pictures of the apparatus, which involved unusually difficult photographic problems.

Reference

1. Stroud, A. N., and P. D. Klein. 1955. Studies on the protective effect of spleen perfusates from X-irradiated and hypoxic mice. Quarterly Report, Biological and Medical Division, Argonne National Laboratory ANL-5486, pp. 69-71.

STUDIES ON THE PROTECTIVE EFFECT OF SPLEEN PERFUSATES FROM X-IRRADIATED AND HYPOXIC MICE

Agnes N. Stroud and Peter D. Klein

Previous studies by Stroud et al.[1] have shown that the regeneration of the spleen following X-irradiation is characterized by foci of "red pulp" wherein extramedullary hematopoiesis takes place. When the organ is perfused with physiological saline solution these foci are less tenaciously retained than is the "white pulp,"* suggesting that it might be possible to remove these centers of immature stem cells selectively. The hypoxic spleen is similarly characterized by high hematopoietic activity, which reaches a level comparable to that of bone marrow.[2] It was deemed of interest to investigate the effect on the survival of irradiated recipients of cells or cellular elements released by perfusion of X-irradiated regenerating spleens and of hypoxic spleens. This report deals with the results of preliminary experiments.

Methods

The spleens used were obtained from mice which had been treated in one of three ways. The first group received 550 r 20 days prior to sacrifice. At this time the spleens are increased 2- to 3-fold in size over the controls, and mitoses in the regenerating foci are 2 to 3 times normal. The second and third groups had been subjected to high altitude acclimatization[3] for periods of $2\frac{1}{2}$ and $4\frac{1}{2}$ days respectively.

Each spleen was removed and quickly perfused with cold heparinized Tyrode's solution. A 24 gauge needle attached to a syringe was inserted into the organ lengthwise and the fluid perfused through the organ with pulsatile flow, permitting the spleen alternately to expand and drain. The perfusates were collected in a chilled beaker and centrifuged; the supernatant fluid was removed and the cells were made up to a known concentration volumetrically with heparanized saline. The perfused spleens were weighed, homogenized in 10 volumes of cold saline, and strained through gauze to remove connective tissue.

Recipient mice received 800 r 1 to 2 hours before injections of cells, homogenate, supernatant fluid or saline. All injections were intraperitoneal and the quantities were as listed in Table 14.

---

*We are indebted to Dr. Hermann Lisco for calling this to our attention.

Table 14

Protection of mice against 800 r by homologous perfusate cells, perfusate supernatant, and perfused spleen homogenate

Spleen source		Perfusate cells	Perfusate supernatant	Homogenate of perfused spleen	Saline
I 20 days after irradiation (550 r)	Weight injected*	100 mg	1 cc	250 mg	--
	Median survival time**	11.4 days	10.3 days	10.5 days	--
	Survival	3/10	0/6	2/8	--
II $2\frac{1}{2}$ days hypoxic	Weight injected	40 mg	2 cc	200 mg	--
	Median survival time	9.7 days	10.2 days	10.5 days	10.4 days
	Survival	3/6	0/10	3/10	0/10
III $4\frac{1}{2}$ days hypoxic	Weight injected	60 mg	2 cc	120 mg	--
	Median survival time	10.7 days	9.6 days	8.0 days	10.7 days
	Survival	4/10	0/10	3/15	0/10

*Assuming cell density of 1.00.

**All values based on 21-day survival.

Results

The median survival times and number of animals surviving for 21 days for each of the groups are shown in Table 14. The data suggest that it is possible to provide protection against an otherwise lethal dose of X-irradiation by injections of cells perfused out of spleens from irradiated or hypoxic animals. A statistical analysis showed that in the second and third experiments significant protection was obtained with the perfusates. In the combined results, no significant difference in protective effect could be found between the perfusate cells and homogenates of the perfused spleens, although, in each experiment, the number of survivors in the homogenate group represented a smaller percentage of the original group. Originally it was hoped that the protective effect would be found to be concentrated in the perfusate cells and, therefore, an excess of perfused spleen homogenate (2 to 5 times the weight of cells) was injected for comparison. However, the survival among the homogenate groups was unexpectedly high. In order to determine whether activity is concentrated in the cells it will be necessary to compare the effects of equal amounts of cells and homogenates, since a saturation effect may occur at a lower homogenate level. In addition, the perfusion of the spleens was in all probability incomplete. In no case was any protective effect noted in the supernatant perfusion fluid.

The protection afforded by the perfusate cells is consistent with the hypothesis that the spleen factor operates by colonizing new centers of hematopoiesis.(4) The perfusate cells were largely of the primitive or stem cell type present in active red pulp, although some cell types from "white pulp" were represented. Both the irradiated and hypoxic spleens might be expected to have larger numbers of the former type since both are characterized by extensive hematopoiesis. Further studies of the effectiveness of perfusates from these spleens are now under way.

References

1. Stroud, A. N., D. M. Chatterley, M. M. Summers, and A. M. Brues. 1955. Regeneration and recovery of the spleen and thymus after single doses of X-irradiation. Quarterly Report, Biological and Medical Research Division, Argonne National Laboratory. ANL-5456, p. 15.

2. Rambach, W. A., J. A. D. Cooper, and H. L. Alt. 1953. Nucleic acid metabolism of the bone marrow and spleen in the rat. NP-4881. United States Air Force Project 21-3501-0001. Report No. 1

3. Klein, P. D., and R. W. Swick. 1955. Design and use of a high altitude chamber. Quarterly Report, Biological and Medical Research Division, Argonne National Laboratory. ANL-5486, pp. 65-68.

4. Barnes, D. W. H., and J. F. Loutit. 1955. Spleen protection: the cellular hypothesis, in Radiobiology Symposium 1954, Z. M. Bacq and P. Alexander, eds. New York: Academic Press.

PROGRESS REPORT: FURTHER EXPERIMENTS ON SPLEEN PROTECTION

Howard S. Ducoff

Protective activity has been shown to reside in the spleens of CF#1 mice X-irradiated 14 days previously with 400 r or 17 to 24 days previously with 550 r. (Protective activity signifies that when homogenates are injected intraperitoneally to CF#1 females exposed 4 or 24 hours earlier to an otherwise uniformly lethal dose of 740 r, a number of the recipients survive for 30 days or more.) Spleens tested 12 days or less and 16 days or more after 400 r to the donors, and spleens tested 16 days or less after 550 r to the donors, exhibited no protective activity . The periods of protective activity appear to coincide with the times of maximum rate of increase in mitotic activity during post-irradiation splenic regeneration, as reported by Stroud et al.[1] Since they also reported a peak of mitotic activity in spleens two days after doses of 200 r, it appeared desirable to test for protective activity in spleens one, two, and three days after 200 r, as well as at longer time intervals. In this set of experiments, again only spleens of animals irradiated 14 days earlier, whether with 200 r or 400 r, exhibited protective activity.

Finally, C_3H mice, 18 days after 550 r, were used as spleen donors for CF#1 females exposed to 740 r. Four of 10 animals receiving the heterologous preparation survived more than 30 days, and three are still alive at the time of writing, 78 days after irradiation.

Reference

1. Stroud, A. N., D. M. Chatterley, M. M. Summers, and A. M. Brues. 1955. Regeneration and recovery of the spleen and thymus after single doses of X irradiation. Quarterly Report, Biological and Medical Research Division, Argonne National Laboratory. ANL-5456, pp. 15-25.

PROGRESS REPORT: AN EFFECT OF AMINOPTERIN ON THE ACUTE EFFECTS OF X-RADIATION

Howard S. Ducoff, Daniel J. Chatterley,* and Mildred M. Summers

During attempts to alter splenic regeneration in irradiated mice and to interfere with the activity of the spleen protective factor, mice were injected intraperitoneally with aminopterin one day prior to X-irradiation. Aminopterin (15 - 40 μg per mouse) did not interfere with splenic regeneration as indicated by spleen weight 14 days after 400 r, nor with the protective activity of such spleens for lethally irradiated recipients. Furthermore, aminopterin at levels of 40 - 120 μg per mouse given one day prior to various doses of X-radiation increased mortality very slightly if at all (Table 15). There is, however, a reduction in mean survival time of non-survivors, due to a sizeable proportion of early (5 - 7 day) deaths. When similar experiments were done with rats, a comparable decrease in mean survival time was found, accompanied by an increased mortality (Table 16). These results suggest additivity of the effects of the two agents on the intestinal tract, rather than on the hemopoietic system.

It is planned to extend these experiments by varying the time interval between injection and irradiation, by bacteriological examination of preselected animals, and by testing substituted purines with clinical effects similar to those of aminopterin.

Table 15

Effect of aminopterin on mice (12 per group)

	120 μg./mouse		Saline	
	Mortality	MST	Mortality	MST
700 r	75%	8 days	83%	13 days
600 r	8%	5	42%	14
500 r	42%	7	25%	15
400 r	25%	4	0	-
0 r	0	-	-	-

*Resident Student Associate

Table 16

Effect of aminopterin on rats (9 per group)

	750 μg./rat		Saline	
	Mortality	MST	Mortality	MST
750 r	100%	7 days	78%	15 days
550 r	78%	7	0	--
0 r	0	-	-	--

LACK OF EFFECT OF CHLORPHENERGAN ON THE LETHALITY OF WHOLE BODY X-IRRADIATION

Robert N. Feinstein

In an earlier report,[1] it was noted that the anti-histaminic, autonomic-depressant drug Phenergan gave some evidence of therapeutic activity in mice and rats which had received lethal doses of whole body X-irradiation. However, the therapeutic action was not sufficiently striking statistically to make the agent of practical importance.

The thought occurred that it might be of value to screen chemically related compounds. In answer to request, the Wyeth Laboratories' Dr. Daniel L. Shaw, Jr., to whom I wish to express thanks, kindly supplied a sample of Chlorphenergan, a compound in which a single chlorine atom is added to the phenothiazine ring of Phenergan. In all other respects, the two drugs are chemically identical.

Chlorphenergan has now been thoroughly tested in both rats and mice for therapeutic or prophylactic effect against whole body X-irradiation. In no case has the compound been found to have any value whatever, either in reducing the percent mortality, or in increasing the average survival time.

Reference

1. Feinstein, R. N. 1955. Effect of Thorazine and Phenergan on survival of rats and mice after lethal doses of whole body X-radiation. Quarterly Report, Biological and Medical Research Division, Argonne National Laboratory. ANL-5426, p. 128.

POSSIBLE RELATIONSHIP OF MOUSE LIVER CATALASE LEVEL TO STRAIN SENSITIVITY TO X RAY

Robert N. Feinstein and Sara Berliner

Catalase, the widely distributed enzyme responsible for the decomposition of hydrogen peroxide, is extremely sensitive, at least in the mammalian organism, to a wide variety of diseases and environmental and other circumstances. This nonspecific sensitivity is attested to by literally hundreds, perhaps thousands, of literature references to the level of catalase activity in the blood and tissues in various conditions. One observation among the deluge was made by the senior author;[1] it was noted that appreciable variation in liver catalase activity often occurred between two shipments of otherwise comparable mice. A further observation of interest was the finding[2] that of a given shipment of rats, those individuals with the lowest blood catalase appeared generally to be the most susceptible to the lethal effects of X-radiation. This combination of observations led us to test the hypothesis that among various strains of inbred mice, there might be a correlation between the level of liver catalase activity and the sensitivity to whole body X-irradiation. Liver catalase was measured, rather than blood catalase, because it has been shown[3] that in the mouse the liver accounts for approximately 67% of the total catalase of the body, while the blood accounts for only approximately 25%.

The following strains of mice were tested:* A/jax, Balb/c, C_3H, and $C_{57}Bl/6$. Only males were used. Catalase assays were done by the perborate method[4] on whole homogenates of liver. Results are given in Table 17, in which catalase data are expressed as the perborate units (PU) per gram of liver. Figures are the mean and the average deviation from the mean.

Table 17

Mouse liver catalase activity and strain sensitivity to X-rays

Strain	No. of mice	Catalase activity (PU/gm liver)	LD_{50} to X-rays (r)
$C_{57}Bl/6$	3	470 ± 57	630
A/jax	3	487 ± 42	545
Balb/c	6	501 ± 75	505
C_3H	6	654 ± 81	590

*We wish to thank Dr. Douglas Grahn and Miss Katherine Hamilton for the mice used, and for information on the LD_{50}.

It is apparent from the data of Table 17 that there is no significant correlation between liver catalase and strain sensitivity to X ray. There is apparently so great a liver catalase variation between litters as to mask any possible strain variance. This is indicated by the fact that two litters of C_3H mice were used; these assayed 708 ± 41 (4 mice) and 545 ± 51 (2 mice), respectively.

References

1. Feinstein, R. N., C. L. Butler, and D. D. Hendley. 1950. Effect of whole body X-radiation and of intraperitoneal hydrogen peroxide on mouse liver catalase. Science 111, 149.

2. Feinstein, R. N., M. Hampton, G. J. Cotter, and J. C. Ballin. 1953. Blood level of catalase or carboxypeptidase inhibitor as possible indicator of individual resistance or sensitivity to whole body X-irradiation. U. S. Air Force Radiation Laboratory, Quarterly Report 7, 55.

3. Feinstein, R. N., M. Hampton, and G. J. Cotter. 1953. Species specificity of catalase. Enzymologia 16, 219.

4. Feinstein, R. N. 1949. Perborate as substrate in a new assay of catalase. J. Biol. Chem. 180, 1197.

AN ACTIVATOR OF DEOXYRIBONUCLEASE IN RAT PLASMA

Robert N. Feinstein and Frank O. Green*

The existence of deoxyribonuclease (DNAase) activity in blood plasma has recently been established by Kowlessar, Altman, and Hempelmann.(1) It has not, however, been previously reported that plasma also contains an activator of DNAase I (pH optimum ca. 7.5).

In observing the effect of blood fractions on the activity of commercial (Worthington) crystalline DNAase by a viscosimetric method,(2) it was noted that the addition of normal plasma caused a considerable surge of activity. In a typical instance, the half-time (i.e., time required to reduce the intrinsic viscosity of the mixture to half its initial value) was 62 seconds for the crystalline enzyme, and 16 seconds for the crystalline enzyme plus normal rat blood plasma. The half-time for the plasma alone (no other enzyme added) was 3212 seconds. On the assumption that these represented first-order reactions, the slopes of the three curves were calculated to be:**

(a) crystalline DNAase alone: 0.5820

(b) crystalline DNAase plus plasma: 0.8275

(c) plasma alone: 0.0144 .

It is thus evident that the enzyme activity of the plasma alone can by no means account for the increase in activity when plasma is added to a preparation of crystalline enzyme.

An independent demonstration of the same phenomenon is afforded by Figure 40. In this case, the diphenylamine reaction of Dische,(4) as applied by Allfrey and Mirsky,(5) was used in order to permit straight-forward addition of effects produced by plasma and by the crystalline enzyme. Here again it is obvious that, in the early stages of the reaction at least, the enzyme activity of the plasma alone cannot account for the increased activity of the crystalline enzyme-plasma combination. Activity is terminated, as shown in the upper curve, by complete solubilization of the DNA present.

---

*Resident Research Associate from Wheaton College.

**We wish to thank Mr. Sylvanus A. Tyler for the calculations.

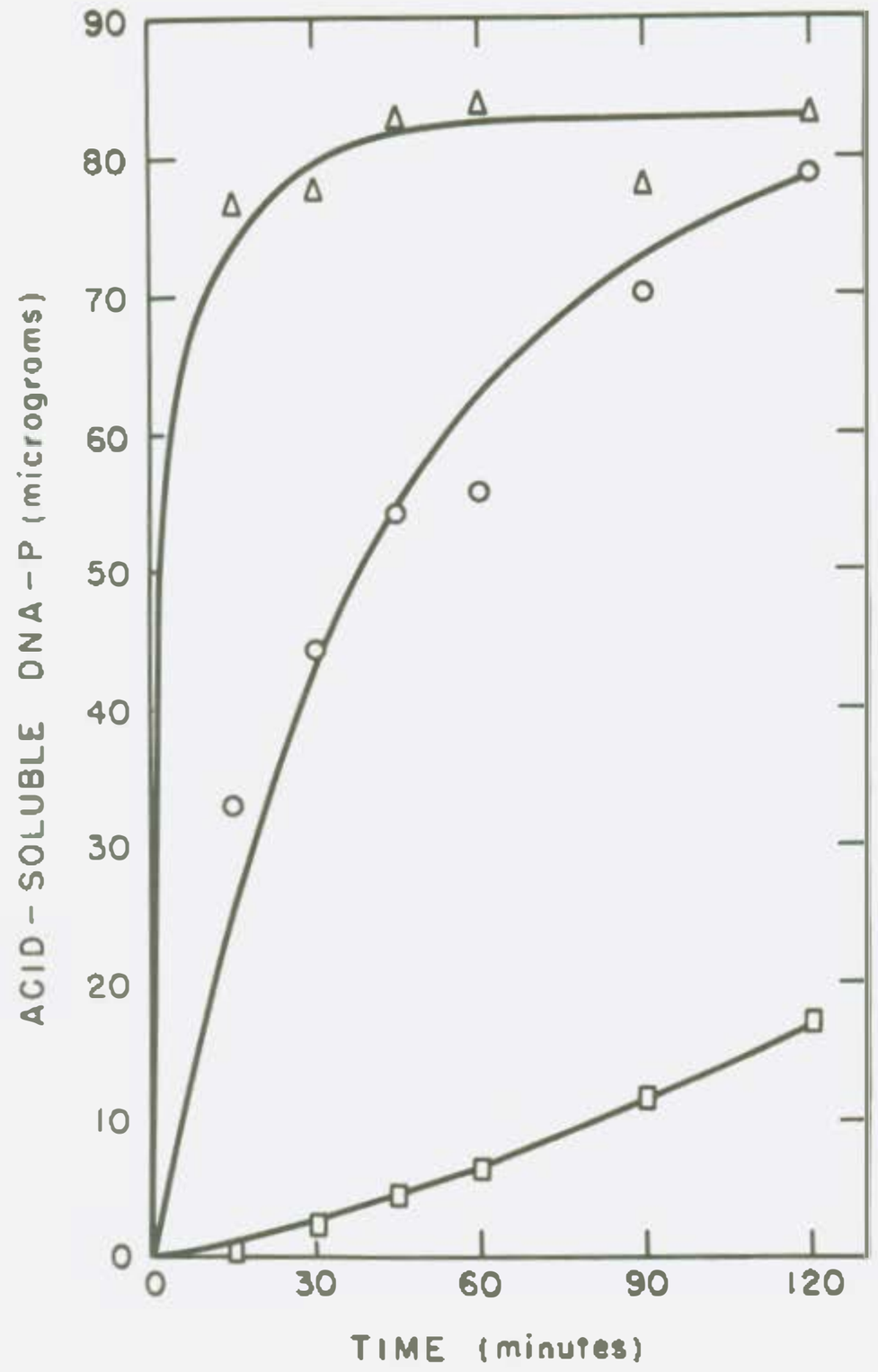

Figure 40 Effect of normal rat blood plasma on DNA and DNAase

plasma alone

crystalline DNAase alone

crystalline DNAase plus plasma

The activator is heat-stable; 100°C for five minutes caused no noticeable loss. The possibility has been considered that the Mg^{++} content of the plasma may be the responsible agent. This is not the case, as evidenced by two considerations: (a) the test systems are already so rich in Mg^{++} (final Mg^{++} concentrations are 0.090 M in the viscosimetric system and 0.043 in the diphenylamine assay system) as to render it unlikely that the slight additional Mg^{++} of the plasma could have any appreciable effect; (b) increase of the Mg^{++} concentration to 0.10 M in the viscosimetric assay and to 0.086 M in the diphenylamine test did not cause activation.

References

1. Kowlessar, O. D., K. I. Altman, and L. H. Hempelmann. 1955. The effect of ionizing radiation on deoxyribonuclease activities of body fluids. II. The plasma deoxyribonucleases after total body irradiation. Arch. Biochem. Biophys. 54, 355-358.

2. Henstell, H. H., and R. I. Freedman. 1952. The viscosimetric determination of desoxyribonuclease inhibition. Cancer Research 12, 341-345.

3. Dische, Z. 1930. Some new characteristic color tests for thymonucleic acid and a microchemical method for determining the same in animal organs by means of these tests. Mikrochemie 8, 4-32.

4. Allfrey, V., and A. E. Mirsky. 1952. Some aspects of the desoxyribonuclease activities of animal tissues. J. Gen. Physiol. 36, 227-241.

THE INITIAL RADIATION SYNDROME IN THE ADULT CHICKEN

S. Phyllis Stearner, Margaret H. Sanderson, Emily J. Christian
and Austin M. Brues

In the adult rooster a dose-rate-dependent early mortality followed exposure to X rays. A moderate decrease in blood pressure occurred soon after irradiation but a critical hypotension was not seen during the initial post-irradiation period. The urate excretion rate increased during the first 10 to 12 hours after exposure, both in 24-hour survivors and in non-survivors. Apparently, the slight fall in blood pressure that follows irradiation is not sufficient to affect renal function directly; in addition, the epithelium of the adult kidney is not radiosensitive as is that of the young chick. In spite of the increased rate of urate excretion, however, the blood concentration of urate increased during this period, indicating an increased rate of formation.

Although adult chickens showed no severe hypotension and maintained a normal renal function after X-irradiation, the initial mortality was comparable to that of similarly exposed chicks. However, there is qualitative evidence of a progressive decrease in circulatory efficiency in the initial period, both in adults and in young chicks; and circulatory failure may be a common factor in the two age groups. Comparison of the effects in the two groups of a period of sustained hypotension induced by hemorrhage indicates that the adults are better able to compensate for severe loss of circulatory volume than are young chicks.

EMBEDDING OF LARGE BONE SPECIMENS

William P. Norris and Lois Woodruff Speckman

"Scotchcast" (Minnesota Mining and Manufacturing Company) is an epoxy-type casting resin designed for electrical insulating; it is being used for embedding large pieces of bone. The "cold pouring" form consists of a viscous resin and a liquid hardener. Upon combination, the mixture polymerizes rapidly at room temperature. This material has several advantages over others currently used for similar purposes: (1) it will cure at room temperature in 3-6 hours without air bubbles, (2) it is characterized by high adhesion and low shrinkage, (3) it is easily machined, and (4) it is resistant to most chemicals. The only disadvantage of this polymer in our work is its reduced transparency due to the pale amber color typical of epoxy resins.

Blocks containing bones have been machined and polished to produce a very flat, smooth surface. Excellent contrast radioautographs can be made from those blocks containing radioactive bones (Figure 41).

The method is currently being refined. After thin longitudinal sections of whole bones have been embedded in this resin, they have been machined and polished down to produce sections 15-30 microns thick in pieces of plastic as thick as ordinary microscope slides.

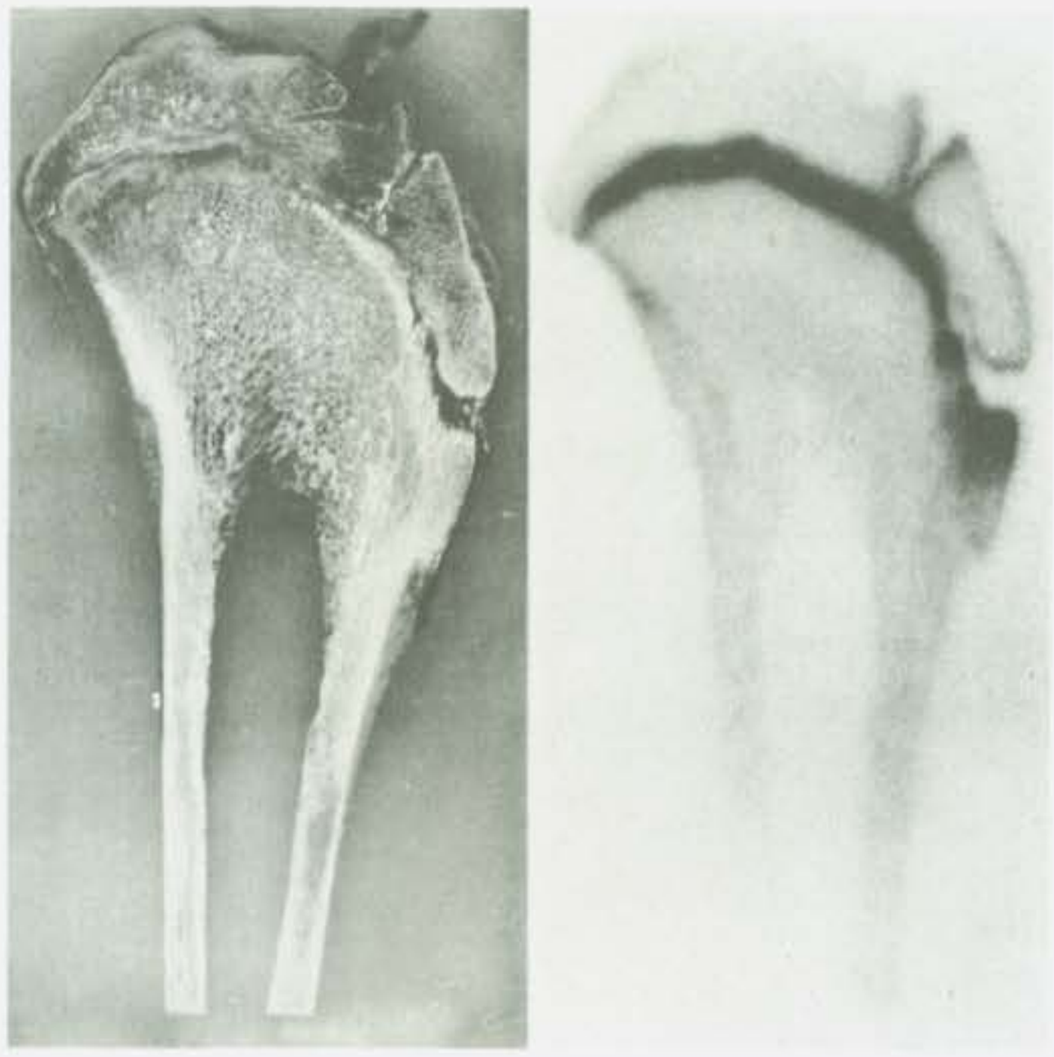

Figure 41 Left: A "Scotchcast" block containing the proximal end of the tibia of an adult pig. Right: A contrast radioautograph of the same block.

FURTHER STUDIES ON THE EFFECT OF IN VIVO FORMATION OF A CHELATING AGENT ON EXPERIMENTAL PLUMBISM

Joan F. Fried and Marcia White Rosenthal

Previous experiments have indicated that in rats intraperitoneal administration of sodium fluoroacetate in sublethal doses results in a marked increase in citrate levels of the tissues[1] due to blocking of the Krebs cycle.[2] Other experiments have shown that injected sodium citrate, either by intravenous or intraperitoneal route, is rapidly excreted and does not accumulate in the tissues.[3] Recently we showed that the enhanced citrate levels induced by sodium fluoroacetate administration are of therapeutic value in experimental plumbism resulting from the intravenous injection of lead nitrate ($Pb(NO_3)_2$) at a level of 70 mg/kg (ca. LD_{90}).[4] It is believed that this protection is brought about by the chelating action of the citrate in the tissues with lead ions to form a soluble inactive complex.

In order to evaluate the extent of this protection a large scale survival study has been conducted. Two groups of 85 healthy Sprague-Dawley female rats, ages 11 and 19 weeks, weighing 230-265 grams were selected. These were evenly distributed into groups according to the dose of Pb injected as shown in Table 18. All animals received $Pb(NO_3)_2$ injected intravenously in the tail vein using a 6.4% solution in distilled water. The treated animals were given a 0.005% solution of sodium fluoroacetate in distilled water, administered intraperitoneally at 22 and at 5 hours prior to the lead injection, and at 8, 19 and 25 hours after the lead injection; the dose was 0.30 mg/kg per injection (a total of 1.5 mg/kg over a 3-day period). The untreated animals were given saline intraperitoneally in equivalent volume at these time intervals. Animals were caged in such a manner as to eliminate all possible "cage effects."

Table 18

Dosage schedules

Pb dose in mg/kg	No. animals	
	Treated	Untreated
50	10	10
55	10	20
60	20	20
65	20	20
70	20	20

Since statistical analysis revealed no significant difference between the results obtained with the two age groups, the data were combined and probit curves made (Figure 42). Examination of the curves reveals a shift in the LD_{50} value of lead nitrate as Pb from 58.2 mg/kg ($\pm\sigma$ 4.3%) for the untreated (saline controls) to 67.7 mg/kg ($\pm\sigma$ 3.1%) for the treated animals. This difference has been found to be significant at the 5% level ($.05 < P < .02$). As was to be expected from a consideration of the mechanism of protection (i.e., a reduction in the concentration of toxic lead ions), the two curves obtained from the treated and untreated animals show no significant difference in slope ($t_b = 0.32$).

While the increase in the LD_{50} value of Pb resulting from fluoroacetate treatment is somewhat small it is of interest in that it demonstrates the possibility of utilizing therapeutically an induced in vivo production of naturally occurring chelating agents.

The authors wish to express their appreciation for the assistance of Mr. Sylvanus Tyler and his group in the statistical analysis of the data, and for the competent assistance of Elizabeth Moretti.

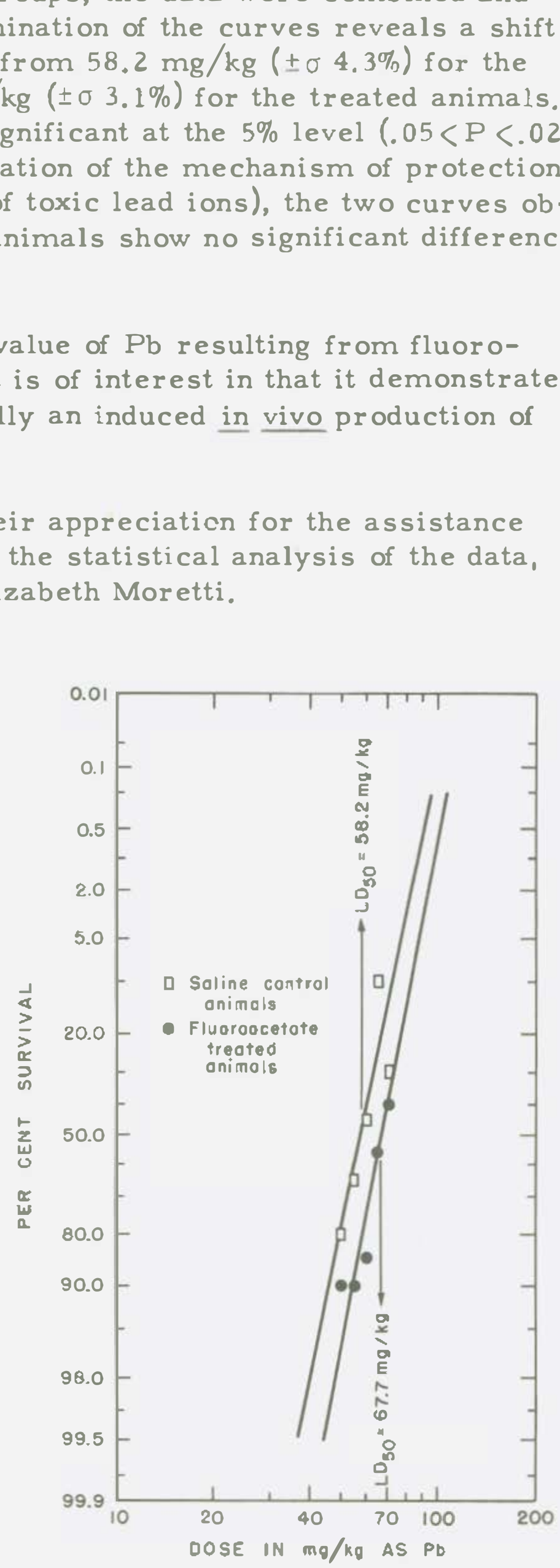

Figure 42 Survival curves of sodium fluoroacetate-treated and saline control groups.

References

1. Lindenbaum, A., M. R. White, and J. Schubert. 1951. Citrate formation *in vivo* induced by non-lethal doses of fluoroacetate. J. Biol. Chem. 190, 585-593.

2. Peters, R., R. W. Wakelin, and P. Buffa. 1953. Biochemistry of fluoroacetate poisoning. The isolation and some properties of the fluorotricarboxylic acid inhibition of citrate metabolism. Proc. Roy. Soc. (London) B, 140, 497-507.

3. Rosenthal, M. W., and J. F. Fried. Unpublished data.

4. Fried, J. F., and M. W. Rosenthal. 1955. The effect of fluoroacetate administration on experimental plumbism. Quarterly Report, Biological and Medical Research Division, Argonne National Laboratory. ANL-5378, p. 178.

ASCITES TUMOR CELLS AND RETENTION OF INTRAPERITONEALLY INJECTED I^{131}-LABELED HUMAN SERUM PROTEIN

Robert L. Straube and Marian S. Hill

The accumulation of intravenously-injected labeled protein in the peritoneal cavities of mice after inoculation with ascites tumor cells apparently involves a primary increase in vascular permeability.(1) Since tumor cells supposedly increase the effective endothelial "pore" size, one might assume that tagged proteins would leave the peritoneal cavity more rapidly in tumor-bearing mice. This, however, does not occur. There is a greater retention of labeled protein after injection into the peritoneal cavities of tumor-bearing mice. Penetration into the blood stream is also less rapid than in the case of normal mice. Thus, 2 hours after inoculation with 20×10^6 tumor cells, 14% of labeled protein is still present in the peritoneal fluid in contrast to the normal retention of about 9%. These levels are reflected in the corresponding blood plasma concentrations (26% versus 37%). This is due in part to the fact that the main route of escape from the peritoneal cavity is through lymph channels rather than by back diffusion into the vascular bed. An analogous distribution of protein occurs in the inflammatory response evoked by a variety of irritants.(2) Menkin(3) ascribes the retention of protein in the inflamed peritoneal cavity to the occlusion of lymphatics by fibrin clots, a consequence of fibrinogen accumulation resulting from the primary increase in vascular permeability.

To further elucidate the role played by the lymphatics, an attempt was made to block these channels: 20% India ink was injected intraperitoneally 4 hours prior to inoculation. This resulted in an increased retention of I^{131}-tagged albumin in the peritoneal cavity (7.3% of the injected activity at 2 hours, as compared to 3.5% in the control animals), but the values never reach that normally produced by tumor cells (11.1%). The retention in blockaded and non-blockaded tumor-bearing groups does not differ statistically.

References

1. Straube, R. L., and M. S. Hill. 1955. Vascular permeability and Krebs 2 ascites tumor growth. Quarterly Report, Biological and Medical Research Division, Argonne National Laboratory. ANL-5378, p. 71

2. Menkin, V. 1953. Recent studies on repair and on the mechanism of suppression by anti-inflammatory steroids. in Mechanism of Inflammation, ed. G. Jasmin and A. Robert, Montreal: Acta. p. 148.

3. Menkin, V. 1950. Newer Concepts of Inflammation. Springfield: Thomas. pp. 40-46.

THYROID DISTRIBUTION AND FUNCTION IN THE GOLDFISH AS DETERMINED BY THE UPTAKE OF TRACER DOSES OF I^{131}

Walter Chavin*

In most teleosts the thyroid consists of scattered follicles along the ventral aorta in the throat area. Recently, however, histologically normal thyroid follicles were found in the lymphoidal pronephric remnants, the head kidneys, of the goldfish, Carassius auratus L. The epithelium of these follicles was found to respond to physiologic stimuli in a manner similar to that of the throat area. This raised the question of the utility of the head kidney follicles in the physiology of the goldfish. The purposes of the present study, therefore, were to determine the radioiodine uptake in goldfish subjected to various experimental conditions, and to localize this iodine histologically by autoradiographic means.

A total of 146 common xanthic goldfish, 1 - 2-1/2 inches in length, and less than one year of age, were used in this study. Tracer doses of radioiodine (5 μc per fish) were administered intraperitoneally. The animals were maintained in groups of four, and all measurements are expressed as mean values for each group. After the injection of NaI^{131} the radioiodine uptake by the throat thyroid reached a maximum of approximately 3% within 1 hour, and this value remained fairly constant for the duration of the 20-day experimental period (Figure 43). In the head kidney the iodine trapping rate was slower, reaching a peak of 5% at 24 hours and remaining at this level. Thus a total of approximately 8% of the administered iodine was retained by thyroid tissue.

On the other hand, after the injection of radioiodinated serum albumin the maximal accumulation of iodine by the throat thyroid occurred at 24 hours after injection, whereas the uptake by head kidney rose during the entire course of the experiment (Figure 44). The total thyroid uptake at 10 and at 20 days was 10% of the injected dose. These total uptake values are much higher than those reported for the goldfish by Berg and Gorbman;[1] this species, although not an avid collector of iodine, apparently falls within the lower range of iodine accumulation characteristic of fresh water teleosts.

The relative activity of the thyroid in the throat and head kidney, as indicated by I^{131} uptake, was variable. In the normal goldfish after maximum uptake had occurred, the head kidney was more active in 47% of the fish, the throat thyroid in 23%, and in 20% the two thyroid areas were approximately equal in activity. In 10% of the fish studied, radioiodine was not accumulated in the head kidney, and histological study of the autoradiographs of this area indicated that thyroid follicles were absent. Counts of the number of follicles in the head kidney and in the throat revealed no correlation between the number of follicles and I^{131} uptake.

---

*Resident Research Associate from Wayne University.

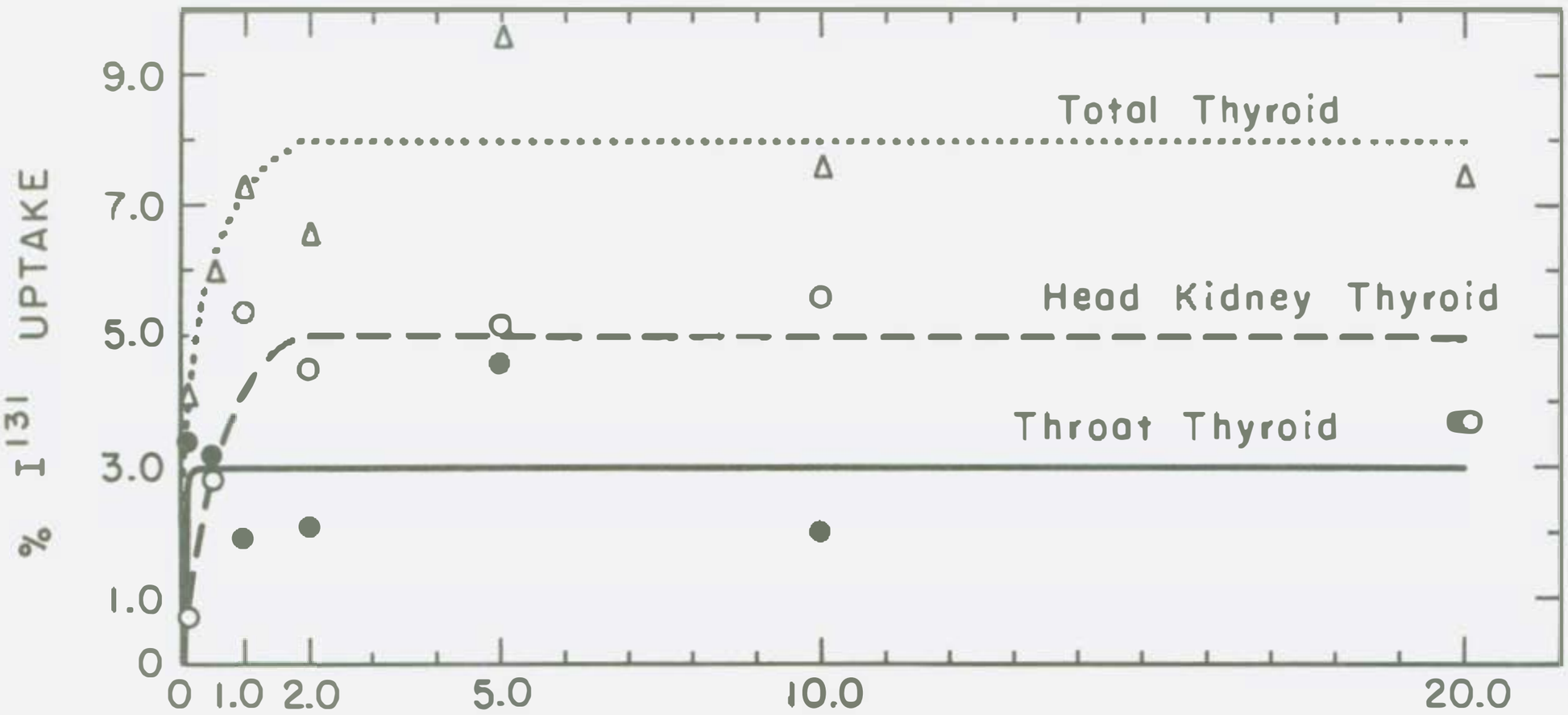

Figure 43 I^{131} uptake of goldfish after injection of 5 μc. NaI^{131}

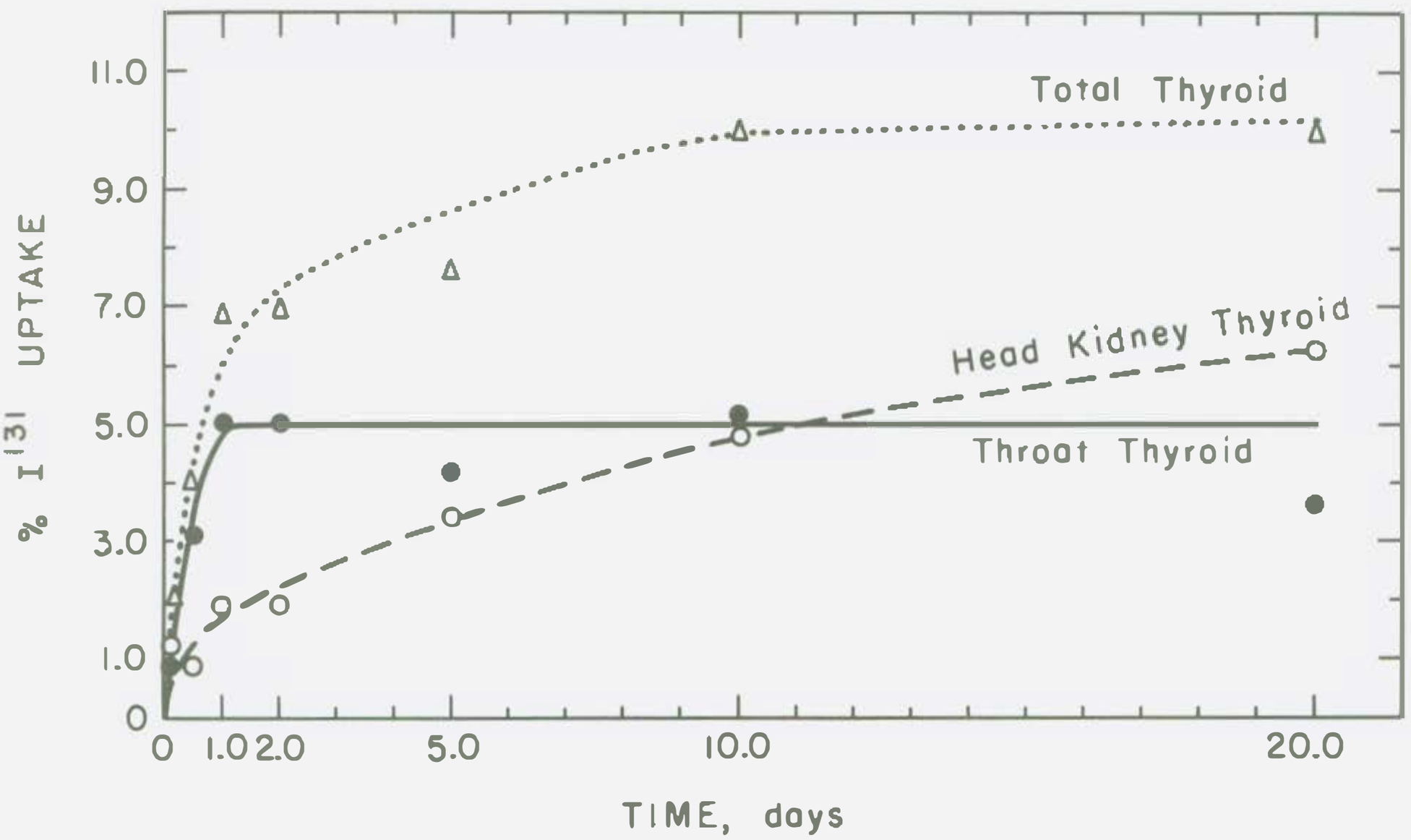

Figure 44 I^{131} uptake of goldfish after injection of 5 μc. radioiodinated serum alubumin

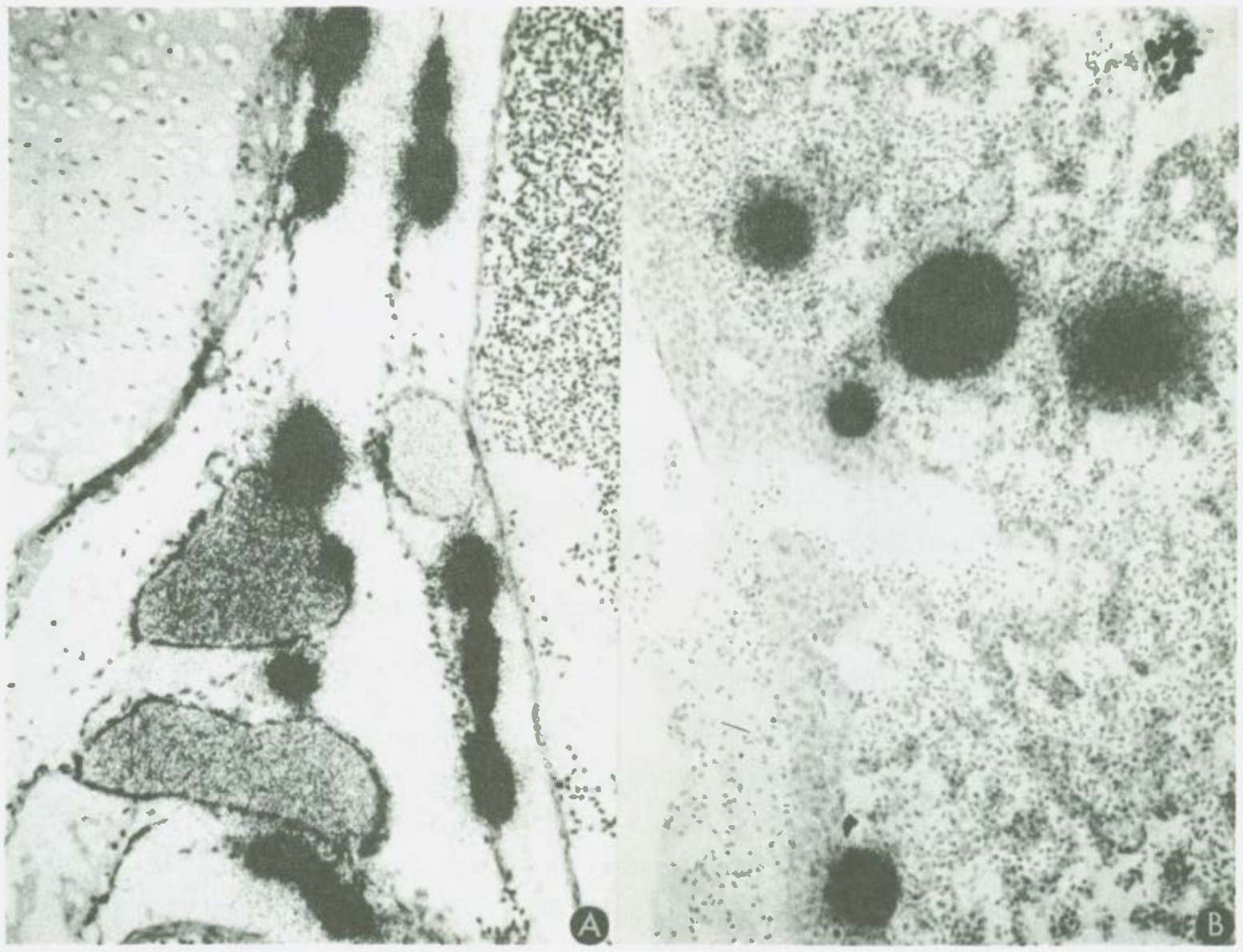

Figure 45 Autoradiographs of normal goldfish thyroid

A. Throat thyroid

B. Head kidney thyroid

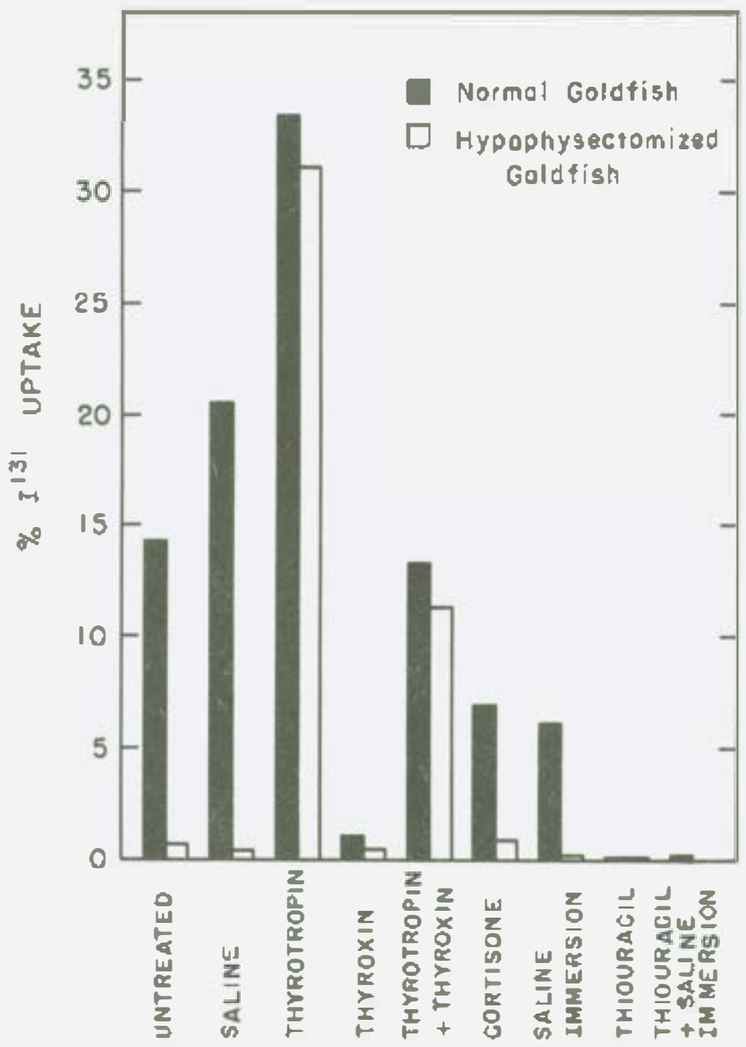

Figure 46 Thyroidal iodine uptake in normal and hypophysectomized goldfish after experimental treatment.

Injected NaI^{131} was rapidly excreted, for within 24 hours after injection, approximately 65% of the radioiodine could be detected in the aquarium water. At 20 days, approximately 16% was retained. I^{131}-bound serum albumin was retained to a considerably greater extent; 87% and 40% of the injected dose remained unexcreted at 1 and 20 days respectively.

Autoradiographs of the head kidney and throat regions reveal that radioiodine was present only in thyroid follicles (Figure 45). The follicular iodine uptake, as indicated by the density of the silver particles in the film, varied considerably. Generally the smaller follicles were more active in trapping iodine (Figure 45A). The animals which had a high head kidney iodine uptake usually had highly active follicles, but not necessarily a larger number.

The throat and head kidney thyroid tissue reacted similarly to experimental treatment, indicating that, functionally as well as structurally, the head kidney thyroid is normal thyroid tissue. That the activity of the goldfish thyroid is controlled by the pituitary is shown by the finding that hypophysectomy decreases iodine accumulation to less than 1/20 of the normal value (Figure 46). Administration of thyrotropin produces a 234% increase in iodine uptake by intact fish, and more than a 3000% increase in hypophysectomized fish. As expected in the light of mammalian studies, thyroxin, cortisone, thiouracil or the stress of saline immersion decreased thyroid activity in normal goldfish, but produced no effect in hypophysectomized fish. Slight stimulation occurred in normal fish after saline injection.

In addition, thyroxin inhibited the response of both normal and hypophysectomized fish to thyrotropin, indicating this action is not mediated via the hypophysis but is a direct effect upon the thyroid cell. Since thyroid epithelial hypertrophy is stimulated to approximately the same extent in thyrotropin and in thyrotropin-thyroxin treated fish, it appears that thyroxin inhibits the iodine trap and thus diminishes hormone synthesis within the cells, as recently postulated for the rat.(2) It would seem, therefore, that the endocrine mechanisms controlling thyroid function in the goldfish are basically similar to those in mammals.

References

1. Berg, O. A., and A. Gorbman. 1954. Normal and altered thyroidal function in domesticated goldfish. Proc. Soc. Exptl. Biol. Med., 86, 156-159.

2. Vander Laan, W. P. 1955. The biological significance of the iodide-concentrating mechanism of the thyroid gland. Brookhaven Symp. Biol., 7, 30-39.

RELATIONSHIP OF BORON NUTRITION TO RADIOSENSITIVITY OF SUNFLOWER PLANTS

John Skok

In plants, the absence of boron for even short intervals results in retardation of cellular activity and in arrest of growth. Since radiosensitivity is related to cellular and metabolic activity, it might be expected that some relationship exists between radiosensitivity and boron nutrition. Experiments designed to test for the presence of such a relationship indicated that it does in fact exist.

Sunflower seeds (var. Mammoth Russian) were sown in quartz sand; one week later the seedlings were transplanted to nutrient solutions either with or without boron. After maintenance in these solutions for as short a time as two days (or in other experiments up to five days), the plants were X-irradiated with 1000 r. (This dosage was selected after 100, 500, 1000, 2000, and 5000 r had been tried. Sunflower was found to be relatively radiosensitive when compared with other higher plants.)

Immediately after X-irradiation or on the following day the plants were transferred to complete nutrient solutions containing boron, where they were maintained for subsequent observations. In some cases they were later transplanted to soil and kept for periods up to 70 days from the time of irradiation.

Typical radiation symptoms, such as speckling and mottling of leaves, distortion of leaves, and general retardation of growth resulted from exposure of young seedlings to 1000 r. At the higher dosages death of the growing tips and eventually death of the entire plant generally resulted. These plants were irradiated when each seedling consisted of an axis and expanded cotyledons, with the first pair of leaves partially emerged but not fully expanded.

In the case of plants not deprived of boron prior to irradiation, these leaf symptoms in response to 1000 r appeared in all subsequently developed leaves up to the 26th to 28th pair, 70 days after irradiation. In the case of plants similarly treated except that they were maintained on boron-deficient solutions for short periods prior to irradiation, the symptoms appeared only in the first 6th to 7th pairs of leaves. After these leaves had been produced the plants recovered completely from the radiation effects; the leaves that were produced subsequently were normal and free from all radiation symptoms. These plants were also considerably less stunted than those in which there were no periods of boron deprivation.

These results conform to what would be expected in the light of our knowledge concerning boron nutrition in plants and to our general knowledge concerning radiosensitivity and radioresistance: a reduced rate of cellular activity brought about by withholding boron results in greater radioresistance. They further suggest the possible utilization of this experimental approach in the study of some of the other essential mineral elements, with the possibility of obtaining further information on their function in growth and cell division.

Th^{227} ACCIDENT

Philip F. Gustafson and Leonidas D. Marinelli

A member of the laboratory received a Th^{227} burden via a puncture wound in the right index finger caused by a pair of forceps. Two days prior to the accident the forceps had been dipped into a newly extracted Th^{227} solution. The first determination of radioactive body burden was made 4 days after the accident by measuring the γ-ray activity with a scintillation counter, using the standard chair position as is done in the case of Ra^{226} burdens.(1) The estimated radioactivity in the index finger was sufficiently high to warrant removal of the tissue surrounding the wound. Total body and index finger activity were measured again after surgery. The γ-ray spectrum of the tissue sample was taken as an aid in determining the relative amounts of Th^{227} and Ra^{223} present, i.e., in determining per cent of secular equilibrium.

Th^{227} has a half life of 18.6 days and alpha decays to Ra^{223} (half-life 11.2 days). Four more alpha and two beta decays occur before a stable isotope of lead is formed; however, all these Ra^{223} daughters have very short half lives so that secular equilibrium is quickly reached.

In order to estimate body burden accurately, the state of equilibrium must be known. Comparison of the gamma spectrum of the tissue sample with spectra of Th^{227} in various stages of equilibrium provided this information. Calibration with sources of Th^{227} and Ra^{223} of known activity then made it possible to calculate the amount of radioactivity removed surgically and to estimate the activity remaining in the body. Some uncertainty remains concerning the first total body estimate, since the degree of radioactive equilibrium present in the vicinity of the wound and in the body as a whole may not have been the same. Subsequent measurements of total body activity were less subject to this uncertainty, since the data was taken by means of a 24 channel analyzer; thus the gamma spectrum emitted from the body as a whole was obtained. The iron room was used in counting the subject in order to obtain higher counting rates relative to background. The gamma spectra of Th^{227} and Ra^{223} were taken at different depths in a suitable "presdwood" phantom (20 x 30 x 30 cm.) using calibrated sources. Composite spectra were then formed by adding fractions of the Ra^{223} spectrum to that of Th^{227}. In this way it was possible to match the total body gamma spectrum and thus determine the degree of equilibrium present. A breakdown of the total body activity in terms of microcuries of Th^{227} and Ra^{223} is given in Table 19.

A comparison of these values with those of simple radioactive decay is shown in Figure 47. The sharp decrease in activity after the first observation is due in part to the administration of Versene.

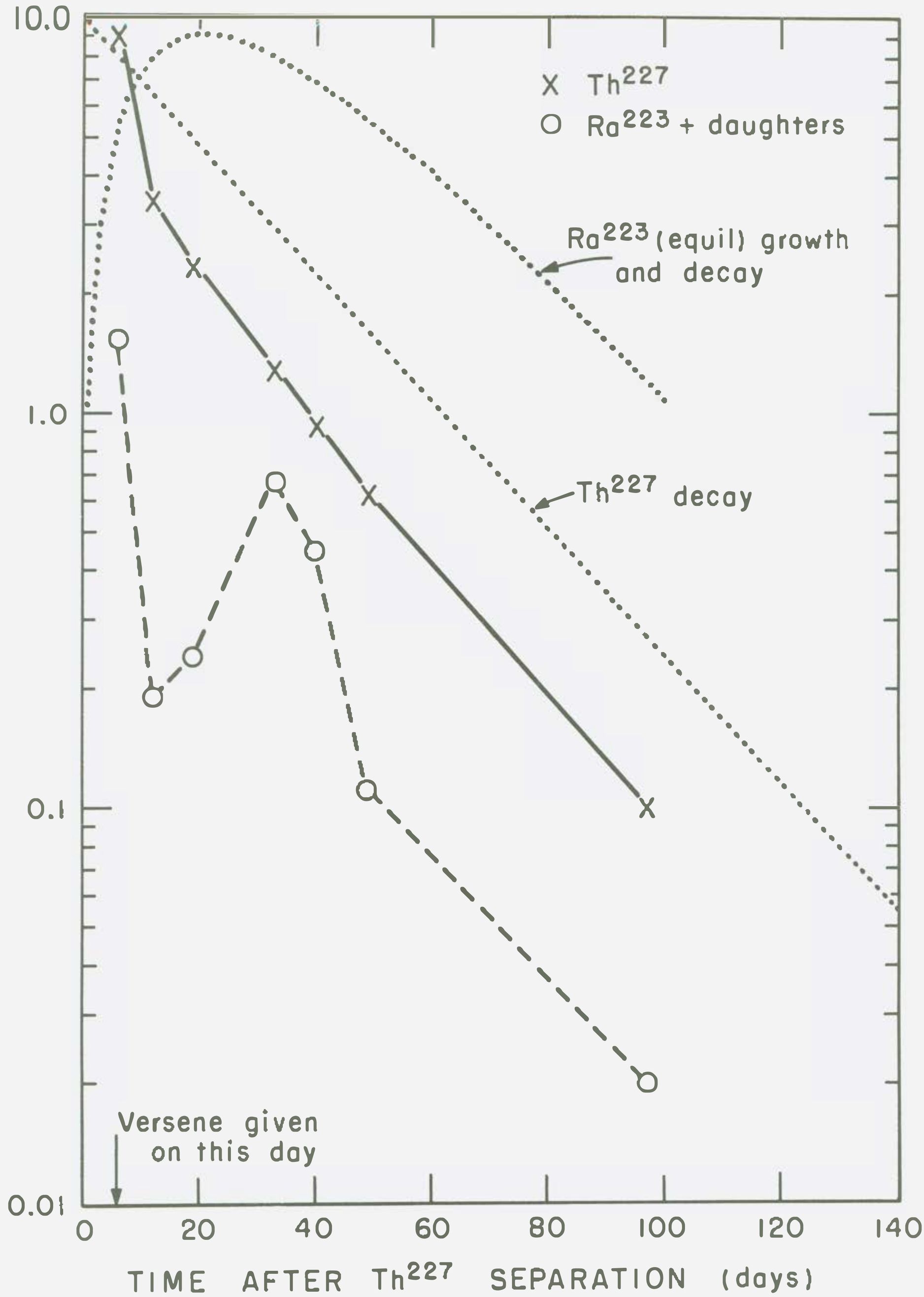

Figure 47 Body burden

Table 19

Days*	μc Th^{227}	μc Ra^{223}**
6	9.28***	1.54***
12	3.49	0.19
19	2.40	0.24
33	1.31	0.68
40	0.95	0.45
49	0.63	0.11
97	0.10	0.02

*Time is expressed in terms of days after preparation of the Th^{227}.

**Ra^{223} in equilibrium with its daughters.

***These values are after surgery during which 1.08 μc Th^{227} and 0.18 μc Ra^{223} was removed.

Readings were also taken with the scintillation probe adjacent to specific parts of the body, again using the 24 channel analyzer. In areas in which the ratio of bone to soft tissue was comparatively large, e.g. the head and knees, the amount of Ra^{223} relative to Th^{227} was roughly twice that in either the liver or the stomach. This would seem to indicate deposition and retention of Ra^{223} in bone.

Further treatment of the total body data will consist of an effort to derive excretion equations which agree at least qualitatively with the body burden pattern and with the excretion data which is available.

Reference

1. L. D. Marinelli, C. E. Miller, P. S. Gustafson, and R. E. Rowland. 1955. The quantitative determination of gamma-ray emitting elements in living persons. Am. J. Roentgenol. Radium Therapy Nuclear Med. 73, 661-671.

KINETIC DATA ON A GAMMA-RAY CLOUD

Howard Walton, Jr.

Although a complete energy budget (in the physical sense) for the detonation of a nuclear weapon may be obtained directly in terms of heat, blast, and radiation,[1] estimates as to the relative contribution to total effect by any one of these may be in error by as much as 10%[2] or more,[1] depending on which form of energy release is considered. It becomes important to reduce the magnitude of this error where possible, particularly in dealing with health hazards from lingering isotopes which comprise the nuclear cloud. If attention is restricted to gamma-ray photons resulting from fission, it is found that 75% of the effective bomb mass is transformed into 40 isotopes of undoubted existence at time zero (diminishing to 27 by 18 hours post-burst). This fortuitous circumstance allows one to account for 99% of the most penetrating components which linger in the cloud after detonation, thereby providing certain information of interest to the biologist who has copied these components in laboratory studies of their physiological effects. It further allows a partial assessment of certain notions on airborne monitoring techniques which might occur to hazard planners, in contemplation of nuclear catastrophe.

Methods

Radiation data for the nuclear cloud were obtained largely from work through 1946, as summarized in the survey by Siegel,[3] most results of which in this instance have remained unaltered over the intervening years. In those cases where subsequent studies have led to modified values for any of the isotopes in question, the 1954 compilation by the Nuclear Data Group of the National Research Council[4] was favored.

In the interests of optimal precision, the only nuclei considered were those for which both atomic number and mass assignment are certain. A further restriction was that the isotope emit either X- or γ-radiation and that the maximum energy of emission be known; in cases in which the magnitude of the latter parameter was a matter for consideration, these isotopes were separated into classes by dividing the energy range at intervals of 100 kilovolts. The decision as to odd or even integer assignment was by conventional rules for the treatment of significant figures,[5] except for the lowest of energy groups (Tables 20 and 21).

Each fission isotope was regarded as if all its radiation were via photons of maximum energy, even where branching is known to occur; the resulting information therefore represents the most dangerous possible situation from γ-ray components of a nuclear cloud. Relative contributions to the total cloud mass by each isotope were computed by the half-life value

Table 20

Cloud components of undoubted existence at time zero

Photon Energy Class (maximum kilovolts)	Isotopes of the Cloud (γ-or X-radiators)
<50	$_{45}Rh^{103*}$, $_{41}Cb^{95*}$, $_{52}Te^{127*}$
100	$_{63}Eu^{155}$, $_{43}Tc^{99*}$, $_{59}Pr^{144}$
200	$_{54}Xe^{133}$, $_{54}Xe^{135}$, $_{58}Ce^{141}$
300	$_{43}Tc^{101}$, $_{45}Rh^{105}$, $_{49}In^{115}$
400	$_{53}I^{131}$, $_{36}Kr^{85}$,
500	$_{54}Xe^{135*}$, $_{56}Ba^{140}$, $_{58}Ce^{143}$
600	$_{56}Ba^{139}$, $_{60}Nd^{147}$, $_{62}Sm^{153}$, $_{39}Y^{91*}$, $_{44}Ru^{103}$, $_{48}Cd^{115}$, $_{53}I^{133}$
700	$_{40}Zr^{95}$, $_{51}Sb^{127}$
800	$_{40}Zr^{97}$, $_{41}Cb^{95}$, $_{41}Cb^{97}$, $_{42}Mo^{99}$, $_{44}Ru^{105}$, $_{45}Rh^{106}$, $_{52}Te^{129}$, $_{55}Cs^{137}$
900	$_{42}Mo^{101}$, $_{47}Ag^{112}$
1100	$_{34}Se^{83}$
1300	$_{38}Sr^{91}$
1600	$_{53}I^{135}$
2300	$_{57}La^{140}$

Table 21

Components of undoubted existence 100 hours
following nuclear detonation

Photon Energy Class (maximum kilovolts)	Isotopes of the Cloud (γ- or X-radiators)
< 50	$_{41}Cb^{95*}$, $_{52}Te^{127*}$
100	$_{63}Eu^{155}$
200	$_{54}Xe^{133}$, $_{58}Ce^{141}$
300	$_{45}Rh^{105}$
400	$_{53}I^{131}$
500	$_{56}Ba^{140}$, $_{58}Ce^{143}$
600	$_{60}Nd^{147}$, $_{62}Sm^{153}$, $_{44}Ru^{103}$, $_{48}Cd^{115}$, $_{53}I^{133}$
700	$_{40}Zr^{95}$, $_{51}Sb^{127}$
800	$_{40}Zr^{97}$, $_{41}Cb^{95}$, $_{42}Mo^{99}$, $_{55}Cs^{137}$
2300	$_{57}La^{140}$,

and fission yield for various times subsequent to detonation. Where the yield for an isotope of undoubted mass assignment and atomic number has not yet been reported, its theoretical value from the yield-mass curve[3] was used.

By the same line of reasoning, the fallout data considered here show the upper limit of danger. Particles of the plume and base surge were grouped with those of the cloud proper so that concentration factors would be maximal. Also, diffusion via turbulence and eddies was neglected so that the data describe the cloud mass as if it remained intact for the longest possible time. Settling rates were obtained by use of Stokes' law, Cunningham's factor, and other relevant information as summarized in the Frank Chart of 1937.[6] In the consideration of external radiation threat per unit volume of space, of course, the kinetics of particle distribution subsequent to early fallout would lead to an attenuation of the hazard.

Results

Results are summarized in the accompanying figures and tables; radiation data are given in Figures 48 through 52 and fallout predictions are found in Figures 53 through 55. Information pertinent both to radiation and to fallout is tabulated in Tables 20 and 21.

In Figure 48 it is seen that the initial half-time of γ-ray photons from fission is 18 hours and that only 5% of the starting activity remains 6 months after detonation. A general notion as to the composition of the cloud in terms of γ-ray photons at given times subsequent to fission may be gained from Figure 49; simultaneous comparisons of energy distribution among radiating particles of the cloud reveal that the relative contribution by each energy class is rather constant during the period from 5 to 20 hours post-burst. It appears, therefore, that monitoring of cloud samples during this interval (during which activity drops 50%) would be useless for fixing the exact time of detonation via relative amounts of γ-radiation (in terms of photon energy). However, Figure 50 shows an irreversible change in the average energy of γ-ray photons from 5 to 100 hours following detonation. This means that the time since fission could be determined from cloud sampling during this interval, even though monitors were not present at detonation. The apparent wave property of the mean energy curve has no special physical significance, but it does reveal that sampling via pulse height analyzers set from about 600 to 700 kilovolts could be used in reconstructing the history of a nuclear cloud during its most dangerous phase of existence.

Although the pulse height criteria would have to be abandoned beyond 100 hours post-burst, Figure 51 reveals that unique time-dependent energy ratios occur among the particles in the period between 250 and 2000 hours following fission. The mean energy method noted above could be resumed

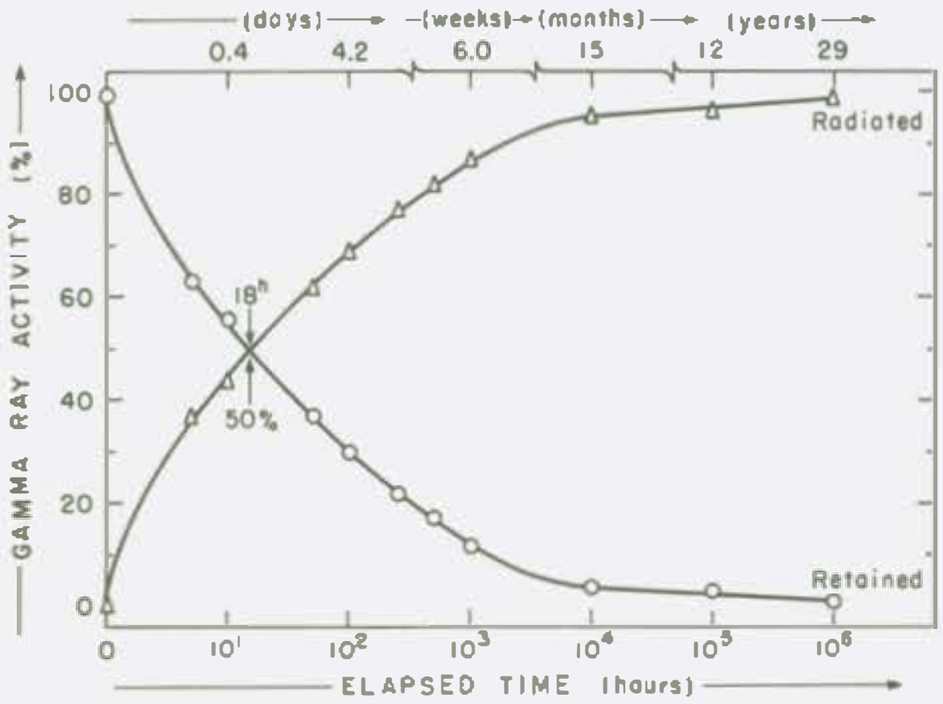

Figure 48 Activity as a function of time for uranium-235 fission fragments.

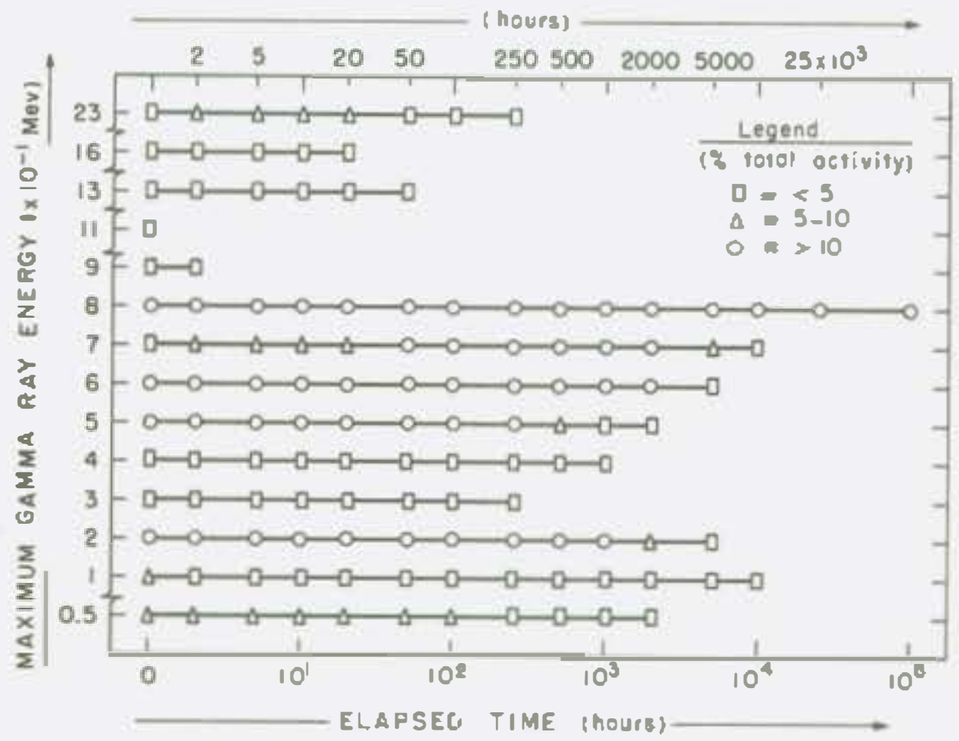

Figure 49 Energy distribution among fission particles as a function of time.

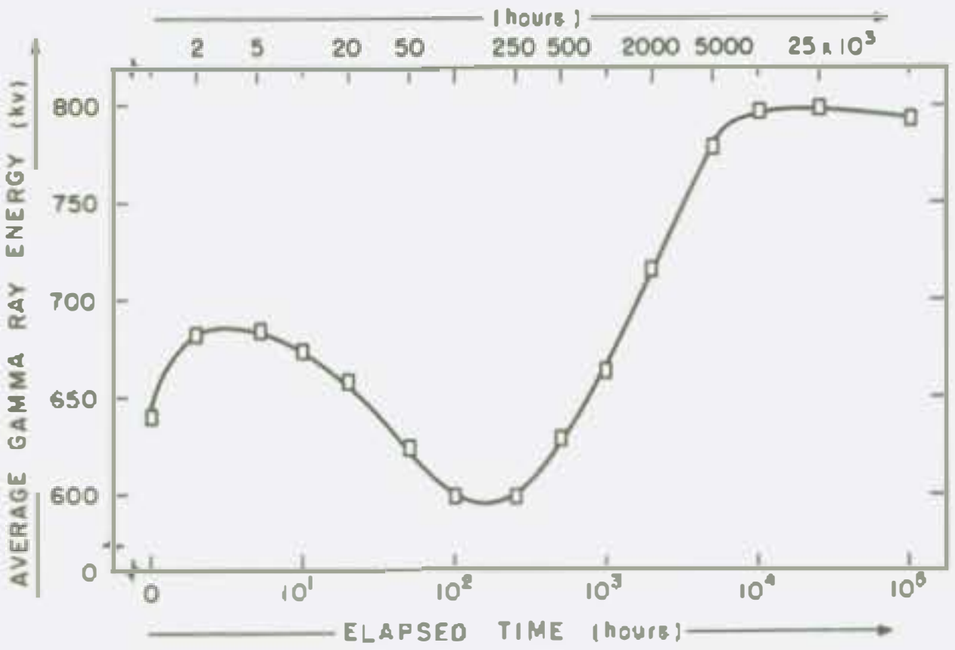

Figure 50 Upper limit of average γ-ray hazard at and subsequent to fission.

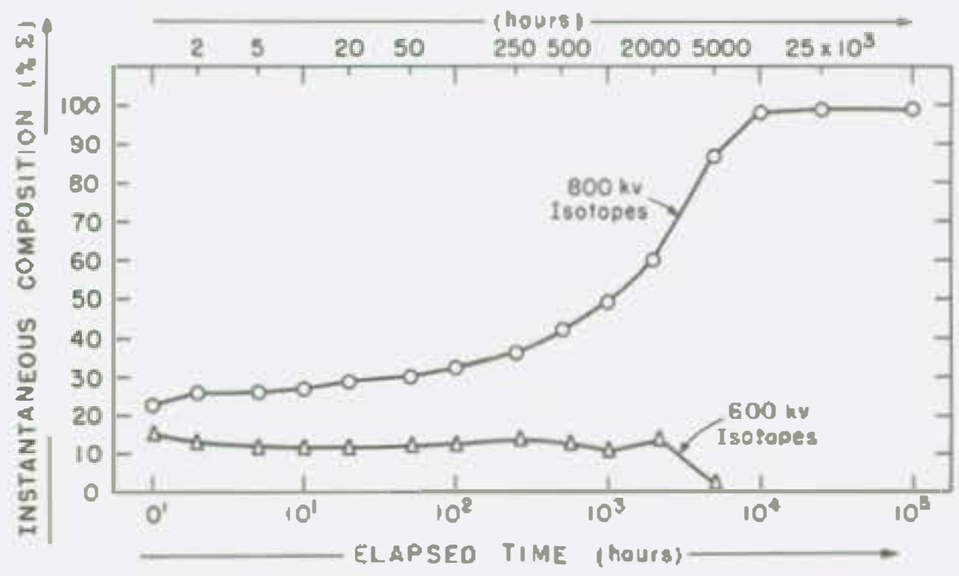

Figure 51 Relative amounts of 600 and 800 kilovolt fission isotopes with time.

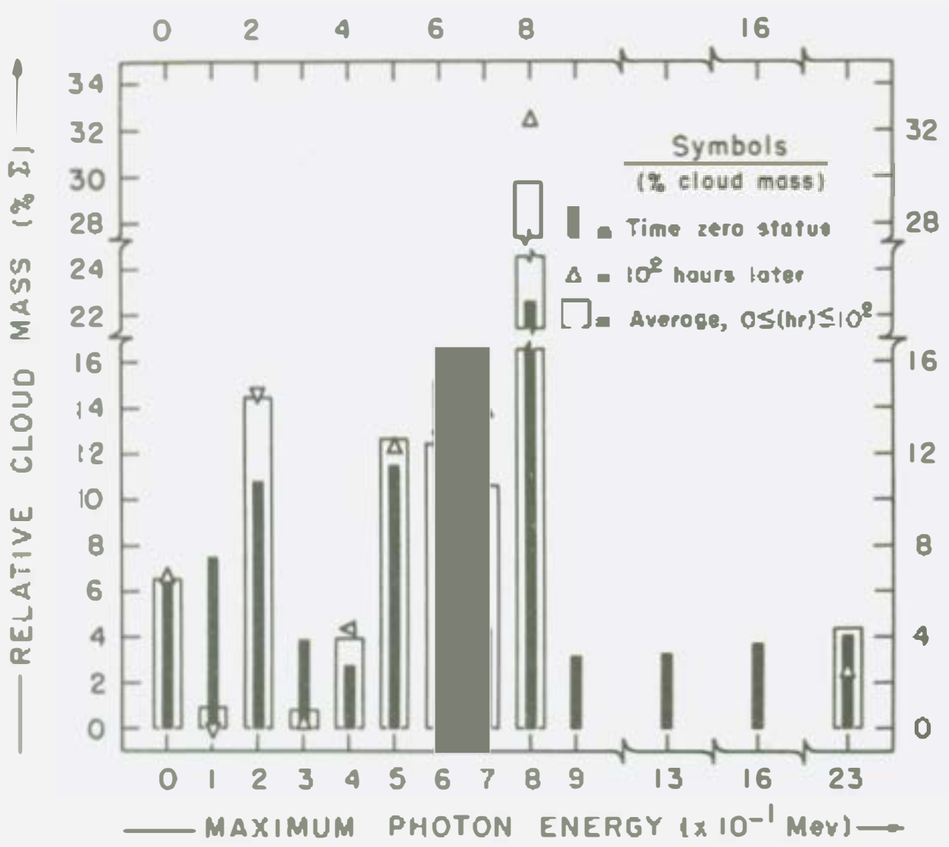

Figure 52 Distribution of γ-radiation within the fission cloud.

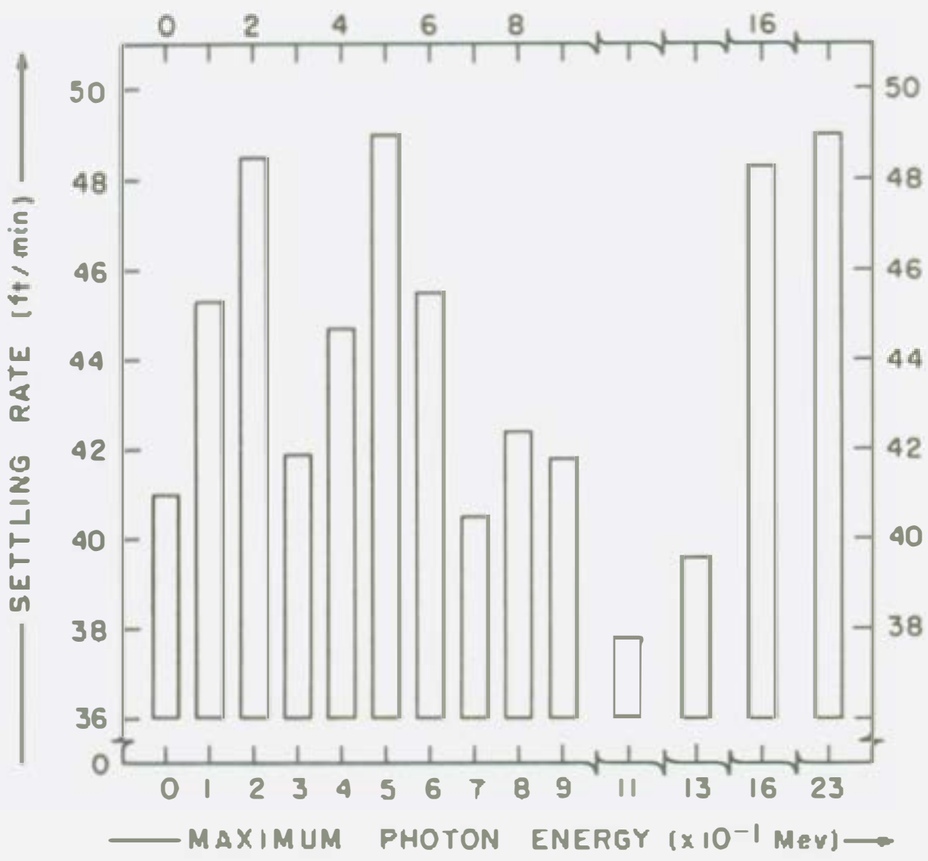

Figure 53 Settling rate relative to energy of γ-ray photons within a fission cloud.

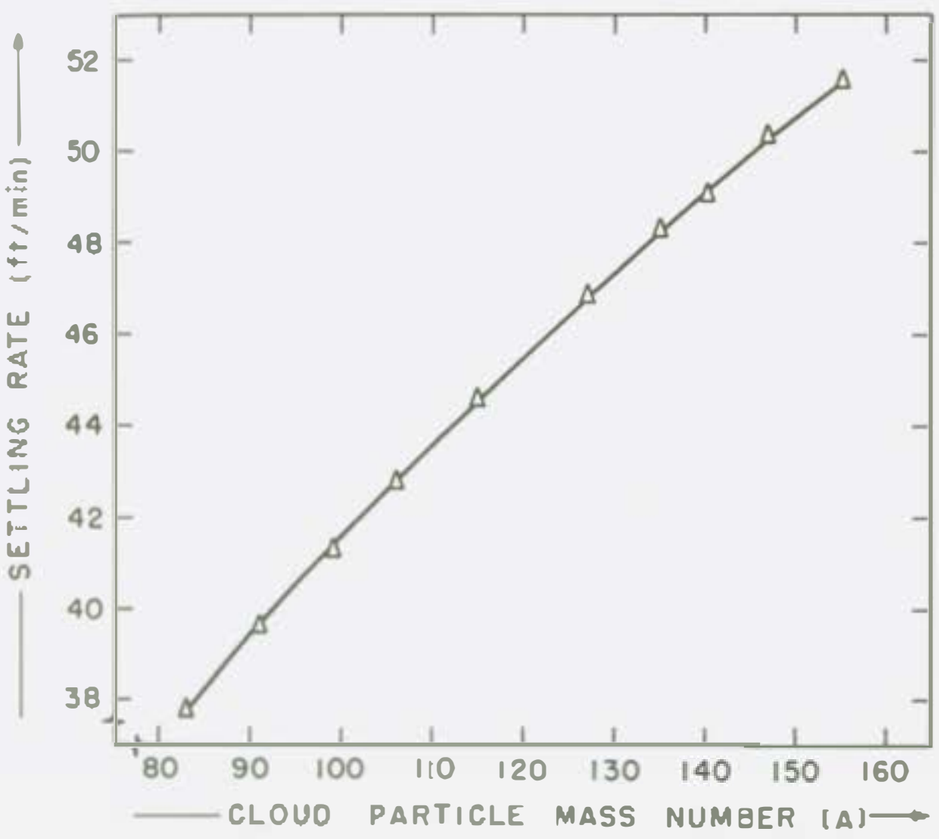

Figure 54 Earthward migration rates by particles within the fission cloud.

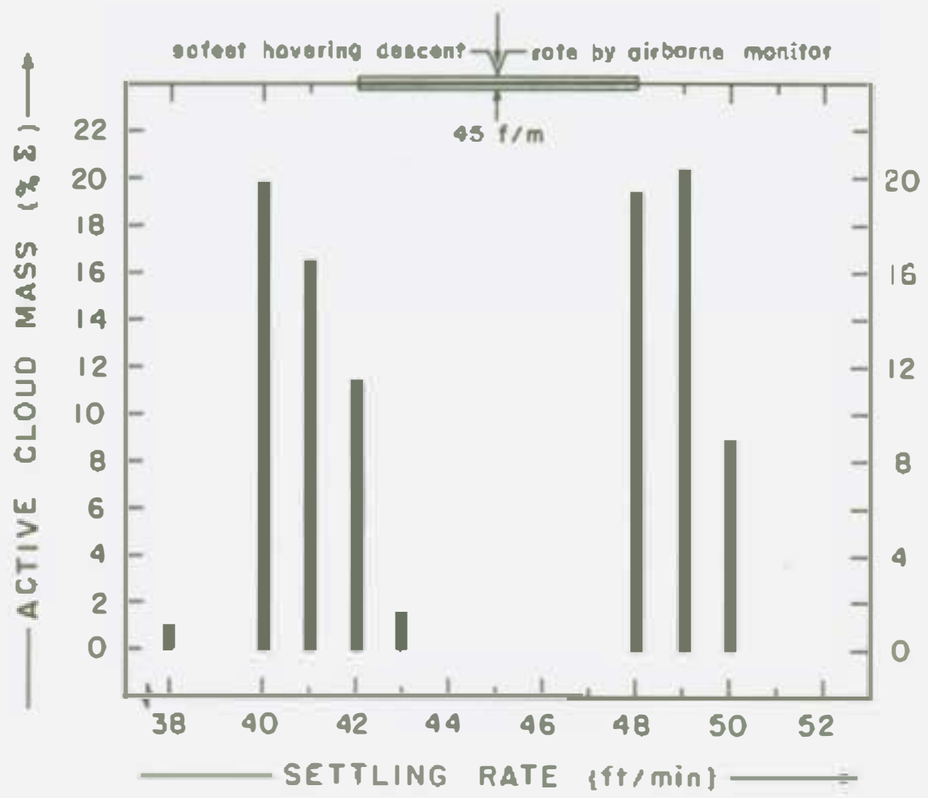

Figure 55 Kinetic guide for migration by airborne personnel through a fission cloud.

for intervals ranging beyond 2000 hours post-burst (but for not more than 5 to 10 thousand hours later), in which case, of course, sampling evidence would come from material-bearing fragments of the cloud, long since dissipated. Another way of fixing time since detonation would be by rather involved radiochemical methods, exploiting such abundance differences as are indicated in Tables 20 and 21.

Information presented here is applicable in biological studies using laboratory copies of γ-ray photons within a nuclear cloud.(7) The extent to which such studies would simulate field conditions can be estimated from data in Figure 52. Average values obtained from simultaneous comparisons among all cloud isotopes at intervals no greater than 5 hours apart, were necessarily based on the first 100 hours post-burst, since the majority (70%) of the γ-radiation is not retained after that time (Figure 48). These data further reveal that appropriate exposure geometry of machines for laboratory simulation of a nuclear cloud(8) would involve a wide range of radiant energies. Thus less than 20% of the most hazardous cloud particles would emit photons with maximum values between 80 and 250 kilovolts; this statement holds, whether applied to time zero, 100 hours later, or any time between. Similar reasoning applied to other energy groups shown in Figure 52 is left to the interested reader.

Fallout data presented here are for particles $5.0 \times 10^{-1}\ \mu$ in diameter and therefore would not apply to a sub-surface burst, where cloud components would be much larger.(6) With this restriction in mind, we see in Figure 53 that the first wave of particles to reach earth from an airborne fission weapon would have peak energies of 200, 500, 1600, and 2300 kilovolts. Figure 54 indicates a rather narrow earthward velocity range, from about 40 to 50 feet per minute. The Hiroshima catastrophe showed that a nominal atomic bomb will inflict maximum blast damage when delivered from about 2000 feet above the target.(9) In that circumstance, the upper limit of danger from early fallout would include migration to the nadir by cloud particles at rates as shown in Figure 54 and in relative amounts noted in Figure 55, in which case they would reach earth at from 6 to 9 hours following detonation.

Actually, most of the radioactive products are carried aloft in the plume and dispersed over a wide area,(10) with attendant dilution. On the other hand, the fate of a nuclear cloud generated during a summer thundershower would be quite like that described. Further study on this subject is still in progress and will be reported in the future.

The radiation data shown above take on additional significance when it is noted that a ten-megaton tnt-equivalent nuclear weapon may release 500-fold the fission activity found in the Hiroshima bomb.(11) Inasmuch as relative values have been shown, these data therefore apply to the γ-ray cloud from the so-called "super" as well as to that from the "Model-T" type of nuclear weapon.

The writer is very grateful to Dr. Austin M. Brues for his encouragement and help with the more difficult portions of the analysis.

References

1. D'Olier, F. and the United States Strategic Bombing Survey (Directors and Complement). 1946. The effects of atomic bombs on Hiroshima and Nagasaki. United States Governmant Printing Office, Washington, D. C., pp. 24-25.

2. Hunter, H. F., and N. E. Ballou. 1951. Fission-product decay rates. Nucleonics, 9(5), C, 2-7.

3. Siegel, J. M. 1946. Nuclei formed in fission: decay characteristics, fission yields, and chain relationships. J. Am. Chem. Soc., 68, 2411-2442.

4. Way, K., G. H. Fuller, R. W. King, C. L. McGinnis, and A. L. Hankins. 1954. New nuclear data, 1954 cumulation, Nuclear Science Abstracts, 8(24B), 1-99.

5. Crumpler, T. B., and J. H. Yoe. 1940. Chemical Computations and Errors. New York: John Wiley and Sons, Inc., pp. 30-35.

6. Frank, W. G. 1937. Size and Characteristics of Air-Borne Solids. Louisville, Ky. American Air Filter Co., Inc.

7. Grahn, D., and G. A. Sacher. 1955. Comparative effectiveness of several X-ray qualities for acute lethality in mice and rabbits. Quarterly Report, Biological and Medical Research Division, Argonne National Laboratory. ANL-5426, pp. 12-19.

8. Walton, H., Jr. 1955. Low-energy X-ray phantom dosimetry. Quarterly Report, Biological and Medical Research Division, Argonne National Laboratory. ANL-5378, pp. 84-90.

9. Hirschfelder, J. O. (Chairman), D. B. Parker, A. Kramish, R. C. Smith, eds., S. Glasstone, exec. ed. 1950. The Effects of Atomic Weapons. New York: McGraw-Hill. p. 134.

10. Smyth, H. D. 1946. Atomic Energy for Military Purposes. Princeton University Press. p. 212.

11. Libby, W. F. 1955. Radioactive fall-out. Bull. Atomic Scientists, 11, 257.